Investigation of a Novel Formulation from Umbilical Cord Blood Stem Cell-Derived Exosomes and Antioxidant (Selenium) in Malignant Melanoma Cells

INVESTIGATION OF A NOVEL FORMULATION FROM UMBILICAL CORD BLOOD STEM CELL-DERIVED EXOSOMES AND ANTIOXIDANT (SELENIUM) IN MALIGNANT MELANOMA CELLS

T. S. H. M. ALTOBALANI

MD

2023

Investigation of a Novel Formulation from Umbilical Cord Blood Stem Cell-Derived Exosomes and Antioxidant (Selenium) in Malignant Melanoma Cells

Tahera Sayed Hashem Mohamed ALTOBALANI

Submitted for the Degree of

Doctorate in Medicine

School of Chemistry and Biosciences

Faculty of Life Sciences

University of Bradford

2023

Abstract

Tahera Sayed Hashem Mohamed Altobalani

Investigation of a Novel Formulation from Umbilical Cord Blood Stem Cell-Derived Exosomes and Antioxidant (Selenium) in Malignant Melanoma Cells

Keywords: Melanoma, CBSC-derived exosomes, selenium, cancer, malignant melanoma, cancer immunotherapy, comet assay, CCK-8, RT–qPCR, Western blotting.

Introduction: Malignant Melanoma (MM), caused by UV radiation-induced DNA damage, is the most invasive form of skin cancer and has an increasing incidence worldwide. The hallmarks of MM include the presence of reactive oxygen species (ROS) and excessive proliferation of tumour cells. Many treatments are available or under investigation as anticancer therapeutics such as cell therapy, immunotherapy, gene therapy and nanotechnology-based strategies but they all have severe complications and side effects that limit their wider use.

Methods: The present *in vitro* study has evaluated the genotoxic and cytotoxic effects of Se and CBSC-derived exosomes, individually and in combination, on lymphocytes from MM patients and healthy controls, and on the CHL-1 melanoma cell line. The comet assay and cell counting kit-8 (CCK-8) assay were used to measure genotoxicity and cytotoxicity, respectively, in all cell types. Molecular mechanisms underlying the observed effects were explored using transcriptional and protein expression profiling of key cell cycle and apoptosis genes, by employing the RT qPCR and Western blotting techniques.

Conclusion: Selenium displays antioxidant and genoprotective effects in human lymphocytes, especially in MM patients. Both Se (10 μM) and CBSC-derived exosomes (120 μL) are well tolerated in lymphocytes, but show significant genotoxicity and cytotoxicity towards the CHL-1 cell line, with combined administration exhibiting a synergistic effect.

Acknowledgements

I would like to thank God for always being with me and showing me the right path, and being on my side even when situations got worse. You have always blessed everyone with the best.

I would like to express my special thanks of gratitude to my supervisor Dr Mojgan Najafzadeh, who made this work possible. Her guidance and advice carried me through all the stages of my project. She has helped me by sharing her experiences, with great respect, for both support and guidance throughout this study. My special thanks also go to my team members, particularly Dr Masya Alhawamda.

I would like to give special thanks to my husband and my family as a whole for their continuous support and understanding when undertaking my research and writing my project. Your prayer for me was what sustained me this far.

Table of Contents

List of Figures

List of Tables

List of Abbreviations

6-4PPs	Pyrimidine (6-4) pyrimidone photoproducts
8-oxoG	8-Oxoguanine
AK	Actinic keratosis
ATP	Adenosine 5′-triphosphate
B cell	B lymphocyte cell
BCC	Basal cell carcinoma
BD	Bowen’s disease
BMDCs	Bone marrow-derived progenitor cells
CAFs	Cancer-associated fibroblasts
CBSC	Cord blood stem cell
CCK-8	Cell counting kit-8
CD	Cluster differentiation
CDK	Cyclin dependent kinase
CDK2	Cyclin dependent kinase 2
cDNA	Complementary DNA
CHL-1	Callisaurus cell line, patented cell line
circRNA	Circular ribonucleic acid
CLND	Complete lymph node dissection
CPDs	Cyclobutanepyrimidine dimers
CSC	Cancer stem cell
CSCD	Chondroitin sulfate–ss–deoxycholic acid
DMSO	Dimethyl sulfoxide
DNA	Deoxyribonucleic acid
dsDNA	Double-stranded deoxyribonucleic acid
ECM	Extracellular matrix
EGFR	Endothelial growth factor receptor
ERK	Extracellular signal-regulated kinase
EtBr	Ethidium bromide
EVs	Extracellular vesicles
FBS	Foetal bovine serum
FDA	Food and Drug Administration, USA
GPX1	Glutathione peroxidase 1

H_2O_2	Hydrogen peroxide
HIF	Hypoxia-inducible factor
HLA	Human leukocyte antigen
HPLC	High performance liquid chromatography
HPLC–ED	HPLC coupled with electrochemical detection
HPLC–MS/MS	HPLC coupled with tandem mass spectrometry
HPV	Human papillomavirus
HSP	Heat shock protein
IC_{50}	Half-maximal inhibitory concentration
IKAP	Subunit of the highly conserved complex, Elongator
IKK-α	Inhibitor of nuclear factor-κB kinase subunit alpha
IKK-β	Inhibitor of nuclear factor-κB kinase subunit beta
IKK-γ	Inhibitor of nuclear factor-κB kinase subunit gamma
IL	Interleukin
ILVs	Intraluminal vesicles
LMA	Low melting agarose
LMP	Low melting point
lncRNA	Long noncoding ribonucleic acid
LPS	Lipopolysaccharide
MAPK	Mitogen-activated protein kinase
MC1R	Melanocyte-stimulating hormone receptor
MDSCs	Myeloid-derived suppressor cells
MET	MET proto-oncogene, receptor tyrosine kinase
MGE	Microgel electrophoresis
miRNA	microRNA
MM	Malignant melanoma
MMPs	Matrix metalloproteinases
mRNA	Messenger RNA
MSA	Methylseleninic acid
MSC	Mesenchymal stem cell
MSC EVs	Mesenchymal stem cell extracellular vesicles
MVB	Multivesicular body
NaCl	Sodium chloride
NaOH	Sodium hydroxide

NC	Negative control
ncRNA	Noncoding RNA
NEMO	IKK-γ (see above)
NER	Nucleotide excision repair
NK	Natural killer
NMP	Normal melting point agarose
NMSC	Non-melanoma skin cancer
OD	Optical density
OTM	Olive tail moment
PBMC	Peripheral blood mononuclear cells
PBS	Phosphate buffered saline
PC	Positive control
PDAC	Pancreatic ductal adenocarcinoma
PD-L1	Programmed cell death ligand 1
PD-L2	Programmed cell death ligand 2
PL	Planar lymphoscintigraphy
PPs	Pyrimidone photoproducts
PUVA	8-Methoxypsoralen and UVA
RB	Retinoblastoma
RCT	Randomised control trial
RNA	Ribonucleic Acid
ROS	Reactive oxygen species
RT	Room temperature
RTCA	Real-time cellular analysis
RT-qPCR	Reverse transcription–quantitative polymerase chain reaction
SCC	Squamous cell carcinoma
SCGE	Single-cell gel electrophoresis
SDS–PAGE	Sodium dodecyl sulfate–polyacrylamide gel electrophoresis
SDT	Sonodynamic therapy
Se	Selenium
SECIS	Selenocysteine insertion sequence
SLN	Sentinel lymph node
SLNB	Sentinel lymph node biopsy
SPECT/CT	Single photon emission computed tomography/computerised tomography

SSB	Single-stranded break
SSL	Simulated sunlight
TBST	Tris-buffered saline containing 0.1% (v/v) Tween-20
T cell	T lymphocyte cell
TGF	Transforming growth factor
TLR4	Toll-like receptor 4
TNF	Tumour necrosis factor
TNM	Tumor, lymph node, metastasis
TRAIL	Tumour necrosis factor-related apoptosis-inducing ligand
Treg	Regulatory T cell
TSG 101	Tumour susceptibility gene 101
UCB	Umbilical cord blood
UTR	Untranslated region
UV	Ultraviolet
UVA	Ultraviolet A
UVB	Ultraviolet B
UVC	Ultraviolet C
UVR	Ultraviolet radiation
VEGF	Vascular endothelial growth factor
WHO	World Health Organization
WJ	Wharton’s jelly

1) Introduction

1.1 Cancer

Cancer is characterised by the uncontrolled growth and spread of specific cell types throughout the body, caused by changes to DNA. Cancerous cells can proliferate and multiply due to unregulated cell division. They have the potential to invade neighbouring tissues and develop into clusters of aberrant tissue known as tumours, which are usually classified as either benign or malignant. Benign tumours are not invasive and do not spread to other body regions, and neither do they return following surgical resection. In contrast, malignant (or cancerous) tumours can invade surrounding tissues and spread to other organs through a process known as metastasis (**Figure 1**), which can lead to significant complications or even death (Boutry et al., 2022).

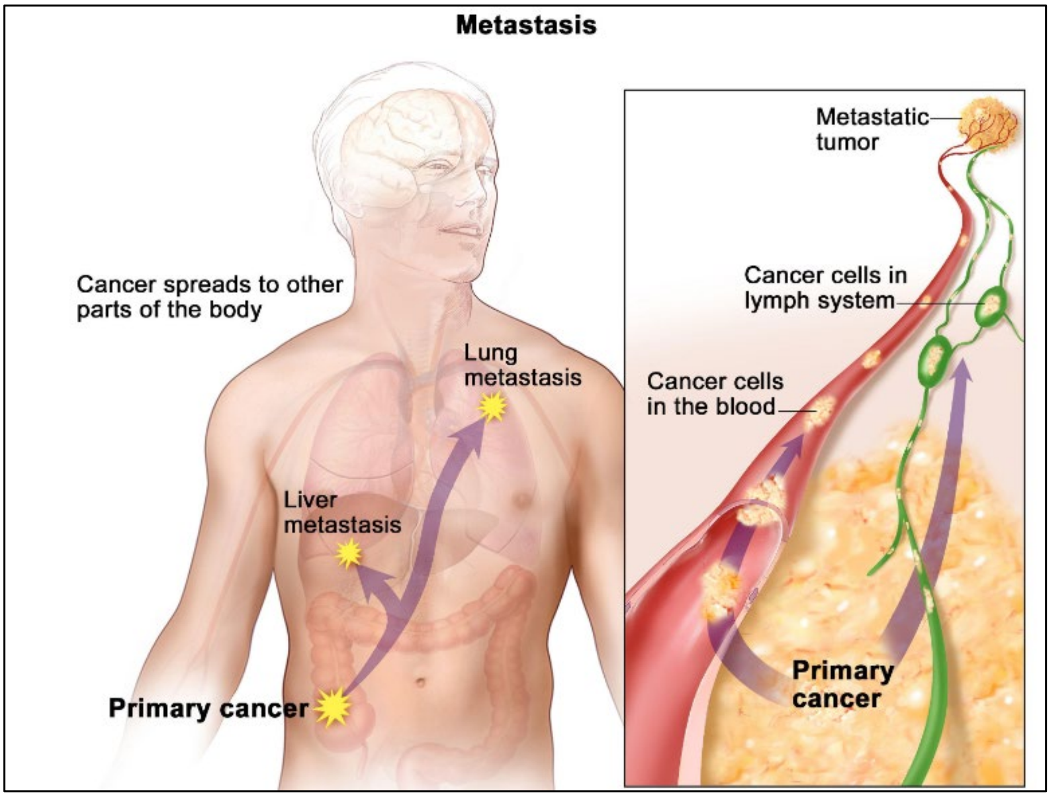

Figure 1. Primary cancer and metastasis (NIH, 2022).

Cancer is mainly caused by changes or mutations to the DNA within cells. The underlying reasons for these changes include smoking, exposure to ultraviolet radiation (UVR), defects in DNA repair mechanisms including nucleotide excision repair (NER), and defects in cell cycle checkpoint genes. For example, UVR can induce direct photochemical damage to DNA and is considered a carcinogen that causes skin cancer (**Figure 2**) (Khan et al., 2018). It is further subdivided into UVC (100–280 nm), UVB (280–320 nm) and UVA (320–400 nm), based on the biological effects of these different wavelength bands (Sorenson et al., 2022). Other known causes of cancer include mutations in the *RB1* (retinoblastoma transcriptional corepressor 1) gene, or in the tumour suppressor genes *TP53* (encoding the protein p53), *CDKN1A* (p21), *CDKN1B* (p27) or *CDKN1C* (p57), all of which are involved in cell cycle regulation.

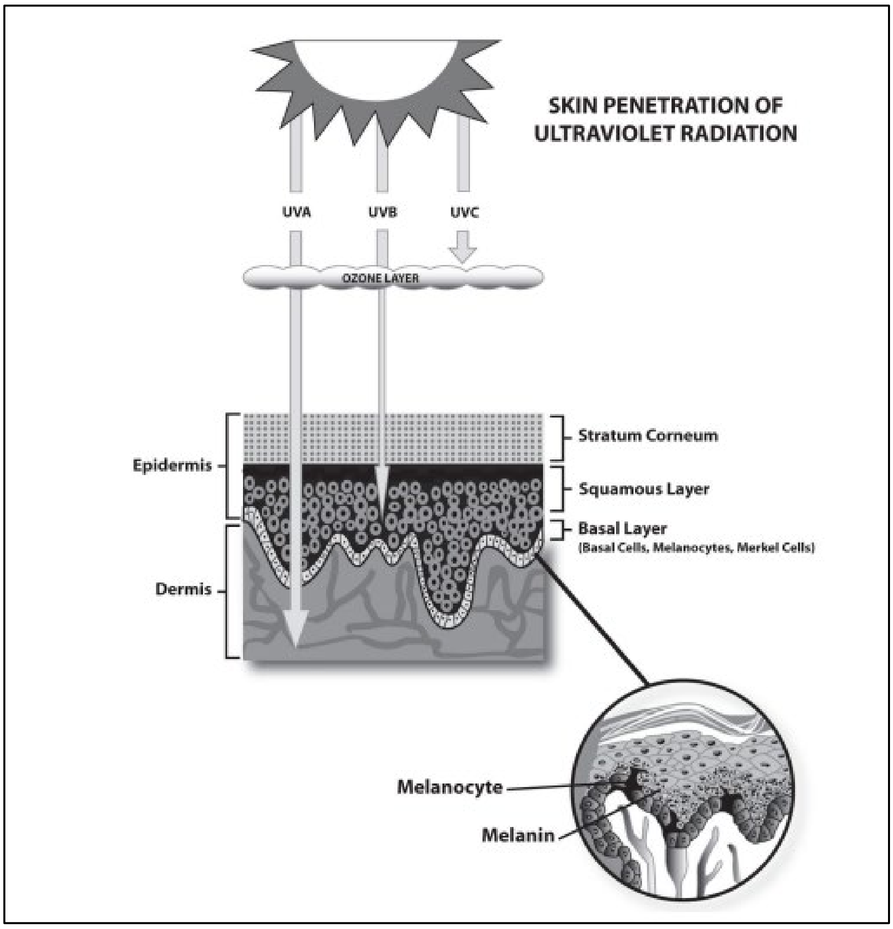

Figure 2. Types of ultraviolet (UV) radiation (UVA, UVB and UVC), and their different degrees of skin penetration (Watson et al., 2016).

Cancer is a heterogeneous disease which is subdivided into various types, including carcinomas, which can develop in the skin or internal organs and account for the vast majority of cases. These tumours usually manifest as solid lumps, and include the most common cancer types such as prostate, breast, lung and gastrointestinal cancers (Maroni & Bendinelli, 2020). Another class of cancers, sarcomas, are a heterogeneous group of rare tumours that arise predominantly from the embryonic mesoderm (Dohnor et al., 2015).

1.2 Skin Cancers

The most prevalent kind of cancer in the US is cutaneous cancer, commonly known as skin cancer (Linares et al., 2015). It also represents the most common malignancy worldwide, with a growing incidence that shows no signs of plateauing. The disease spans all ethnicities, socioeconomic groups and geographical regions, and covers the entire lifespan. Most skin cancers are caused by a combination of both non-modifiable (e.g., genetic) and modifiable (e.g., environmental) risk factors. The most common modifiable risk factor for skin cancer is exposure to UVR (Gandini et al., 2011).

In general, skin cancers are most common among sun-sensitive populations, with non-Hispanic whites being approximately 25 times more likely to develop melanoma compared with blacks, and Hispanics experiencing six-fold higher incidence. Overall, the disease is more common among males, although incidence is higher for females below the age of 50. In common with incidence, mortality increases with age and is also higher among males. Whites have the highest incidence and mortality rates, but black and Hispanic populations are often diagnosed at later stages and consequently have poorer survival outcomes.

1.2.1 Types of Skin Cancer

The three major types of skin cancer are basal cell carcinoma (BCC), squamous cell carcinoma (SCC) and malignant melanoma (MM). Among these, BCC and SCC are sometimes grouped together as non-melanoma skin cancers.

1.2.1.1 Basal Cell Carcinoma

BCC is the sixth most common malignancy in the UK, and its incidence is rising due to the influence of cumulative sun exposure and an ageing population. The disease develops in the deepest, or basal, layer of the epidermis (known as the stratum basale, or stratum germinativum), and is further classified according to its various clinicopathological manifestations (Tanese, 2019). It typically appears as a tiny, bright pink or pearly-white lump with a transparent or waxy look, and a red, scaly patch that occasionally contains some black or brown pigment. Most of the time, BCC does not spread to other parts of the body (Kim et al., 2019). It has low mortality but can cause significant morbidity, primarily through local destruction. Around 147,000 new cases of non-melanoma skin cancer (i.e., BCC and SCC) are diagnosed each year in the UK (NIH, 2022), but despite this high incidence, the metastasis and age-adjusted mortality rates are estimated at only 0.0028–0.5% and 0.00012%, respectively. A similarly high prevalence of BCC is found in other countries (Kocarnik et al., 2022).

The disease is more common in Fitzpatrick skin types I and II (usually white individuals), with a lifetime risk estimated at 30%. Other risk factors for BCC include light eye colour, freckles, and blonde or red hair. The most important environmental risk factor is UVR exposure, with other known examples including childhood sunburn, family history of skin cancer, tanning bed use, chronic immunosuppression, photosensitising drugs, ionising radiation, and exposure to carcinogenic chemicals (especially arsenic). In particular, intense and intermittent sun exposure during childhood strongly correlates with BCC development.

The incidence of BCC is approximately doubled in HIV-positive patients and is 5–10 times greater in organ transplant recipients, with around half of these patients developing the disease within 10 years of surgery. These tumours are more likely to be the thinner, more superficial histological subtype and to occur in younger patients. In individuals with allogeneic organ transplants and receiving immunosuppressive drugs—such as systemic corticosteroids, azathioprine and cyclosporine— different pathways may be activated that lead to induction and promotion of skin malignancies. Furthermore, methotrexate use in patients with rheumatoid or psoriatic arthritis has been shown to have a dose–response relationship with BCC incidence.

Given its low metastatic potential, BCC treatment is primarily directed towards local control. Several factors must be considered when comparing the cure rates for treatments based on different studies, including the duration of follow-up and the percentage of high-risk and recurrent tumours. For example, recurrences are often diagnosed after five years due to the slow growth rate of BCCs. In a randomised controlled trial (RCT) of surgical excision, recurrence rates were 3% and 12% at 2.5 years and 10 years post-treatment, respectively, with 56% of all recurrences diagnosed after more than five years (Kim et al., 2019).

1.2.1.2 Squamous Cell Carcinoma

SCC is the less common form of non-melanoma skin cancer, and originates from epidermal keratinocytes or adnexal structures (such as eccrine glands or pilosebaceous units). As with BCC, the most significant risk factor is exposure to UVR and sunlight, with SCC usually developing on sun-exposed skin as a firm pink lump with a rough or crusted surface. There is minimal chance of cutaneous SCC migrating to the lymph nodes or other organs (Kallini et al., 2015). The average age of onset is during the mid-sixth decade of life, but it can present in individuals as young as 20–30 years of age in regions such as Australia, Florida, New Zealand and southern California (Kocarnik et al., 2022). Overall incidence is higher in males, but SCC originating on the legs is more common in females. In addition to UVR and sunlight exposure, other identifiable risk factors for cutaneous SCC include Fitzpatrick skin types I and II, outdoor occupations (e.g., farming, construction work), and exposure to human papillomavirus (HPV). Other studies have demonstrated a direct correlation between combined 8-methoxypsoralen therapy and UVA (PUVA) exposure, used as a treatment for psoriasis, and SCC incidence (Stern et al., 1984). In patients treated with PUVA, exposure to more than 350 PUVA treatments was found to significantly increase the risk for SCC.

This disease is generally uncommon in dark-skinned individuals. Sun exposure is a less frequent aetiology since their more pigmented skin possesses higher amounts of epidermal melanin, which protects against the carcinogenic effects of UV light. However, SCC does represent the most common cutaneous cancer in African-Americans (Kocarnik et al., 2022), where it usually occurs in non-sun-exposed areas. Actinic keratosis (AK) often precedes SCC in darker skin.

Certain chronic conditions increase the likelihood of developing cutaneous SCC, and as with BCC, its incidence is much higher in transplant patients than in the general population. For example, 70% of transplant recipients in Australia develop the disease within 20 years of surgery (Kocarnik, et al., 2022). Multiple reasons have been postulated for this, including specific polymorphisms in human leukocyte antigen (HLA) and glutathione *S*-transferase genes (Kallini et al., 2015).

1.2.1.3 Bowen's Disease

Bowen's disease (BD), or SCC in situ, is a slow-growing, precancerous dermatosis and a precursor to cutaneous SCC. It can develop in any region of the skin or mucosa, but embraces different clinical presentations depending on the site and aetiology, and may also appear very similar to other skin lesions. It usually affects older people in their sixties and seventies, and is regarded as a very early form of skin cancer that can be easily managed through chemotherapy and surgery (Neagu et al., 2017).

The disease has multifactorial risk factors, including Caucasian race, fair skin, photosensitivity, and high total occupational and recreational sun exposure. Cumulative exposure to UVR produces DNA damage and immunosuppression, facilitating clonal expansion of the underlying p53 driver mutations found in the majority of cases (Kim et al., 2022). Consistent with these findings, aneuploidy and genomic instability are high in the lesional skin. In immunosuppressed individuals (including transplant patients), Merkel cell polyomavirus has been associated with BD, which is also known to arise following ionising radiation exposure, thermal skin injury, inflammatory dermatoses (e.g., chronic lupus erythematosus or lupus vulgaris), and as an adverse effect of PUVA therapy.

Morphology differs based on the age of the lesion, the site of origin, and the degree of keratinisation. In areas with no keratinisation, BD lesions are erythematous and velvety, while in lesions occurring over keratinised epithelium, the erythema is masked by scaling. The clinical presentation is also altered in intertriginous, moist or hyperkeratotic surfaces. Lesions are usually solitary, but 10–20% of affected individuals have multiple lesions.

The treatment modality depends on factors such as the tumour size, location, thickness, and number of lesions, as well as the patient's age, immune status, comorbidities, concomitant medication intake, compliance, desired aesthetic outcome, and equipment availability. The patient's preferences and clinician's expertise are also important aspects of treatment decisions. Where the disease is multicentric, immunosuppression and arsenicosis should be considered. Notwithstanding this, each potential therapeutic modality has its place, and the treating physician should weigh the associated merits and demerits. Because BD occurs mostly in older individuals and is frequently located in regions with poor wound healing, non-invasive treatments are generally preferred (Palaniappan, 2022).

1.2.1.4 Actinic Keratoses

Actinic keratoses, also known as solar keratoses, are dry, scaly skin patches caused by sun exposure damage. The patches can be pink, red or brown, and vary in size from a few millimetres to a few centimetres. Like BD, actinic keratosis is not classed as a cancerous lesion, but there is a slight risk of progression to SCC if left untreated (Radu & Pantanowtiz, 2013).

1.2.2 Malignant Melanoma

MM is the most aggressive type of skin cancer, and also the most lethal. It is a relatively common form of cancer that originates in melanocytes, the pigment-producing cells located in the epidermis, and is derived from genetic mutations in these cells. Cancerous changes can be triggered by damage due to UV light exposure from the sun, along with other sources such as tanning beds. However, MM can also develop in areas of the body that are not exposed to the sun (Linares, et al., 2015), and this includes seemingly counterintuitive locations such as the nasal passages and throat. It is the fifth most prevalent male cancer and the seventh most common female malignancy, and with an estimated 325,000 new cases in 2020, it accounts for 1.7% of all cancer diagnoses worldwide. Although it only represents around 5% of skin malignancies, over 80% of skin cancer deaths are due to MM (Rebecca et al., 2020; Saginala et al., 2021). The WHO has reported a 50% increase in MM incidence over the past decade, with an associated 32% increase in deaths. A further 20% rise is predicted by 2025, reaching 74% by the year 2040 (Rogoża-Janiszewska et al., 2021).

Histological features favouring a diagnosis of MM include asymmetry, ulceration, cytological atypia, pagetoid involvement of the epidermis, lack of maturation, and deep and/or atypical dermal mitosis (Filosa & Filosa, 2018). Melanomas may develop in or near a previously existing precursor lesion, with common acquired nevus, dysplastic nevus, congenital nevus, and cellular blue nevus recognised as MM precursor lesions. Conversely, if MM develops in previously healthy-looking skin, it is said have arisen de novo (with no evidence of a precursor lesion). While solar irradiation induces many MMs, as noted above, they may also occur in unexposed skin areas including the palms, soles and perineum. MMs have two distinct growth phases, radial and vertical. During radial growth, malignant cells grow radially in the epidermis. With time, most cases eventually progress to the vertical growth phase in which the malignant cells invade the dermis (**Figure 3**) and develop metastatic potential (Hida, 2020).

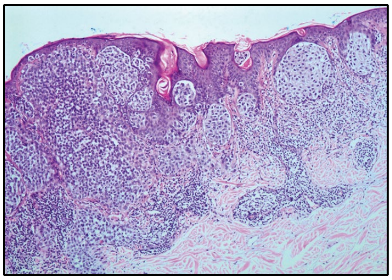

Figure 3. Histopathology of MM, showing proliferation of atypical melanocytes singly and in nests within the epidermis, papillary and superficial portion of the reticular dermis, with smaller nests of atypical melanocytes located within follicular ostia filled with keratin plugs (H&E stained section, 10× objective) (Đorđević Brlek et al., 2019).

1.2.2.1 Major Subtypes of MM

The four forms of MM—superficial spreading melanoma, nodular melanoma, lentigomaligna melanoma, and acral lentiginous melanoma—can readily be differentiated by their distinctive development patterns. The majority of melanomas, around 70%, are of the superficial, spreading type. These lesions are often flat in the initial stages but can subsequently become uneven and elevated, averaging 2 cm in diameter and displaying a spectrum of colours, with either notches or indentations at the periphery. Nodular melanoma is distinguished by tumours that are typically blue-black but may occasionally be colourless, and accounts for about 15–30% of all MM cases. Lentigomaligna melanoma is less common, making up around 4–10% of MM diagnoses. It starts as tiny, freckle-like lesions that often reach a diameter of more than 3 cm, are brown and flat, and have prominent border notching (Kallini et al., 2013). Acral lentiginous melanoma, in its advanced stages, is characterised by flat, tan or brown spots with uneven borders and deep brown or black subungual lesions with ulcerations. These cases account for 2–8% of MMs in whites, but a much higher proportion (35–60%) in people of colour.

Even in the early 21st century, MM is still a potentially lethal cancer whose incidence continues to rise, in contrast to the declining prevalence of many other tumour types. Although most patients are diagnosed with localised disease and are treated by surgical removal of the underlying tumour, many people later develop metastases (Huang & Zappasodi, 2022). One clinical management strategy is to monitor sentinel nodes (the first lymph nodes draining a cancerous region) for signs of metastatic disease, usually by biopsy. In breast cancer, for example, these nodes are typically located in the armpit. If the sentinel nodes test negative for cancer, it is unlikely that the disease will have metastasised more widely. If cancerous cells are detected, other lymph nodes are removed to ascertain the extent of spread (Rutgers, 2008).

1.2.2.2 Aetiology of MM

Although UVR exposure increases the chance of developing MM, the exact origins of the disease are largely unknown. Current opinion suggests that various genetic, epigenetic and environmental factors are associated with malignant transformation of melanocytes and act to permit their unchecked proliferation and acquisition of invasiveness, thereby contributing to progressive development of MM (Varamo et al., 2017). Other mechanistic studies have proposed that reactive oxygen species (ROS) and oxidative stress are central to MM pathophysiology (Obrador et al., 2019). Accumulating evidence suggests that melanoma is an oxidative stress-associated disease (Bisevac et al., 2018), and that oxidative stress is involved at all stages of its development (Emanuelli et al., 2022). A systematic review by Cannavò et al. (2019) concluded that melanoma cells appear to be adapted to elevated levels of ROS, and genetic variation of the melanocyte-stimulating hormone receptor (*MC1R*) leading to higher baseline ROS levels has been causally associated with the disease (Rebecca et al., 2020).

1.2.2.3 DNA Damage Induced by UVA

DNA directly absorbs UVB and UVC radiation, causing photochemical formation of cyclobutanepyrimidine dimers (CPDs), pyrimidine (6-4) pyrimidone photoproducts (6-4PPs), and their Dewar valence isomers. However, UVA does not directly induce any significant formation of these photoproducts because DNA is unable to readily absorb in this wavelength range. Rather, UVA promotes photosensitisation of DNA triggered by either singlet oxygen (type II photosensitisation), electron abstraction (type I photosensitisation), or hydroxyl radicals. Therefore, oxidative DNA damage is still expected upon UVA exposure. Pioneering early work by Tyrrell and Webb (1973) reported the induction of CPDs in bacterial DNA by very pure, narrow-band 365 nm UVA, with increased formation of thymine–thymine (TT) CPDs and reduced damage excision relative to 254 nm UVC. The same group reported induction of single-strand breaks (SSBs; i.e., alkali-labile bonds) by UVA in bacterial and phage DNA.

In the 1990s, the availability of new and sensitive methods advanced this field considerably by permitting efficient characterisation of various DNA lesions for the first time. These innovations included the comet assay; commercially available specific antibodies for DNA repair enzymes; HPLC coupled with electrochemical detection (HPLC–ED) to detect 8-oxoguanine (8-oxoG); and subsequently, HPLC coupled with tandem mass spectrometry (HPLC–MS/MS) to additionally characterise and quantify the various bipyrimidine photoproducts. Thus, our understanding of UVA-induced DNA damage was greatly improved. Based on their different substrate specificities, the *Escherichia coli* Fpg and Nth enzymes are now used to reveal oxidation products of purine (mainly 8-oxoG) and pyrimidine bases, respectively, and the Nfo (Endo IV) nuclease reveals abasic sites. Yousefzadeh et al. (2021) recently showed that UVA radiation induces SSBs, oxidised pyrimidines and oxidised purines in mammalian cells, with the most abundant oxidative DNA damage being 8-oxoG. Using sensitive methods, UVA-induced CPDs have also been detected in mammalian cells, including in human skin. These photoproducts are produced around 100-fold less efficiently by UVA than by 254 nm UVC, and in agreement with the original studies in bacteria, the distribution of UVA-induced CPDs differed drastically from that produced by exposure to UVC, UVB, or simulated sunlight (SSL). In contrast, 6-4PPs were barely detected using specific antibodies. Furthermore, UVA induces CPDs predominantly at TT sites with little formation of CC dimers. Analysis using HPLC-MS/MS supported the prevalence of TT over CT and TC CPDs, whereas CC CPDs and 6-4PPs were similarly undetected. The relative extent of formation of CPDs, 8-oxoG, oxidised pyrimidines and SSBs is 10:3:1:1, meaning that interestingly, CPDs are the major lesions induced by UVA in mammalian and human cells (Girard et al., 2011).

1.2.2.4 Epidemiology of MM

The worldwide increase in MM incidence represents a critical socioeconomic problem. While it was a rare cancer a century ago, the average lifetime risk has reached 1 in 50 in many Western populations (Grau-Pérez et al., 2022). MM now stands as one of the most common malignancies in fair-skinned groups due to an ongoing increase in its prevalence in Caucasian populations that began in the 1960s (Bai et al., 2022). In the United States, the incidence of MM grew by 270% between 1973 and 2002, making it the fifth most prevalent cancer in males and the sixth in females, such that the disease will now affect 1 in 63 Americans at some point in their lifetime (Rastrelli et al., 2014). The Surveillance, Epidemiology, and End Result Program (SEER) of the United States has estimated that there are 793,283 people currently alive in the country with a history of invasive melanoma (385,054 men and 408,229 women) (Rigel, 2010).

According to data gathered between 1998 and 2002, MacKie et al. (2009) found that Queensland, Australia had the highest documented occurrence of melanoma in the world, with an incidence of 55.8 and 41.1 per 10,000 population per annum for males and females, respectively. A high prevalence of the disease was also recorded in New Zealand ($34.8/10^5$ per annum for men and $31.4/10^5$ per annum for women). In Europe, the highest reported incidence was in Switzerland, followed next by the Scandinavian countries (Norway, Sweden and Denmark). Compared with data from the Baltic states of Latvia, Lithuania, Estonia, Belarus and Serbia, occurrence rates in Europe were greater in the more developed nations. However, recent data also show an increasing incidence in several Eastern European nations.

Mediterranean populations are thought to be at minimal risk of developing MM, but Italy has an incidence of 5–7 per 100,000 population per year (i.e., $50–70/10^5$ per annum). Given that this information is from a later report than the MacKie et al. (2009) paper referred to above, it suggests a gradient in disease occurrence across Europe, with the northern countries having the highest rates of MM and the southern nations having the lowest. One plausible explanation is the improved UV protection experienced by persons with more highly pigmented skin, such as those who reside in Southern Europe, but it is also due to the sun's unusual pattern in the region (chronic rather than intermittent) (Rastrelli et al., 2014).

1.2.2.5 Diagnostic Criteria for MM

Diagnosis of MM is facilitated by the "ABCD" identification method originally described by Friedman et al. (1985). Four clinical characteristics were initially assessed for systematic identification of the disease: Asymmetry, Border irregularity, Colour variegation, and a Diameter above 6 mm. It was later recognised that morphological change over time can also be considered in early or in situ melanomas that lack the features of "ABCD" (Hazen et al., 1999), and as a result, the acronym was later expanded to "ABCDE" to include Evolving (Abbasi et al., 2004).

Proper initial staging of MM is based on clinical assessment and histological confirmation. Once the suspect lesion has been histologically confirmed, additional characteristics that contribute to the tumour stage include overall tumour thickness, the presence of ulceration, and the presence of mitosis in lesions below 1 mm in thickness (Rastrelli et al., 2014). The American Joint Committee on Cancer's tumour–node–metastasis (TNM) staging system is used based on the clinical and pathological features. The earliest stage is stage 0 (melanoma in situ), then the scale ranges from stages I (1) to IV (4). Some stages are further subdivided, as denoted by suffixed capital letters (A and B). As a rule, the more advanced the stage (i.e., the higher the number), the more the cancer has spread.

Diagnosis mainly relies on biopsy of the suspicious lesion. Recently, novel approaches based on lymphoscintigraphic imaging have been explored to predict metastatic involvement of the sentinel lymph node (SLN). The most commonly used radiotracers are ^{99m}Tc-labelled colloids, but newer options such as ^{99m}Tc-Tilmanocept may offer superior performance. Alternatively, single photon emission computed tomography/computerised tomography (SPECT/CT) is now becoming a routine diagnostic technique in oncology, and substantial evidence supports its superior diagnostic efficacy over lypmhoscintigraphy to detect metastatic SLN involvement in MM. Researchers are also looking into new hybrid techniques that combine functional and anatomical imaging to visualise the SLN, but additional validation is still needed to establish their utility (Quartuccio et al., 2020).

1.2.2.6 Pathophysiology of MM

As discussed above, MM may develop in or near a previously existing precursor lesion. The disease may also occur in healthy-looking skin, in which case solar irradiation exposure is often the cause. Unexposed areas of the skin (e.g., palms, soles and perineum) can also be affected, and certain types of lesions are considered to be precursor lesions for MM (e.g., common acquired nevus, dysplastic nevus, congenital nevus, and cellular blue nevus). Initial radial growth of the malignant cells most often progresses to the vertical growth phase, wherein they invade the dermis and acquire metastatic capability.

Clinically, MM lesions are classified according to their depth: thin (<1 mm), moderate (1–4 mm), or thick (>4 mm) (Heistein et al., 2022). As introduced above, the four major types of MM are categorised according to their growth pattern. Superficial spreading melanoma is the most common form, constituting around 70% of cases. These lesions are usually flat (but may become irregular and elevated in later stages), with an average diameter of 2 cm along with variegated colours and peripheral notches, indentations, or sometimes both of these features (Trindade et al., 2021). Nodular melanomas (approximately 15–30% of MM diagnoses) are typically blue-black but may sometimes lack pigment. Lentigomaligna melanomas (4–10% of cases) are often larger than 3 cm, flat and tan, with marked notching of the borders. They begin as small, freckle-like lesions. Acral lentiginous melanoma accounts for only 2–8% of MM in whites but 35–60% in dark-skinned people. These lesions can appear on the palms and soles as flat, tan or brown stains with irregular borders. Subungual lesions can be brown or black with ulcerations in later stages (Goydos & Shoen, 2016).

1.2.2.7 Current Treatments for MM

Many treatment modalities are available for MM, including surgical excision, chemotherapy, photodynamic therapy, immunotherapy and targeted therapy. Surgery is the gold standard for early-stage MM, and pharmaceutical intervention is usually reserved for adjuvant treatment of highly locally advanced or metastatic disease (Lens & Eisen, 2003). However, it is important to note that in most cases, none of the available treatments will achieve an absolute cure, and metastatic disease can develop even if a localised MM is surgically removed. The five-year survival rate is 98.3% for localised MM, but this drops to 16% for metastatic disease, indicating that clinical management of advanced MM remains challenging (Villani et al., 2022).

Historically, treatment relied on various chemotherapeutic agents, with little evidence for efficacy. The only FDA-approved general chemotherapy drug for advanced MM is dacarbazine, which has been in use since the 1970s, although the response rate is low (20%) and the median response duration is less than six months (Lacy et al., 2012). Other chemotherapy drugs have shown poor responses and significant side effects. Newer targeted therapies were developed for advanced MM, which can benefit patients with mutations in certain genes (*BRAF*, *NRAS* and *NF1*), although not all cases respond to treatment, and secondary resistance can develop (Davis et al., 2019; Jenkins & Fisher, 2021). Recently, immune checkpoint blockade (e.g., anti-PD-L1 therapy) has improved the outlook further, but this ultimately only benefits around half of patients (Huang & Zappasodi, 2022). Some combinations of the aforementioned treatments have also been investigated clinically, with response rates typically ranging from 50–70%, although serious side effects are encountered in some cases (Jenkins & Fisher, 2021). Other clinical studies have shown that hyperthermia, or 'heat shock', can enhance the treatment effect on MM (Falk & Issels, 2001).

Taken together, the current situation illustrates the need for new, more broadly applicable MM treatments with improved clinical safety. Development of new therapeutic options for MM therefore remains an active research area, and this is the context of the current study, which is focused on two potential treatment modalities with promising safety profiles; i.e., selenium (Se) and cord blood stem cell (CBSC)-derived exosomes.

Elsewhere, Liu et al. (2018b) designed a novel system combining chemotherapy with sonodynamic therapy (SDT), which targets tumours using ultrasound. They constructed a redox/enzyme/ultrasound-responsive, chondroitin sulfate–chlorin e6–lipoic acid self-assembling nanoplatform loaded with docetaxel, for antiproliferative and antimetastatic treatment of melanoma. Safety and efficacy were demonstrated in tumour-bearing mice, offering proof-of-principle that these intelligent, multifunctional nanomaterials might pave the way for more effective cancer therapies in the future. In a separate study, the same group synthesised redox/enzyme-responsive chondroitin sulfate–ss–deoxycholic acid (CSCD) nanoparticles, using cystamine as linker, which were capable of self-assembly in an aqueous environment. When loaded with docetaxel, these nanoparticles showed antitumour efficacy in mice with a favourable pharmacokinetic profile and low toxicity, identifying them as a promising drug delivery system for successful management of melanoma (Liu et al., 2018a).

Recently, monoclonal therapeutic antibodies and cancer vaccines have also shown significant potential for MM treatment. Furthermore, mesenchymal stem cell (MSC)-derived exosomes—which have been used in many genetic conditions, albeit with variable responses—have also been investigated in several studies for their utility in treating melanoma (Karimi et al., 2022). Alternatively, stem cell-derived exosomes are known to influence the pro-metastatic behaviour of melanoma cells by modulating intracellular pathways activated by both oncogenes and noncoding RNAs (ncRNAs). For example, overexpression of miRNA-222 in melanoma cells drives tumorigenesis by repressing *CDKN1B* (p27) and *FOS* (c-Fos) gene expression. This capability can be efficiently transferred to recipient cells by exosomes, activating the PI3K/AKT pathway required for enhanced MM cell proliferation (Felicetti et al., 2016).

Cancer-related exosomes are produced by cancer cells, cancer stem cells (CSCs) and tumour microenvironment associated cells, and their contents span many molecular categories including proteins, DNA, mRNAs, miRNAs, lncRNAs and circRNAs. These vesicles can promote neo-angiogenesis and the ability of cancer cells to invade proximal and distant tissues, with such activities seemingly regulated by immunomodulatory and pro-angiogenic cargo molecules including interleukin (IL)-6, vascular endothelial growth factor (VEGF), and in particular, matrix metalloproteinases (MMPs) (Tucci et al., 2018). Remodelling of the extracellular matrix (ECM) by MMPs is essential for tumour cell invasion and metastasis, because focal degradation of the ECM is the first step in this process.

The SLNs are the first lymph nodes to receive drainage from a primary tumour, and are therefore the most likely to contain cancerous cells if MM has spread. Sentinel lymph node biopsy (SLNB) is consequently indicated in patients with melanoma (stages T1b–T4) without clinically evident locoregional or distant metastases, once excision of the primary lesion with a narrow margin has been performed (Wong et al. 2018). The rationale for identifying (and potentially removing) the first node in the lymphatic chain draining the primary tumour lies in the low probability of subsequent metastatic nodes, if histological examination of the SLN is negative. Relatedly, if required, SLN removal avoids the side effects of complete lymph node dissection (CLND), and prospective trials have nevertheless failed to demonstrate a survival improvement for MM patients undergoing CLND. This procedure should, therefore, be preferentially reserved for cases with positive SLN histopathology (Moncayo et al., 2020).

1.3 The Cell Cycle and its Checkpoints

The cell cycle is a complex process that regulates cellular proliferation and growth, and concludes with division of a parent cell into two daughter cells. It consists of five different phases: G0 (quiescent or resting phase), G1 (gap 1 or prereplicative phase), S (synthesis or DNA replication phase), G2 (gap 2 or growth 2 phase) and M (mitosis). The entire process is tightly controlled, regulated by a variety of factors including the cyclin, cyclin dependent kinase (CDK), and CDK inhibitor protein families. Importantly, the cell cycle includes a number of checkpoints, or decision windows, that determine progression to the next phase, with the most important being the G1/S and G2/M checkpoints (Barnum & O’Connell, 2014; Matthews et al., 2021). These checkpoints protect against DNA damage or other cellular defects to ensure the integrity of cellular function and replication.

Disruption of the cell cycle can result in unrestrained cellular growth, potentially leading to cancer, and many cancer-associated mutations affect cell cycle-related genes. Neoplastic changes can result from genetic damage, for example due to UVA overexposure, which affects protein function and causes dysregulation of the cell cycle or its checkpoints. It has long been known that inactivation of cell cycle checkpoints is a common feature in cancer, particularly for the G1/S transition where cells commit to replication (Molinari, 2000). For example, the retinoblastoma protein (formally, retinoblastoma transcriptional corepressor 1) is a CDK4/6 substrate that plays a role in S phase entry. Mutations in this protein have been found in multiple cancer types, including most cases of retinoblastoma (Yan et al., 2022). Another important class of cell cycle regulatory genes is the tumour suppressor genes, which normally act to restrain cellular growth, promote DNA damage repair, and activate cell cycle checkpoints (Lee & Muller, 2010). Sometimes referred to as anti-oncogenes, they mainly regulate the proliferation of healthy cells, and mutations in these genes are often associated with cancer (Wang et al., 2018). Important examples include *BRCA1* and *BRCA2*—where germline mutations are associated with increased risk of breast or ovarian cancer in women, and breast and prostate cancer in men—and *TP53*, which is inactivated in more than 50% of human cancers (Lee et al., 2014). Cancer can also be caused by other oncogenes, which are mutated forms of proto-oncogenes (i.e., the normal, fully functional forms), and have the potential to drive malignant transformation. One notable example is *HER2*/*ERBB2*, which is amplified in 25–30% of human breast cancers (Cui et al., 2019).

1.3.1 Role of the Cell Cycle Proteins p53 and p21 in MM

Tumour suppressor p53 is a 393-amino acid phosphoprotein that functions as a transcription factor to regulate cell cycle arrest, apoptosis, DNA repair and senescence in response to cellular stresses, including oncogene activation (Lee et al., 2014). In particular, p53 has a major role in activating the G1/S cell cycle checkpoint, thereby preventing replication of damaged cells, by upregulating expression of its downstream target *CDKN1A* (p21) (Brown et al., 2007). Functionally, p21 binds directly to CDKs to inhibit their activity and prevent cell cycle progression. This in turn facilitates DNA repair, which is also co-ordinated by p53 (Williams & Schumacher, 2016). Later in the cell cycle, p53 is also involved in control of the G2/M checkpoint (Chung & Bunz, 2010).

Although p53 is not often mutated in MM, its activity is compromised in the vast majority of cases (Box et al., 2014), which is important given its role in co-ordinating cellular responses to UVR-induced DNA damage (Loureiro et al., 2020). Thus, treatments that can reactivate p53 have been proposed as a possible therapeutic approach in MM. While p21 is important in cell cycle regulation, as mentioned above, it is also known to be overexpressed in some melanomas, where it acts as tumour-promoting factor through inhibition of apoptosis (Šestáková et al., 2010). This apparent paradox was explained in terms of the transcription factor activity of p21, which is distinct from its CDK-inhibitory function, and suggests that therapies capable of downregulating p21 may benefit at least a subset of MM patients.

1.3.2 S100 Family Proteins in MM

The S100 family of calcium-binding proteins consists of 24 members with both intracellular and extracellular functions. Among other roles, these factors are involved in cellular proliferation, apoptosis and migration (Donato et al., 2013). Overexpression of S100 proteins in melanoma is well known, and appears to be strongest for S100A1, S100A13 and S100B (Xiong et al., 2019). Among these proteins, S100B is used as a prognostic biomarker of MM in current Swiss and German guidelines (Revythis et al., 2021), although the evidence in support of this is limited. Other family members, such as S100A2, are highly expressed in primary but not metastatic disease. Interestingly, the S100 proteins S100A1, S100A2, S100A4 and S100B are all known to interact with p53 to modulate its activity (van Dieck et al., 2010), suggesting one possible underlying mechanism for the reduced p53 activity that is generally observed in MM (independent of *TP53* mutations), as noted above.

1.3.3 Mechanism of Apoptosis and Associated Genes

Apoptosis is a form of programmed cell death which is considered fundamental for maintenance of genome stability and normal cellular turnover. Impaired apoptotic function may promote dysregulated cell proliferation, tumorigenesis and cancer progression, and in addition, this pathway may either increase or decrease the sensitivity of malignant cells to chemotherapeutic drugs, depending on the mode of action (Hall et al., 2009; Gottesman et al., 2016). Thus, it is important to consider apoptosis when developing potential new treatments. The process is mediated by the caspase family of effector proteins (including caspase-3) via two distinct pathways: intrinsic and extrinsic apoptosis (Fulda & Debatin, 2006).

The intrinsic (mitochondrial) pathway is regulated by BH3-only proteins—such as the Bcl-2 family of pro-survival factors and the pro-apoptotic Bax protein—to control mitochondrial membrane permeability and the release of various apoptosis factors (including caspase-3). The extrinsic pathway is monitored by two different mechanisms: (i) binding of tumour necrosis factor-related apoptosis-inducing ligand (TRAIL) to the DR4 and DR5 cytoplasmic death domains; and (ii) binding of Fas ligand (FasL) to DR2; in either case leading to activation of caspase-8 (Cavalcante et al., 2019). The balance between pro- and anti-apoptotic genes mediated by p53 ultimately determines the fate of a cell, and the loss-of-function *TP53* mutations commonly found in cancer are associated with elevated anti-apoptotic and reduced pro-apoptotic signalling (Lee et al., 2014). Given the low p53 activity in most MM cases, modulation of apoptotic signalling may be an important consideration when investigating potential new treatments for the disease.

1.3.4 Role of the Apoptosis Proteins Caspase-3 and Bcl-2 in MM

Caspase-3 is activated downstream of p53 signalling (Hussein et al., 2003), hinting that impaired apoptosis may be a molecular feature of MM, although other findings suggest a more complex picture. Using patient samples, Liu et al. (2013) demonstrated that caspase-3 is expressed in non-apoptotic melanoma cells and is associated with metastasis. Consistent with this, knockdown or inhibition of caspase-3 reduced migration and invasion in MM cells. In another study, the caspase-3 released by irradiated melanoma cells undergoing apoptosis was found to promote the growth of surrounding live cells via an apparent paracrine signalling mechanism, and these results were confirmed *in vivo* (Donato et al., 2014). The observed effect was attenuated on knockdown of caspase-3. In contrast, early work on Bcl-2 suggested that this protein is downregulated in MM compared with healthy melanocytes (Hussein et al., 2013). The current evidence is more mixed. Higher levels have been associated with decreased survival, and cellular studies have suggested that Bcl-2 overexpression might enhance metastatic potential in MM (Trisciuoglio & Del Bufalo, 2021). Given the apparent association of both caspase-3 and Bcl-2 with metastatic MM, it seems important to investigate their roles in the disease further, and to establish the modulating effect of proposed new treatments on apoptosis pathways.

1.4 Umbilical Cord Blood Stem Cell (CBSC)-Derived Exosomes

MSCs are multipotent progenitor cells that can differentiate into multiple cell types depending on their location. They are found in many tissues, particularly in bone marrow, adipose tissue and cord blood. In this study, our focus is on exosomes derived from umbilical cord blood (UCB) MSCs. Stem cells have a diverse secretome containing extracellular vesicles (EVs), microvesicles, soluble proteins, lipids and nucleic acids. Among these, EVs play crucial roles in intercellular communication and are now recognised as a cornerstone of stem cell function, despite the fact that they were initially regarded as merely excretory vesicles. Exosomes are the smallest (50–100 nm) of the three EV classes, with the others being microvesicles (100–1,000 nm) and apoptotic bodies (50–4,000 nm). The stem cell populations in bone marrow and UCB contain both MSCs and hematopoietic stem cells (HSCs) (Dixit & Katare, 2015; Zhao et al., 2018; Colicchia et al., 2019; D'Arrigo et al., 2019), and recent research has revealed that exosomes are essential for the immunomodulatory action of MSCs (Gupta et al., 2020).

Exosomes are constitutively derived from late endosomes, which are formed by inward budding of the limited multivesicular body (MVB) membrane. Invagination of late endosomal membranes results in formation of intraluminal vesicles (ILVs) within large MVBs (Colicchia et al., 2019). Exosome-producing immune cells of the innate and adaptive immune systems have been discussed at length in the systematic review by Wang et al. (2010). Through this form of intracellular communication, immune cells such T lymphocytes, B lymphocytes, natural killer (NK) cells, dendritic cells and macrophages can be activated, differentiated and propagated. While these processes are usually beneficial, dysregulation may result in tumorigenesis, autoimmune diseases, or graft versus host disease. For example, the role of exosomes in multiple myeloma, a currently incurable type of blood cancer, has recently been reviewed by Zhou et al. (2018). Certain chemokines and cytokines can promote tumorigenicity by suppressing apoptosis (Moloudizargari et al., 2019). Similarly, some microRNAs play a role in the spread of multiple myeloma, and differential expression of certain microRNAs has also been explored as a potential predictive, diagnostic or prognostic approach in melanoma (Varamo et al., 2017).

1.4.1 Structure of CBSC-Derived Exosomes

The main constituents of exosomes are proteins and lipids (**Figure 4**), with the exact nature of these components depending on the originating cell type. Exosomes can contain complex proteomes, as illustrated by a representative recent study that identified nearly 10,000 individual proteins in exosomes using mass spectrometry (Muthu et al., 2021). Most of these are cargo proteins, which are the basis for intercellular communication.

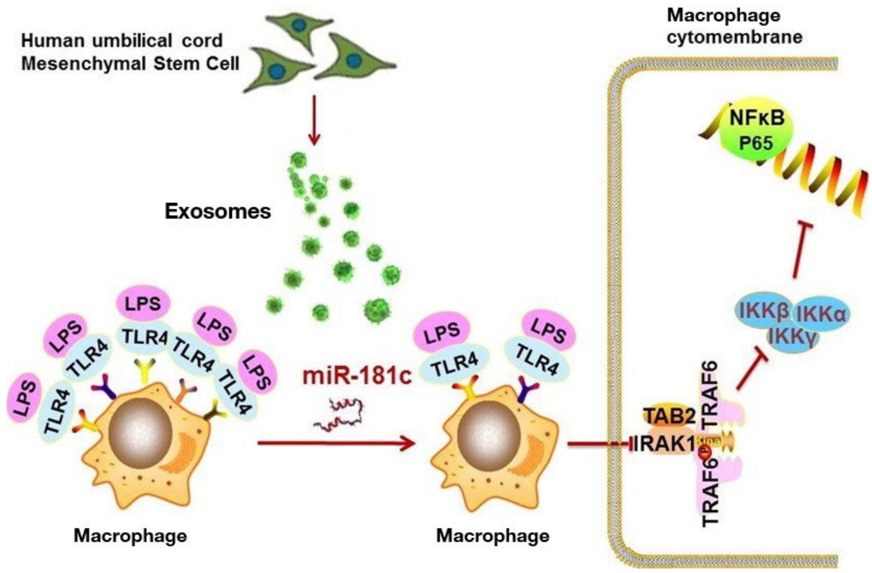

Figure 4. Exosomes derived from human umbilical cord MSCs and their function. Toll-like receptor 4 (TLR4) is a type I transmembrane glycoprotein that recognises pathogen- and damage-associated molecular patterns. TLR4 is part of the receptor complex that binds lipopolysaccharide (LPS) from the Gram-negative bacterial cell wall, and endogenous ligands. Upon stimulation, TLR4 activates the IKK complex, where IKK-α and IKK-β are the two catalytic subunits, and two additional molecules, IKK-γ/NEMO and IKAP, have also been described as integral members. Macrophages are a class of phagocytic white blood cells that kill microorganisms, remove dead cells, and stimulate other immune system cells (Li et al., 2016).

The major protein constituents of exosomes are fusion proteins, transport proteins (annexins and flotillins), heat shock protein (HSP)-70, cluster differentiation proteins (CD9, CD81), phospholipases, and various lipid-associated proteins. Exosomal RNAs (usually microRNAs and mRNAs) also function primarily as cargo molecules, and the same report mentioned above found approximately 2,800 microRNAs and 3,400 mRNAs in the exosomes studied (Muthu et al., 2021). Exosomes also contain diverse lipids, which are essential components of their membrane. It is estimated that over 1,000 different types of lipid can be found in exosomes, and it is also well known that certain lipids are enriched in exosomes compared with their parent cells.

1.4.2 Mechanism of Action of CBSC-Derived Exosomes

To determine the molecular mechanisms underlying immune modulation by CBSCs, the action of exosomes released from these cells was recently explored by Hu et al. (2020). The authors isolated exosomes from CBSC cultures using ultracentrifugation, and confirmed their identity using different markers. Activated T cells and purified monocytes from peripheral blood mononuclear cells (PBMCs) were treated with CBSCs in the presence or absence of the purified exosomes, followed by functional and flow cytometric analysis of phenotypic changes using various immune cell markers. The results showed that CBSC-derived exosomes exert multiple immunomodulatory effects, primarily on monocytes, and could be useful for treating autoimmune diseases (Hu et al., 2020). The CBSC-derived exosomes were quickly bound by monocytes, within 2–3 h. Thus, treating the patient's immune cells with CBSC-derived exosomes allows transport of the latter into the body for cancer treatment, promoting additional type 2 macrophage (M2) differentiation and tolerance induction.

These observations have other implications. Conversion of isolated monocytes into M2 macrophages using CBSC-derived exosomes offers new insights into the molecular pathways that underlie the immunological education and induction of immune tolerance seen in cancer immunotherapy. Furthermore, the multiple immunomodulatory effects of CBSC-derived exosomes on monocytes may enable them to contribute to immune education in clinical treatment of autoimmune diseases. Through their immunoregulatory properties, CBSC-derived exosomes also have the potential to completely transform the way that cancer is treated (Hu et al., 2020).

Exosomes are known to be important in the clinical pathology of MM, particularly in metastatic disease. Among other mechanisms, melanosomes activate cancer-associated fibroblasts (CAFs) through aberrant production and transfer of microRNAs (miRNA-149, -211, -23, -let7a and -let7b) that activate the ErbB/EGFR receptors upstream of MAPK signalling (e.g., García-Silva & Peinado, 2016), in contrast to exosomes, which uniquely stimulate the Wnt pathway. Exosomes enriched in miRNA-let7a, miRNA-let7i, miRNA-191 and miRNA-222 promote tumour growth and invasiveness while also being able to impair immune system activity, leading to defective maturation of dendritic cells, impaired cytotoxicity of T cells, and the expansion of suppressive populations including regulatory T cells (Tregs) and myeloid-derived suppressor cells (MDSCs). Through overproduction of various microRNAs (miRNA-149, -211, -23, -let7a and -let7b), MM cells similarly stimulate collagen-associated fibroblasts of the dermis to promote increased proliferation of cancerous cells.

In addition, exosome-induced upregulation of the endocytic receptor CD169/SIGLEC1 is a key step in the recruitment of MM cells to lymph nodes (Tucci et al., 2018), whose colonisation by metastatic cells is also favoured by α5-integrins, hypoxia-inducible factor (HIF)-1α, and tumour necrosis factor (TNF). Furthermore, MET-expressing exosomes drive specific organotropism that results in mobilisation of bone marrow-derived progenitor cells (BMDCs), which have been implicated in neo-vasculogenesis and pre-metastatic niche formation. Finally, in another potential application of exosomes, the combination of Se and CBSC-derived exosomes might prove beneficial to promote cell growth and migration of human dermal fibroblasts for wound regeneration. These properties were more enhanced with Se-stimulated, CBSC-derived exosomes than with Se or CBSC-derived exosomes, thereby further promoting wound healing *in vivo* (Heo, 2022).

1.5 Selenium and its Roles in Biology and Cancer

The biological trace element selenium was discovered by Swedish chemist Jons Jakob Berzelius in 1817, although its importance in biology and human health did not come into view until the latter part of the 20^{th} century. Its functional roles are now well-studied in many systems of the body, including the endocrine, reproductive and immune systems. Mechanistically, Se is involved in cellular proliferation, apoptosis, and control of cell signalling cascades and transcriptional regulation. The most important bioactive metabolites are hydrogen selenide (H_2Se) and selenic acid (H_2SeO_4). Selenium is directly incorporated into proteins as selenocysteine—the "21^{st} amino acid"—at defined sites through co-translational UGA recoding mediated by a selenocysteine insertion sequence (SECIS) in the 3′-UTR of mRNAs. There are around 30 selenium-containing proteins, usually referred to as selenoproteins, which have variable function and tissue distribution (Avery & Hoffmann, 2018). For example, during thyroid hormone synthesis, the selenoproteins GPX1, GPX3 and TR1 are upregulated and confer thyroid cells with significant protection from peroxidative damage (Beckett & Arthur, 2005). In the reproductive system, Se is essential for spermatogenesis, mammalian fertility, and reproduction (Qazi et al., 2019).

Of the most relevance to cancer, Se has an essential role in human immunity (Cassidy et al., 2013). Most of the known selenoproteins are involved in immunological function in humans, and this especially includes the immune response against malignancies. As mentioned above, Se influences cellular proliferation and programmed cell death, and this applies in both health and disease. In addition to immune responses, it is also involved in multiple other cellular processes such as DNA damage reduction, oxidative stress, inflammation, detoxification of carcinogens, changes in DNA methylation, cell cycle regulation, and inhibition of angiogenesis.

Conversely, Se deficiency adversely affects immune cell activation, differentiation, and proliferation (Huang et al., 2012). The role of Se in the immune system therefore has broad implications for human disease treatment and prevention. There are many existing animal studies on Se deficiency, supplementation and toxicity. In humans, preclinical and clinical studies of Se deficiency and supplementation have demonstrated similar effects. The most common dietary source of Se for humans is selenomethionine, which is a popular and widely available nutritional supplement.

In the immune system, individual selenoproteins are involved in immunity and inflammation, and Se supplementation produces immunostimulatory effects. In immune cells, Se and selenoproteins are related to redox signalling, oxidative burst behaviour, calcium flux, and subsequent effector functions (Huang et al., 2012). Other relevant mechanisms following Se supplementation include T cell proliferation, exaggerated NK cell activity, increased innate immune cell function and augmented cytokine production. In the case of Se inadequacy, supplementation will improve T cell proliferation and exert other effects on immune function, with some inflammatory and immune aspects being particularly affected. In some cases, sexually dimorphic trends can be seen for different Se levels. It has additionally been observed that Se supplementation increases poliovirus vaccine response, and is also able to restore the antioxidant capacity of the lungs in patients with respiratory distress syndrome (Cassidy et al., 2013).

Selenium affects the adaptive immune system through its role in activating T cells and B cells, and promoting their proliferation. Animal studies have investigated low, medium and high Se diets and their relationship to immune function, and have helped establish the importance of adequate Se levels for initiating immunity, and mitigating excessive immune responses and chronic inflammation. On the contrary, Se deficiency adversely impacts immune cell activation, differentiation and proliferation. This is partly due to increased oxidative stress, but other processes may also be impaired in immune cells under Se-deficient conditions, such as protein folding and calcium flux.

The role of Se in cancer risk is currently unclear, however. The proposed anticancer effects of Se are both direct and indirect, given its antioxidant properties as well as its incorporation into selenoproteins. Beginning in the late 1960s, many studies suggested that the higher the level of dietary Se intake, the lower the risk of cancer; and some laboratory studies also found that Se can inhibit cancer cell growth (Miura & Green, 2015). Many epidemiological studies have therefore asked whether higher levels of Se can protect against cancer. Some research has found that greater Se intake correlates with a higher incidence of malignancy, whereas a number of other reports, including meta-analyses, have indicated no such relationship. Recent work has shown that lower levels of Se are associated with a shorter survival duration in melanoma patients (Ravindranathan et al., 2021). Furthermore, Se supplementation was shown to mitigate the neutropenia caused by some cancer treatments, and Se can also shift macrophage polarisation towards antitumour M1 macrophages (Da Silva et al., 2014).

A recent Cochrane review analysed 10 RCTs that investigated the prevention of cancer, or of cancer progression, with Se (Vinceti et al., 2018). Most of the included studies employed Se supplementation in the form of selenomethionine, but selenite (SeO_3^{2-}) was occasionally used. Either way, all 10 trials showed negative results. However, Se did demonstrate a beneficial effect across approximately 70 observational cohort studies with over 60,000 total participants. Here, higher Se exposure was associated with lower cancer incidence and mortality, and these observations held for cancers of the stomach, colon, breast, bladder and prostate. The main disadvantage of cohort studies is that there is no uniformity in study design and interpretation, or the dosage of Se, or other nutritional or lifestyle factors. Furthermore, the dose–response relationship between Se and cancer risk has not yet been studied (Rogoża-Janiszewska et al., 2021).

1.6 Experimental Approaches

1.6.1 Cell Counting Kit-8 (CCK-8)

Currently, the real-time cellular analysis (RTCA) and CCK-8 assays are two of the most sensitive techniques for quantitatively evaluating cell viability. Unlike the RTCA, which monitors electrochemical changes around cultured cells and requires specialised equipment, the colourimetric nature of the CCK-8 assay makes it a convenient choice for cell viability experiments. There is no way to directly compare these two approaches since the detection principles are fundamentally different. Nevertheless, it is known that the physicochemical properties of drug formulations (e.g., optical and electrochemical properties) have a close relationship with the quantitative outcome of methodologies used to assess cancer cell cytotoxicity. Such assays are, however, a critical source of quantitative data of therapeutic relevance; namely, in identifying and comparing the efficacy of anticancer drugs (Li et al., 2022).

Cytotoxicity specifically refers to agents that induce cell death (e.g., through apoptosis or necrosis), and is sometimes taken to also include cytostatic agents (i.e., those which arrest mitosis) (Istifli et al., 2019). Either mechanism would result in reduced cell viability of proliferating cancer cells.

As rapid development brought high-throughput technologies to the pharmaceutical industry, an urgent need arose for compatible drug screening and toxicity assays. Although *in vivo* data is necessary for comprehensive preclinical evaluation, *in vitro* cell-based assays are preferred in the early stages of drug discovery. These screening systems utilise various signal types as readouts, and include colourimetric assays, luminogenic assays, electrochemical processes, and cell counting methods. Because of their high sensitivity and ease of use, colourimetric methods such as the CCK-8 assay have been widely used for many years to assess drug cytotoxicity. The CCK-8 assay uses a highly water-soluble tetrazolium salt, allowing for higher detection sensitivity than other tetrazolium salt-based assays. The WST-8 dye [2-(2-methoxy-4-nitrophenyl)-3-(4-nitrophenyl)-5-(2,4-disulfophenyl)-2*H*-tetrazolium, monosodium salt] is reduced by the dehydrogenase activity of live cells to an orange, water-soluble compound (formazan) that is then detected colourimetrically. The amount of formazan dye generated is directly proportional to the number of live cells, and is measured using a microplate reader by recording the optical density (OD) of each test well at 450 nm, allowing for quick evaluation of cell viability. Thus, the CCK-8 assay is a representative endpoint approach with a simple colourimetric readout, although it is only suitable for measurement at a single time point. Care must also be taken to avoid the presence of substances that might interfere with colourimetric detection.

The high sensitivity of the CCK-8 assay relies on a co-reagent, 1-methoxyphenazine methosulfate (1-methoxy-PMS), which acts as an "electron mediator" to couple intracellular dehydrogenase activity to extracellular reduction of the WST-8 dye (in contrast to other formazan-based assays, which require intracellular localisation of the tetrazolium dye). The CCK-8 assay is commercially available as a cell counting kit, and its reliability is well-established. The components are stable at room temperature for up to six months, making it a convenient choice for long-term projects such as this study. The assay is straightforward, quick to perform, and easily amenable to detection of drug cytotoxicity (Huang et al., 2022).

1.6.2 The Comet Assay

In 1984, Ostling and Johanson developed the first method using microgel electrophoresis to identify DNA damage in living cells (**Figure 5**), now known as single-cell gel electrophoresis (SCGE), or more commonly the 'comet assay' due to the appearance of electrophoresed samples (**Figure 6**). The underlying principle is that damaged DNA fragments in the gel, when exposed to an electric current, will be more prone to migrate from the nucleus towards the anode, creating the characteristic comet shape. Several researchers have adapted the original protocol to develop new variations of the comet assay.

Due to its low cost, rapid turnaround time and high sensitivity, the method has become widely used to assess the extent of DNA damage caused by drugs and other chemical, biological or environmental factors. Therefore, the comet assay is useful for assessing genotoxicity, which is a distinct concept from cytotoxicity, and can be defined as a destructive effect on a cell's genetic material that affects its integrity (Shah, 2012), but does not necessarily cause cell death. This effect is sometimes further delineated as either primary genotoxicity (i.e., direct DNA damage, such as that from UVR exposure) or secondary genotoxicity (e.g., from ROS generated during an inflammatory response) (Schins & Knappen, 2006).

The comet assay only requires a small sample input (10,000 cells) for sensitive detection, making it economically attractive and widely applicable across many different research settings (Cordelli et al., 2021). At alkaline pH (>13), anodic electrophoresis produces comet-like features for cells with DNA damage (Lewis & Aitken, 2005; Cordelli et al., 2021). Once the alkalinity has been eliminated, ethidium bromide staining can be used to visualise the DNA. According to Azqueta et al. (2022), DNA structures with longer tails were shown to be more severely deteriorated when viewed by fluorescence microscopy. The comet assay is the most popular technique for evaluating the *in vitro* and *in vivo* genotoxicity of herbal remedies. It has also been applied to assess the degree of genetic harm brought on by various environmental and lifestyle factors, or potentially genotoxic substances, in humans. For example, it was used by Chatterjee & Walker (2017) in their investigation of DNA repair and environmental biomonitoring, including genomic sensitivity to carcinogens (Bajpayee M et al., 2013).

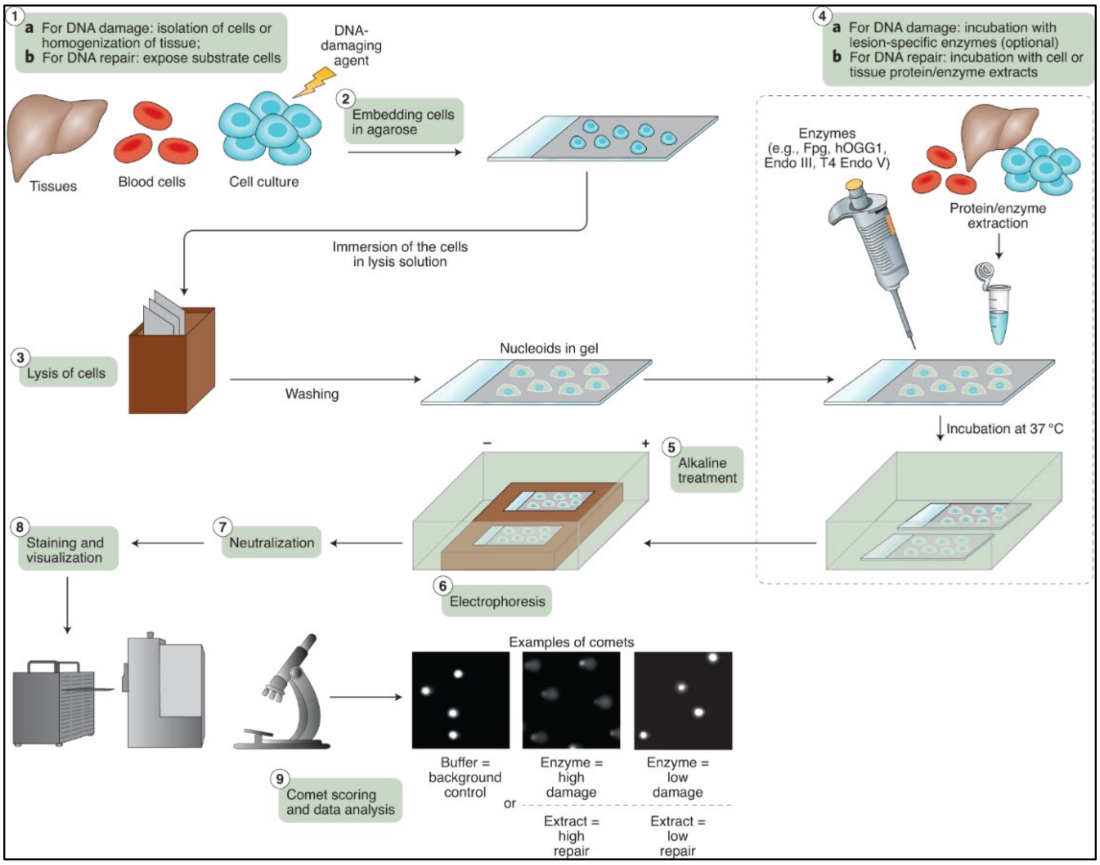

Figure 5. Schematic of the comet assay procedure (Møller et al., 2020).

Since the comet assay is compatible with blood samples and only needs a minimal number of cells, it was chosen for use in this study. Although the technique is versatile, quantitative, easy to perform, and sensitive, appropriate care must be taken to maintain consistent experimental conditions to ensure assay reproducibility. The comet assay can also distinguish between single- and double-stranded DNA breaks at the single-cell level. Electrophoresis can be performed under standard (alkaline) conditions to detect both single-stranded and double-stranded DNA breaks, or under neutral conditions to detect double-stranded breaks only (Dunkenberger et al., 2022).

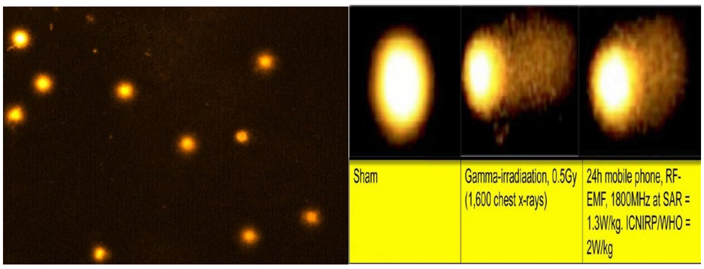

Figure 6. Lymphocytes were analysed using a comet assay, and the cellular DNA was visualised by ethidium bromide staining (Speit et al., 2015).

1.6.3 Reverse Transcription–Quantitative PCR (RT-qPCR)

In biomedical research, changes in gene expression are frequently measured using reverse transcription (RT) coupled with quantitative polymerase chain reaction (qPCR). Total RNA is extracted from cells, then reverse transcribed to complementary DNA (cDNA) to provide a template for PCR. The PCR technique exploits thermostable DNA polymerases to achieve exponential cyclical amplification of double-stranded DNA (dsDNA). It was originally developed by Kary Mullis, who was awarded the Nobel Prize in 1993 for the discovery (Mullis, 1990). DNA polymerases require a primer with a 3′-OH group to initiate replication, which then proceeds via sequential synthesis of a complementary DNA strand to the template, in the 5′ to 3′ direction. In PCR, two primers are designed with opposite directionality, one for each strand of the template DNA, allowing for repeated copying of the intervening region. Thermal cycling is used to achieve the desired amplification of the target region. Each cycle includes a number of steps: denaturation (causing dissociation of dsDNA into its separate strands and releasing any bound primers), annealing (hybridisation of each primer with its target sequence), and primer extension (new DNA synthesis). These steps are typically carried out at 95 °C (denaturation), 45–72 °C (annealing, where the choice of temperature depends on the T_m of the primers), and 68 °C or 72 °C (extension). The qPCR method for measuring gene expression levels (**Figure 7**) was developed shortly after the original discovery of PCR. It was first reported in 1992, meaning that it has now been used for over 30 years (VanGuilder et al., 2008). In this technique, gene-specific primers are designed for the target gene(s) of interest, then PCR is carried out in the presence of SYBR Green, a dye that fluoresces upon binding to DNA. Measurement of fluorescence intensity therefore enables the progress of the reaction (i.e., the quantity of newly synthesised DNA) to be monitored in real time. Various PCR methods based on this principle are widely used for both research and diagnostic purposes.

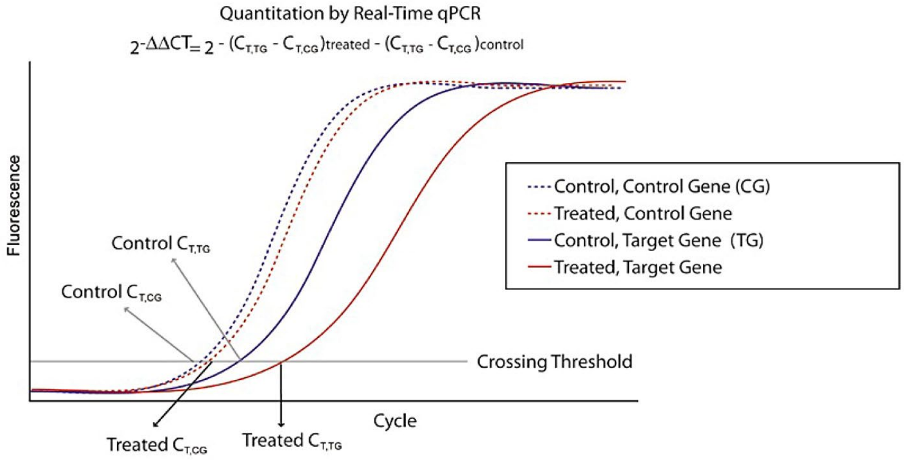

Figure 7. Principle of gene expression quantification using the $2^{-\Delta\Delta CT}$ qPCR method. Expression levels between samples are compared based on the crossing threshold (C_T), the number of PCR cycles required for the SYBR Green fluorescence to exceed an assay-dependent cutoff value (adapted from VanGuilder et al., 2008).

1.6.4 Western Blotting

Western blotting, sometimes referred to as protein immunoblotting, is a standard technique in cell and molecular biology. It has diagnostic and therapeutic applications, in addition to its widespread use in academic research (Pillai-Kastoori et al., 2020). Under optimised conditions, it allows for quantitative analysis of the levels of target protein(s) present in a sample of interest, such as a cell lysate (Mahmood & Yang, 2012). The target proteins are detected and measured from the initial mixture using three key stages (**Figure 8**). First, the proteins in the sample are separated by size and molecular weight using denaturing polyacrylamide gel electrophoresis (SDS–PAGE). Secondly, the proteins are transferred from the gel to a thin membrane in a process known as blotting. In the third and final stage, the membrane is first blocked with a protein solution (e.g., BSA) to cover any nonspecific protein-binding areas. Then, detection and imaging are carried out using a primary antibody that recognises a protein of interest, followed by a secondary antibody modified to permit visualisation of the target protein bands (e.g., through conjugation to an enzyme such as horseradish peroxidase or alkaline phosphatase). In each step, unbound antibody is removed by washing the membrane. Western blotting is a highly sensitive technique, and as little as 1 ng of the target protein can be detected with high specificity.

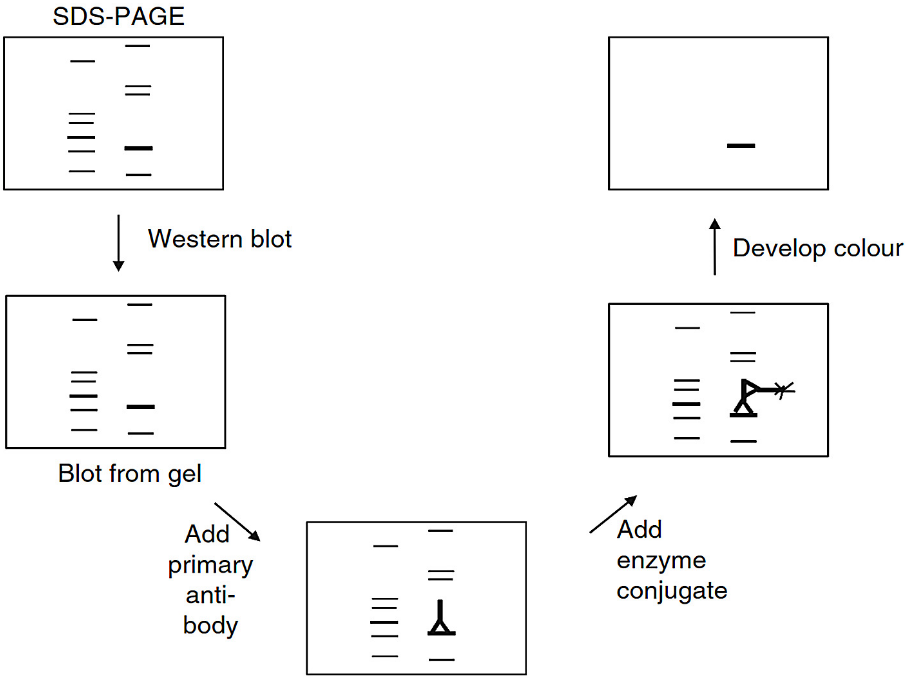

Figure 8. Basic steps in the Western blotting workflow (adapted from Kurien & Scofield, 2006).

1.7 Aims and Objectives

1.7.1 Aims

- Investigate the genotoxicity, and protective effect against oxidative stress, of Se on lymphocytes from MM patients, compared with healthy controls.
- Investigate the same effects for treatment with CBSC-derived exosomes.
- Similarly, assess the genotoxic and protective effects of combined Se and CBSC-derived exosome treatment on lymphocytes from MM patients and healthy controls.
- Measure the genotoxic, cytotoxic and protective effects of Se and CBSC-derived exosomes, separately and in combination, on the CHL-1 melanoma cell line.
- Determine the influence of Se and CBSC-derived exosomes, separately and in combination, on expression levels of cell cycle and apoptosis genes in oxidatively stressed CHL-1 cells.

1.7.2 Objectives

- Use the CCK-8 assay to determine cell viability and cytotoxicity upon Se treatment of oxidatively stressed MM lymphocytes, control lymphocytes and CHL-1 cells.

- Measure the effect of CBSC-derived exosomes, either alone or in combination with Se treatment, in parallel CCK-8 assays using the same cell types.
- In oxidatively stressed CHL-1 cells, use RT-qPCR to determine the expression changes for cell cycle (*TP53*/p53, *CDKN1A*/p21), apoptosis (*BCL2*/Bcl-2, *CASP3*/caspase-3) and *S100B* genes upon treatment with Se, CBSC-derived exosomes, or both.
- Under the same conditions, use Western blotting to assess the effect on expression of these genes at the protein level.
- Based on the results, evaluate the potential of Se and CBSC-derived exosomes for treatment of MM.

2) Materials and Methods

2.1 Materials

2.1.1 Reagents

The list of reagents used in this study is presented in Table 1 below along with the supplier's name and catalogue (or CAS) number.

Table 1. List of chemicals and reagents used in the study along with their CAS/CAT numbers.

Chemical or Reagent	Company or Distributor	Catalogue/CAS Number
Black box	Sigma–Aldrich, UK	Z742411
Bradford Protein Assay Kit 1	Bio-Rad	5000201
Bovine serum albumin	Sigma–Aldrich, UK	9048-46-8
Caspase-3 (*CASP3*) human qPCR primer pair	Origene	HP207674
CHL-1 cells	ATCC	CRL-9446
Cell counting kit-8 (CCK-8)	Sigma–Aldrich, UK	96992
Cover glass	VWR	No. 631
Distilled water (dH_2O)	n/a	n/a
Dimethyl sulfoxide (DMSO)	Sigma –Aldrich, UK	67-68-5
Donkey anti-rabbit IgG H&L	Abcam, UK	ab6802
Dulbecco's Modified Eagle's Medium	Sigma–Aldrich, UK	56436C
Eppendorf tubes (1 mL)	Sigma–Aldrich, UK	n/a
EDTA ($Na_2EDTA.2H_2O$)	Sigma–Aldrich, UK	10378-23-1
Ethidium bromide	Sigma–Aldrich, UK	1239-45-8
Exosomes (CBSC)	Cure Stem, Korea	141942
Ethanol	Sigma–Aldrich, UK	64-17-5
Foetal bovine serum	Sigma–Aldrich, UK	F7524
Falcon tubes	BD, Swindon, UK	N/a
FAST SYBR Green	Sigma–Aldrich, UK	163795-75-3
Anti-GAPDH antibody [EPR16891] – loading control	Abcam	ab181602
Hs_ACTB_1_SG QuantiTect	Qiagen	QT00095431
Hs_BCL-2_1_SG QuantiTect	Qiagen	QT00025011
Hs_CDKN1A-va.1	Qiagen	QT00062090
Lithium heparin tube 9 mL (LH)	Greiner Bio-One, Austria	455084/A1803 3VS
iScript cDNA Synthesis Kit	Bio-Rad, UK	1708890
Lymphoprep	Axis-Shield, Norway	66720-17-0

Chemical or Reagent	Company or Distributor	Catalogue/CAS Number
Low melting point agarose	Invitrogen, UK	39346-81-1
2-Mercaptoethanol	Sigma–Aldrich, UK	60-24-2
Mini gel tank	ThermoFisher Scientific	A25977
Normal melting point agarose	Invitrogen, UK	9012-36-6
Pipette tips	VWR	n/a
Phosphate buffered saline	Sigma–Aldrich, UK	n/a
Protease inhibitor	Sigma–Aldrich, UK	66701-25-5
p53 primer	Qiagen	QT00050785
Recombinant anti-p53	Abcam, UK	ab32049
Recombinant anti-p21	Abcam, UK	ab109520
Recombinant anti-Bcl-2	Abcam, UK	ab32124
Recombinant anti-caspase-3	Abcam, UK	ab32351
S-100 Antibody	Abcam, UK	ab34686
S-100 beta (*S100B*) human qPCR primer pair	Origene	HP209246
Selenium	Sigma–Aldrich, UK	PHR1359
Sodium chloride (NaCl)	Sigma–Aldrich, UK	7647-14-5
Sodium hydroxide (NaOH)	Sigma–Aldrich, UK	1310-73-2
Superfrost microscope slides	ThermoFisher Scientific	10504182
Triton X-100	Sigma–Aldrich, UK	9002-93-1
Trizma base	Sigma–Aldrich, UK	77-86-1
Tween-20	Sigma–Aldrich, UK	9005-64-5
RPMI-1640 medium	Sigma–Aldrich, UK	R8758
RIPA lysis & extraction	ThermoFisher Scientific	88900
Penicillin–streptomycin	Sigma–Aldrich, UK	P4333
QIAamp RNA Blood Mini	Qiagen	52304
Western ECL substrate, 200	Bio-Rad	1705060
20× Bolt MES SDS	ThermoFisher Scientific	B0002
4× Bolt LDS sample	ThermoFisher Scientific	B0007
10× Bolt sample	ThermoFisher Scientific	B0009
96-well plates	VWR	10861-666

2.1.2 Equipment

The list of equipment items and materials used in this study are listed below in Table 2.

Table 2. Equipment used in this project.

Equipment	Company/Distributor
Nitrocellulose blotting membrane	GE Healthcare Life Sciences, Germany
BioDrop Touch Duo Spectrophotometer	BioDrop Ltd, Cambridge, UK
Bolt welcome pack + iBlot 2 system	ThermoFisher Scientific
BRAND filter flask with lateral socket / vacuum glass bottle	Sigma–Aldrich, UK
BRAND staining trough / incubation box with tray	Sigma–Aldrich, UK
Centrifuge Mistral 3000	MSE, Albertville, USA
Centrifuge (Biofuge 28 RS)	Heraeus, Sepatech, Germany
CCD camera	Hitachi KPMI/EK Monochrome
Coplin jar	VWR, Lutterworth, UK
Corning 15 mL centrifuge tubes	Sigma–Aldrich, UK
Corning cell culture flasks (25 cm^2)	Sigma–Aldrich, UK
Culture flasks (25 & 75 cm^3)	Corning Incorporated Costar, NY, USA
Dry incubator (37 °C) LKB BIOCHROM	Leech Ltd, Nottingham, UK
Electrophoresis power supply	Consort (E861), Belgium
Electrophoresis tank (HU20)	Scie-Plas, Renfrewshire, UK
Falcon tubes	BD, Swindon, UK
Freezer −20 °C	Sanyo, Japan
Freezer −80 °C	Sanyo, Japan
Fluorescence microscope	Leica, Weztler, Germany
Fume cupboard	Milton, UK
Fume hood Ray Air	Maiche Aire, Bolton, UK
Ice maker (Scotsman AF 100)	Namur, Belgium
Incubator 37 °C with 5% CO_2	Andor Technology Ltd, Belfast
Light microscope	Nikon, Japan
Komet 6 software	Kinetic Imaging, Nottingham, UK
Microcentrifuge MSE	GMI, Alberville, USA
Microplate reader	Dynex Technology, Sussex, UK
StepOnePlus real-time PCR detector	Applied Biosystems, Warrington UK
Waldmann F15/T8-PUVA tubes	Villingen-Schwennigen, Germany
Water bath	Grant Instruments, Cambridge, UK

2.2 Human Participants and Blood Samples

2.2.1 Ethical Approval

Peripheral blood was collected after informed consent from all patients and healthy individuals.

Whole blood was collected by venepuncture from 20 healthy individuals and 20 patients. Samples were diluted with a 1:1 ratio of RPMI-1640 medium (Sigma–Aldrich) supplemented with 10% DMSO, aliquotted into Eppendorf tubes, then immediately stored at −80 °C until use in the experiments. This study received approval from Leeds East Research Ethics Committee (REC number: 12/YH/0464), the University of Bradford Research Ethics Sub-Committee on Research in Human Subjects (Ref: 0405/8), and the Research Support and Governance Office, Bradford Teaching Hospitals, NHS Foundation (Ref: RE DA 1202).

2.2.2 Volunteer Recruitment

Each volunteer was given a participant information sheet relating to the research, which included two parts. Part 1 showed the participant the purpose of the invitation, the reason for the study, and the consent to give the blood on a voluntary basis. Part 2 provided information about what would happen to participants if they took part in the research, and explained that the study results would not be prognostic for the participants. Details of the patient group are provided in Table 3. Blood samples were not taken from patients who had received chemotherapy or radiotherapy.

Table 3. Details of the MM patients who provided blood samples.

Number	Sample Code	Age	Ethnicity	Gender	Smoking History
1	162-F	53	Caucasian	F	N
2	157-F	68	Caucasian	M	N
3	156-M	42	Caucasian	M	Y
4	144-F	69	Caucasian	M	Y
5	145-F	49	Caucasian	M	Y
6	156-M	58	Caucasian	M	Y
7	190-F	77	Caucasian	M	Y
8	204-F	40	Caucasian	F	N
9	203-F	57	Caucasian	M	Y
10	181-F	52	Caucasian	F	Y
11	182-F	68	Asian	F	Y
12	190-F	66	Asian	M	Y
13	188-M	65	Asian	F	N
14	180-M	63	Asian	M	N
15	189-M	41	Asian	F	N
16	185-M	73	Asian	F	N
17	10624	91	Asian	F	N
18	10622	52	Asian	F	N

Number	Sample Code	Age	Ethnicity	Gender	Smoking History
19	143-F	73	Asian	F	N
20	158-F	58	Asian	M	Y

The healthy student and staff volunteers, over 18 years of age and of various ethnicities, were recruited from within the University of Bradford to take part in this study. Further details on these healthy volunteers are given below in Table 4. The inclusion criteria for these individuals included:

- The willingness to complete the consent form.
- The agreement to store blood samples at the University of Bradford.
- No family history of cancer.
- Preferably non-smokers.

Table 4. Details of the healthy individuals who provided blood samples.

Number	Sample Code	Age	Ethnicity	Gender	Smoking History
1	11958	33	Caucasian	F	N
2	11962	34	Caucasian	M	N
3	11973	20	Caucasian	F	N
4	11974	39	Caucasian	F	N
5	11977	21	Caucasian	M	N
6	11980	20	Caucasian	M	N
7	11981	21	Caucasian	M	N
8	11986	22	Caucasian	M	N
9	11988	21	Caucasian	F	N
10	11983	22	Caucasian	F	N
11	11988	24	Asian	F	N
12	11989	35	Asian	F	N
13	11979	37	Asian	M	N
14	11975	40	Asian	M	N
15	11960	45	Asian	F	N
16	11898	35	Asian	M	N
17	11987	40	Asian	F	N
18	11988	35	Asian	F	N
19	11982	37	Asian	M	N
20	11968	39	Asian	M	N

2.3 Methods

2.3.1 Determination of H_2O_2 Concentration

This step aimed to find the dosage of H_2O_2 that produced the highest level of DNA damage so that it could be used as a positive control (PC) for the comet assays in this study. Four H_2O_2 concentrations were tried: 25 µM, 50 µM, 75 µM and 100 µM. Comet assays were carried out as described below in Section 2.3.6 Comet Assay Protocol, using whole blood samples from healthy subjects. The olive tail moment (OTM) and % tail DNA were assessed to quantify the DNA damage. The experiment was repeated five times and the results were averaged. After statistical analysis, the optimal dose of H_2O_2 (for triggering the maximum amount of DNA damage) was determined to be 75 µM. This dose served as a PC for subsequent comet assays.

2.3.2 Preparation of Selenium Solutions

Stock solutions with different concentrations of Se (10, 25, 50, 75, 100 µM) were prepared. They were combined with 1,000 µL of DMSO and stored in the refrigerator overnight. After 5 min on a heater, the solutions were mixed by vortexing until the Se was completely dissolved.

2.3.3 Cell Viability

Cell viability was determined after incubation with a range of doses of Se (10, 50, 75, 100 µM) for 30 min. Cells were collected by centrifugation at 160 × *g* for 3 min, then 10 µL of cell suspension was combined with an equal volume of 0.4% trypan blue stain and the mixture was allowed to settle for 30 sec. Samples were transferred to the Neubauer haemocytometer for analysis. If the cell membrane is compromised, trypan blue will permeate the membrane to produce a blue colour, which indicates cell death (Phillips, 1973). Therefore, the haemocytometer was used to determine the proportion of cells that rejected the dye. Trypan blue exclusion of this cell demonstrated that the viability of freshly separated lymphocytes from both groups was usually over 75%, and therefore, a cell viability of at least 75% was used in all lymphocyte assays (Henderson et al., 1998).

2.3.4 Cell Counting Kit-8 (CCK-8) Cytotoxicity Assay

Cell viability and cytotoxicity were determined using a colourimetric technique. As appropriate, isolated human lymphocytes from healthy individuals or melanoma patients, or CHL-1 melanoma cells, line distributed into 96-well plates at 5,000 cells/well. The cells were treated with various doses of Se (10, 50, 75, 100 μM) for 24 and 48 h at 37 °C, in a humidified incubator with 5% CO_2. Then, 10 μL of CCK-8 solution was added to each well and the cells were incubated at 37 °C for a further 4 h. Absorbance was measured at a wavelength of 450 nm, using a microplate reader.

2.3.5 Lymphocyte Isolation from Whole Blood

Blood was mixed in a 1:1 ratio with 0.9% normal saline and mixed gently. In a Falcon tube, diluted blood (6 mL) was carefully overlaid onto 3 mL of Lymphoprep, and the sample was transferred to the centrifuge. After centrifugation at room temperature (RT) and 600 × *g* for 20 min, the white layer of lymphocytes was obtained from the top of the Lymphoprep, within the plasma interface of the sample, and washed with saline in a universal tube. Then, the suspension was centrifuged at 375 × *g* for 15 min at RT, and the supernatant was treated with 2% Virkon before being discarded. The pellet was resuspended in 900 μL of foetal bovine serum (FBS), transferred to an Eppendorf tube containing 100 μL of DMSO. The tubes were tightly closed, mixed, then stored overnight at −20 °C before being transferred to a −80 °C freezer for prolonged storage.

2.3.6 Comet Assay Protocol

2.3.6.1 Cell Treatment for the Comet Assay

The frozen whole blood samples were allowed to defrost at ambient temperature. Then, 1,000 μL of RPMI-1640 medium (with $NaHCO_3$, without L-glutamine, sterile-filtered, suitable for cell culture) was added to 100 μL samples of whole blood that had been incubated at 37 °C for 30 min with various test agents. The test agents comprised: 75 μM H_2O_2 (PC), Se (10, 25 and 75 μM), and a combined treatment with 10 μM Se and 75 μM H_2O_2. An untreated sample served as the negative control. Immediately after incubation and adding RPMI-1640 medium, the tubes were centrifuged at 160 × *g* for 3 min, then 900 μL of the supernatant was discarded to leave 100 μL of particulate material in the tube. Next, 100 μL of 0.5% low melting point (LMP) agarose was added and the mixture was resuspended, then 100 μL aliquots of this solution were applied in duplicate to individually labelled slides that had been coated with 1% normal melting point (NMP) agarose. The samples were covered with cover slips and moved to a cold surface for

5 min, ensuring that they remained cool.

2.3.6.2 Cell Lysis

At this stage, the cover slips were removed and the slides were immersed in a black box containing 200 mL of fresh cold lysis solution and kept at 4 °C overnight. The lysis solution was composed of 178 mL lysis stock solution (2.5 M NaCl, 100 mM EDTA, 10 mM Tris, 10% DMSO, 1% Triton X-100, pH 10). This solution has a high salt concentration to break down protein–DNA interactions without damaging the DNA, a detergent (Triton X-100) to disrupt the cell membrane, and a free radical scavenger (DMSO) to neutralise the radicals generated from haemoglobin, to prevent DNA damage (Olive, 2002).

2.3.6.3 DNA Unwinding and Electrophoresis

After cell lysis, the slides were placed into a horizontal electrophoresis tank and incubated in 2,000 mL of freshly prepared alkaline electrophoresis buffer. This solution consisted of 70 mL of buffer concentrate (10 M NaOH, 200 mM EDTA, pH >13) mixed with 1,930 mL of cold distilled water. The samples were incubated for 30 min at 4 °C to facilitate DNA unwinding, then electrophoresis was performed at 25 V, 300 mA (0.78 V/cm for the electrophoresis tank used) for 30 min using a compact power supply. All procedures were conducted at 4 °C.

2.3.6.4 Neutralisation

Sample slides were removed from the electrophoresis buffer and placed horizontally on a flat surface. They were covered with neutralising buffer (0.4 M Tris pH 7.5) for 5 min. This process was repeated three times, to prevent further action of the alkaline buffer.

2.3.6.5 Slide Staining and Comet Scoring

The samples were stained by adding 60 µL of 20 µg/mL ethidium bromide (EtBr) to each slide. The slides were covered with cover slips, in a dark room with dim light, then individually coded and kept in a closed and damp box at 4 °C until scoring. For each slide, 100 nuclei were scored with a fluorescent microscope at 20× magnification in conjunction with a CCD camera, using the Komet 6 software and Kinetic Imaging (Andor Technology Ltd, Belfast). The OTM and % tail DNA were used together to decrease variability in the results (Najafzadeh et al., 2016).

2.3.7 CCK-8 Assay on the CHL-1 Melanoma Cell Line

The same technique was used for the melanoma cells as for the lymphocytes (Section 2.3.4 Cell Counting Kit-8 (CCK-8) Cytotoxicity Assay), with the same dosage of Se. Cytotoxicity readings were taken at 24 and 48 h.

2.3.7.1 Melanoma Cell Line Culture

First, the frozen cells were thawed at 37 °C in a water bath, inside a laminar flow hood to avoid contamination. After thawing, the 1 mL cell suspension was added to 9 mL of complete growth medium: RPMI-1640 supplemented with 1% penicillin–streptomycin and 10% FBS. The suspension was centrifuged for 5 min at 1,000 rpm. The supernatant was discarded and the pellet was resuspended in 2 mL of complete medium. For routine subculture, the cells were seeded into T75 flasks with 15–17 mL of complete medium, and the flasks were maintained in an incubator at 37 °C with 5% CO_2 until the cells reached 80% confluence. At this point, the medium was discarded and the cells were washed twice with 6–7 mL of PBS to remove residual medium and dead cells. Next, 1–2 mL of trypsin solution was added for 3–5 min to detach the cells from the surface the flask. To deactivate the trypsin, 6–9 mL of complete medium was then added. The resultant cell suspension was transferred to a 15 mL Falcon tube and centrifuged at 1,000 rpm for 5 min. After centrifugation, the supernatant was discarded and the pellet was again resuspended in 1 mL of complete medium. For storage of cell aliquots, the supernatant was discarded, then complete growth medium (1 mL) combined with DMSO (200 µL) was added to the cell pellet before freezing.

2.3.8 Comet Assay with Primary Lymphocytes and CHL-1 Cells

After establishing cultures of primary cell lines and CHL-1 cells, test treatments were applied to cells as relevant, and the comet assay was performed to evaluate the effects of the treatment. The procedure was as follows: Cells were distributed into six-well plates at 2.5×10^5 cells/well in 2–3 mL of complete growth medium (as specified above). Plates were incubated at 37 °C with 5% CO_2 until the cells reached confluence. After achieving maximum cell growth, the medium in each well was discarded and replaced with 1 mL of fresh medium, then the treatments were added. If necessary, part of the growth medium was removed according to the volume of the treatments added to each well. Negative and positive controls were used, along with different concentrations of Se.

2.3.9 Cord Blood Stem Cell (CBSC)-Derived Exosome Assays

First, the exosomes were diluted by adding 5 mL of PBS, then 10 μM of the diluted solution was added to 990 μM of DH_2O.

2.3.9.1 CCK-8 Cytotoxicity Assay with Exosome Treatment

Using the identical method as above (Section 2.3.4 Cell Counting Kit-8 (CCK-8) Cytotoxicity Assay), the CCK-8 cytotoxicity assay was performed. The stated exosome concentrations were based on protein concentration, as measured by UV absorbance (A_{280}). Different dosages of exosome therapy (10, 30, 60, 90 and 120 μL) were used initially, to determine the optimal treatment dosage that maintained sufficient viability. The results indicated that the three optimal dosages were 10, 90 and 120 μL.

2.3.9.2 Comet Assay with Exosome Treatment

The comet assay was performed on 20 lymphocyte samples from healthy individuals, 20 lymphocyte samples from melanoma patients, and three melanoma cell lines, using the three most effective dosages of exosome therapy. The test agents comprised a PC (75 μM H_2O_2), and exosomes (10, 90 120 μL) with all dosages co-administered with 75 μM H_2O_2. The comet assay was carried out using the same method described above (Section 2.3.6 Comet Assay Protocol).

2.3.10 Statistical Analysis

The final reported data are expressed as mean values with standard errors, based on 100 cells scored on each slide. In total, 48 comet assays were included in this project: five assays for H_2O_2 at different concentrations, to determine the PC conditions; three assays for the different melanoma cell lines; and 40 patient samples (20 from healthy individuals and 20 from melanoma patients). The results were analysed using one-way analysis of variance (ANOVA) with Dunnett's post hoc multiple comparison test, using GraphPad Prism 9.4.0, which was also used to generate the graphs included in the figures below. Where comparisons between experimental groups were statistically significant ($p < 0.05$), this is indicated on the graphs as follows: * = $p < 0.05$; ** = $p < 0.01$; *** = $p < 0.001$, with 'ns' used to denote 'not significant'.

2.3.11 Combined Treatment Using Selenium and Exosomes

2.3.11.1 CCK-8 Cytotoxicity Assay for Combined Treatment of CHL-1 Cells

The CHL-1 melanoma cell line was tested using combined treatment with exosomes and selenium, done at four different concentrations (90 µM exosomes + 5 µM Se, 120 µL exosomes + 10 µM Se, 90 µL exosomes + 15 µM Se, and 120 µL exosomes + 20 µM Se). Cytotoxicity was determined using the CCK-8 assay using the same method as before (Section 2.3.4 Cell Counting Kit-8 (CCK-8) Cytotoxicity Assay). The PC was 75 µM H_2O_2. Readings were taken at 3 h, 12 h, 24 h and 48 h time points. The results indicated that the optimal dosage for combined treatment was 10 µM Se together with 120 µL exosomes.

2.3.11.2 Comet Assay for Combined Treatment of CHL-1 Cells

Three melanoma cell line samples were treated with 10 µM of Se and 120 µL of exosomes, co-administered with 75 µM H_2O_2. The same method as described above (Sections 2.3.6 Comet Assay Protocol and 2.3.8 Comet Assay with Primary Lymphocytes and CHL-1 Cells) was used to perform comet assays.

2.3.11 Gene Expression Analysis by RT–qPCR

2.3.11.1 Cell Culture and Treatments

The CHL-1 cell line was used for these experiments. Cultures were established from frozen stocks that were in a suspension of 2 × 10^6 cells/mL, prior to being cryopreserved. In this case, the treatment groups were PC (75 µM H_2O_2), 10 µM Se, 120 µL exosomes, and10 µM Se in combination with 120 µL exosome (with 75 µM H_2O_2 co-administered in all cases). The negative control group was left untreated.

2.3.11.1 RNA Isolation from CHL-1 cells

The RNeasy Mini Kit (QIAGEN) was used following the manufacturer's protocol. Cells were transferred to a sterile flow cabinet and centrifuged at 400 × *g* for 3 min. The supernatant was removed and 350 µL of lysis buffer (RLT, supplemented with 10 µL/mL of 2-mercaptoethanol) was added to the pellet, followed by centrifugation for 2 min at high speed. The lysate was then added to a QIAshredder spin column that was already placed in a 2 mL collection tube, and the sample was centrifuged at full speed for another 2 min. The lysate was recovered and the QIAshredder assembly was discarded. Then, 70% ethanol (600 µL) was added to the lysate and mixed well by careful pipetting. The samples, including any precipitate formed, were then transferred into a new QIAamp spin column placed in a 2 mL collection tube, and centrifuged for 15 s at 8,000 × *g*. The column was rinsed by adding 700 µL of RW1 buffer (guanidine salt and ethanol) and centrifuging for 15 s at 8,000 × *g*. The column was placed in a new 2 mL collection tube, then 500 µL of RPE buffer RPE was pipetted into the column. Samples were centrifuged at 8,000 × *g* for 3 min to remove any residual ethanol. Finally, the column was transferred into a 1.5 mL microcentrifuge tube and 50 µL of RNase-free water was added directly onto the QIAamp membrane, followed by centrifugation at 8,000 × *g* for 1 min to elute the RNA. The concentration and purity of the isolated RNA were measured using a NanoDrop 1000 spectrophotometer, with purity judged using the $A_{260/280}$ ratio. The RNA samples were ultimately stored at −80 °C.

2.3.11.2 Complementary DNA Synthesis

The iScript cDNA synthesis kit was used to synthesise complementary DNA (cDNA) from total RNA. This was done by mixing 4 µL of 5 × iScript Reaction Mix with 1 µL of iScript Reverse Transcriptase, 20 µL of nuclease-free water and 1 µL of thawed extracted RNA, in PCR tubes. The reaction mixtures were then transferred to a Bio-Rad PTC-200 Peltier Thermal Cycler (Bio-Rad Laboratories, Inc., USA) and incubated for 5 min at 25 °C, then 20 min at 46 °C, and finally for 1 min at 95 °C, with the samples being additionally held for 10 min at 4 °C. The cDNA samples were then stored at −20 °C until use.

2.3.11.3 Quantitative Real-Time PCR and Analysis

Following cDNA synthesis, the genes of interest were quantified by performing real-time PCR reactions in a 96-well plate (MicroAmp). The assay was conducted in triplicate to minimise variation in the results. Each well contained 10 µL of Fast SYBR Green Master Mix, 2 µL of target gene primers (*TP53*, *CDKN1A*, *BCL2*, *CASP3* or *S100B*), 4 µL of diluted cDNA, and 4 µL of RNA-free water, with care taken to ensure that all components were properly mixed. The plate was sealed using MicroAmp Optical 8-Cap Strips and briefly spun using a plate spinner to remove any bubbles, before being transferred to a StepOnePlus Real-Time PCR Detection System (Applied Biosystems, Warrington, UK). The following settings were used: denaturation at 95 °C for 10 min, followed by 40 cycles of denaturation at 95 °C for 15 s, then annealing and extension at 60 °C for 1 min. The internal housekeeping gene was β-actin (*ACTB*).

The data was analysed using the CFX Manager software to evaluate the expression levels of target genes. The $2^{-\Delta\Delta CT}$ method (Figure 7) was used to represent differences in gene expression in terms of fold change between cells treated with PC (75 µM H_2O_2), 10 µM Se, 120 µL exosomes, and 10 µM Se in combination with 120 µL exosomes. The negative control was left untreated.

2.3.11.4 Statistical Analysis

Each experiment was conducted three times in triplicate, using the same experimental groups, to compare between PC, 10 µM Se, 120 µL exosomes, and 10 µM Se in combination with 120 µL exosomes. Untreated cells were used as a negative control. The results are presented as mean ± SEM. Data analysis was done using GraphPad Prism 9, with two-way ANOVA and multiple comparison tests. Statistically significant p values are indicated as $p < 0.01$ (**), $p < 0.001$ (***), or $p < 0.0001$ (****), respectively.

2.3.12 Western Blot Assay

2.3.12.1 Cell Culture

Three biological replicates of CHL-1 cells, with 1×10^6 cells/well, were cultured in six-well plates in Dulbecco's Modified Eagle's Medium (DMEM) supplemented with 10% FBS and 1% penicillin–streptomycin, under aseptic conditions. Plates were incubated at 37 °C and 5% CO_2 until the cells were fully confluent. The cells were then treated and labelled. The treatment groups comprised a PC (75 µM H_2O_2), 10 µM Se, 120 µL exosomes, and 10 µM Se in combination with 120 µL exosomes. The negative control group was left untreated.

2.3.12.3 Protein Extraction

The cultured cells were recovered by scraping, transferred into Eppendorf tubes, and centrifuged at 400 × *g* for 3 min. The supernatant was removed and the cell pellets were rinsed twice with cold PBS, then resuspended in 100 µL of RIPA buffer with 2 µL of protease inhibitor cocktail. The samples were incubated on ice for 30 min, after which they were sonicated briefly (~5 s), then centrifuged at 16,000 × *g* for 20 min at 4 °C. Next, the supernatant was collected, and 10 µL of the extracted protein solution was taken for protein quantification. The remaining lysate was stored at −80 °C.

2.3.12.4 Protein Quantification

Quantification of total protein was carried out using the Bradford Assay Kit (Bio-Rad). This assay relies on the absorbance shift (colour change) of Coomassie dye, from red to blue, upon protein binding. The blue colour has a maximum absorbance at 595 nm, and the absorbance of the solution at this wavelength is directly proportional to the amount of bound dye, and therefore to the concentration of protein present. A standard curve was constructed using bovine serum albumin (BSA) at various concentrations (0.125, 0.25, 0.5, 0.75, 1.0, 1.5 and 2.0 mg/mL). For all standards and test samples, 10 µL aliquots were added in triplicate into 96-well plates, then 200 µL/well of diluted Bio-Rad dye reagent was added. The absorbance of the BSA standards and test samples was then read at 595 nm using a microplate reader.

2.3.12.5 Sodium Dodecyl Sulfate–Polyacrylamide Gel Electrophoresis (SDS–PAGE)

For resolving and stacking gels, Tris buffer was prepared (with pH 6.8 and pH 8.8, respectively). Catalyst (ammonium persulfate) and tetramethylethylenediamine were also added, along with a calculated amount of acrylamide to ensure a final concentration of 10.4% in the polyacrylamide gel. A resolving gel (pH 8.8) was poured at the bottom of the tank, to a level of 1 cm below the teeth of the comb, then 0.1% (w/v) SDS solution was poured on top of it. After the resolving gel had solidified, a 4% (w/v) stacking gel solution (pH 6.8) was poured on top of it. The protein samples were prepared by mixing each sample (1:1) with 2× Laemmli sample buffer containing 2-mercaptoethanol, followed by heating in boiling water for 5 min. The sample buffer contained bromophenol blue dye to make the samples distinguishable.

Gels were then submerged in electrophoresis buffer (25 mM Tris, 192 mM glycine, 0.1% [w/v] SDS). The samples were briefly centrifuged and carefully loaded into separate gel lanes, with 30 µg/well of total protein. A pre-stained protein ladder (10 µL of Precision Plus Protein Dual Colour Standards) was loaded into the first lane for reference purposes. The gels were run using a Power Pack Basic (Bio-Rad, UK) operating in constant voltage mode, at 50 V initially (to help give sharp bands), which was then increased to 100 V for the remainder of the run. By visualising the pre-stained ladder and the position of the bromophenol blue within the gel, the end of the electrophoresis run could be determined (approximately 2 h). The SDS–PAGE gel was used to separate the proteins based on their size. Due to the presence of the SDS detergent, which neutralises charge differences between the proteins, the proteins in the sample were separated depending on their size and not their charge. Lower percentage gels are used to resolve larger proteins, and higher percentage gels are used to separate smaller protein molecules.

2.3.12.6 Membrane Transfer

Following electrophoresis, proteins were transferred to a blotting nitrocellulose membrane using the iBlot Gel Transfer Device (Invitrogen) at a constant voltage of 25 V for 7 min.

2.3.12.7 Blocking

After transfer, nitrocellulose membranes were incubated in 5% (w/v) BSA in Tris-buffered saline (150 mM NaCl, 20 mM Tris, pH 7.4) containing 0.1% (v/v) Tween-20 (TBST) for 1 h at room temperature on a gentle shaker. The membranes were then washed three times with TBST for 10 min.

2.3.12.8 Primary Antibody Incubation

A solution of the appropriate primary antibody, in blocking solution (TBST containing 5% [w/v] BSA), was then added. The dilutions of the primary antibodies were as follows: anti-p53 (1:1,000); anti-p21 (1:1,000); anti-Bcl-2 (1:1,000); anti-caspase-3 (1:1,000); anti-S-100 (1:1,000), and anti-GAPDH (1:10,000). An anti-GAPDH monoclonal antibody was used as a housekeeping (loading) control, and a monoclonal antibody was selected due to its higher specificity and better signal. In every case, for antibody binding, membranes were incubated overnight at 4 °C with the primary antibody solution using a gentle shaker. After this, membranes were washed three times with TBST for 10 min.

2.3.12.9 Secondary Antibody Incubation

A secondary antibody was added to determine where the primary antibody was bound. A donkey anti-rabbit IgG H&L (HRP) was used as secondary antibody, at 1:3,000 dilution in blocking buffer (TBST containing 5% [w/v] BSA), as before. Membranes were incubated for 1 h on a gentle shaker at room temperature, then washed with TBST three times for 10 min each.

2.3.12.10 Detection

Each membrane was stained with a chemiluminescence (ECL) kit, by incubation with an equal (1:1) mixture of the ECL solutions for a few minutes at room temperature. Then, membranes were individually placed in a G-Box instrument (Geneflow, UK). Excess detergent was removed, then images were finally captured.

2.3.12.11 Data Analysis

Expression of the proteins of interest was assessed by band densitometry using the ImageJ software, with GAPDH serving as a loading control. Results are presented as the mean ± SEM derived from three biological samples. Comparisons between experimental groups were made using one-way ANOVA, followed by Dunnett's post hoc test, to determine the significance of differences between treatments, using GraphPad Prism 9.

3) Cytotoxicity and Genotoxicity Assessment

3.1 Introduction

Exposure to UVR can directly induce DNA damage, as outlined above (Section 1.2.2.3 DNA Damage Induced by UVA), but it can also stimulate generation of ROS that may cause additional genotoxicity (Wu et al., 2021). This offers one potential reason why MM has increasingly been characterised as an oxidative stress-associated disease, as was also discussed earlier (Section 1.2.2.2 Aetiology of MM). In this study, induction of oxidative stress was therefore used as an *in vitro* model for MM, to assess the potential for new treatments based on an antioxidant (selenium), and CBSC-derived exosomes.

Exosomes are able to induce reprogramming of cancer cells through horizontal transfer of their biomolecular cargo. This has been reported for both MM and breast cancer cells, with morphological changes noted in the latter (Zhou et al., 2017; Li et al., 2014); and exosome-mediated reprogramming has also been suggested to suppress malignancy through induction of pluripotency (Kim & Zaret, 2015). Furthermore, MSC-derived exosomes were previously found to promote wound healing in a rat skin burn model (Zhang et al., 2015), and they have also been demonstrated to aid recovery in cellular and mouse models of liver injury through attenuation of oxidative stress (Yan et al., 2017). The latter example is particularly relevant to the current study, since the observed antioxidant effect relied on exosome-delivered glutathione peroxidase 1 (GPX1)—an enzyme which detoxifies peroxides and is also a selenoprotein (Jerome-Morais et al., 2013)—for protection against oxidative stress, both *in vitro* and *in vivo* (Yan et al., 2017).

In this work, hydrogen peroxide (H_2O_2) was used as a chemical stressor to mimic the heightened oxidative stress in MM. It has often been used to induce oxidative stress and ROS production in cellular studies (e.g., Coyle et al., 2006; Lin et al., 2015; Nowak et al., 2017), and is also a well-established genotoxic agent, including in human lymphocytes, where it was previously shown to generate both oxidised pyrimidines and DNA strand breaks (Duthie et al., 1999).

As introduced in Section 1.6.2 The Comet Assay, the comet assay is widely used to assess genotoxicity due to its simplicity, rapidity and cost-effectiveness. In human monitoring studies, it is most commonly used with white blood cells, particularly lymphocytes (Cortés-Gutiérrez et al., 2011); as is the case here, where lymphocytes isolated from either MM patients or healthy controls were used. As well as the proportion of DNA in the 'tail' (% tail DNA), the Olive tail moment (OTM) was also measured, which represents the product of the % tail DNA and the tail length; i.e., the distance between the intensity centroids (or 'centres of gravity') of the head and tail areas, along the x-axis of the comet (Intranuovo et al., 2018). The higher the OTM, the greater the extent of DNA damage (Fernandes et al., 2021). In parallel experiments to the lymphocyte assays, the treatment effects on CHL-1 melanoma cells were also investigated. This cell line contains mutated *TP53* (Wu et al., 2017), potentially allowing for the effect of CBSC-derived exosomes and/or Se on p53-dependent apoptosis pathways to be evaluated. Finally, in addition to assessing genotoxicity, the CCK-8 assay (also introduced above, in Section 1.6.1 Cell Counting Kit-8 (CCK-8)) was also used to monitor cytotoxicity, in the same cell types and for the same treatment groups as above. As a convenient and straightforward readout of cellular viability, these results were expected to allow for direct comparison of the cytotoxic and genotoxic effects of the proposed MM treatments.

3.2 Materials and Methods

For both assays (comet assay and CCK-8 assay), the reagents and equipment used are listed in Table 1 and Table 2, respectively. Human lymphocytes were isolated from whole blood as described in Section 2.3.5 Lymphocyte Isolation from Whole Blood. The comet assay procedure was performed as detailed in Sections 2.3.6 Comet Assay Protocol and 2.3.8 Comet Assay with Primary Lymphocytes and CHL-1 Cells, while the protocol for the CCK-8 assay is given in Section 2.3.4 Cell Counting Kit-8 (CCK-8) Cytotoxicity Assay.

3.3 Results

3.3.1 Antioxidant Effects of Selenium Treatment in MM

3.3.1.1 Optimal Dosage of H_2O_2

An initial dose–response step was performed to establish the optimal H_2O_2 concentration for subsequent experiments; i.e., to find the concentration that caused the most DNA damage without a significant reduction in cell viability. Four concentrations of H_2O_2 (25, 50, 75 and 100 µM) were used with whole blood samples from healthy individuals, alongside untreated samples that were used as a negative control (NC). The % tail DNA and OTM were both measured. As outlined in Section 2.3.10 Statistical Analysis (Statistical Analysis), GraphPad Prism 9.4.0 was used to graph the results, and asterisks are shown to denote the level of statistical significance (where relevant) between treatment and control samples.

As can be seen in Figure 9, increased DNA damage was observed when the whole blood samples from healthy individuals were incubated with H_2O_2. The comet assay was performed five times, and the optimal dosage was identified as 75 µM H_2O_2, which significantly damaged the DNA based on both the % tail DNA and OTM results (*** p <0.001). Therefore, 75 µM H_2O_2 was selected as a positive control (PC) for assays to evaluate the treatment effects of Se and exosomes.

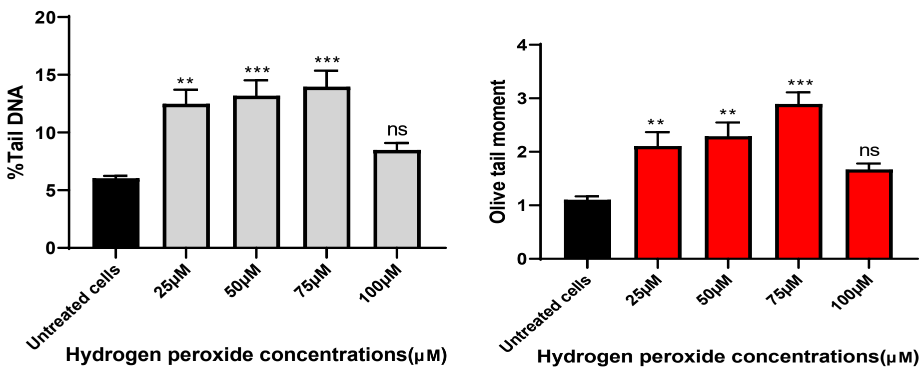

Figure 9. Effect of H_2O_2 at different concentrations on lymphocyte DNA, from healthy individuals, measured using % tail DNA and OTM. Error bars show mean ± SEM, n = 5 (* p <0.05; ** p <0.01; *** p <0.001; ns = not significant). All results for treated groups were compared against the NC (untreated) group, and analysed using one-way ANOVA with Dunnett's multiple comparison test, in GraphPad Prism 9.4.0. Data analysis was performed similarly for subsequent figures, as described above (Section 2.3.10 Statistical Analysis).

3.3.1.2 Cytotoxicity of Se in Stressed Healthy Lymphocytes

Lymphocytes from healthy individuals were stressed with 75 µM H_2O_2 (PC) and treated with various concentrations of Se, then the cell viability was determined using the CCK-8 assay after 24 h and 48 h (

Figure **10**). After 24 h, it can be clearly seen that the percentage (%) of surviving lymphocytes was reduced following treatment with 50, 75 or 100 µM Se (*** p <0.001), but the cells were less affected at 25 µM, and there was no significant effect at 10 µM. Therefore, the two doses of 10 µM and 25 µM were regarded as suitable for the comet assay at this time point. For a 48 h treatment, 10 µM was deemed as the optimal concentration. Overall, 10 µM Se is the most appropriate dose for healthy lymphocytes.

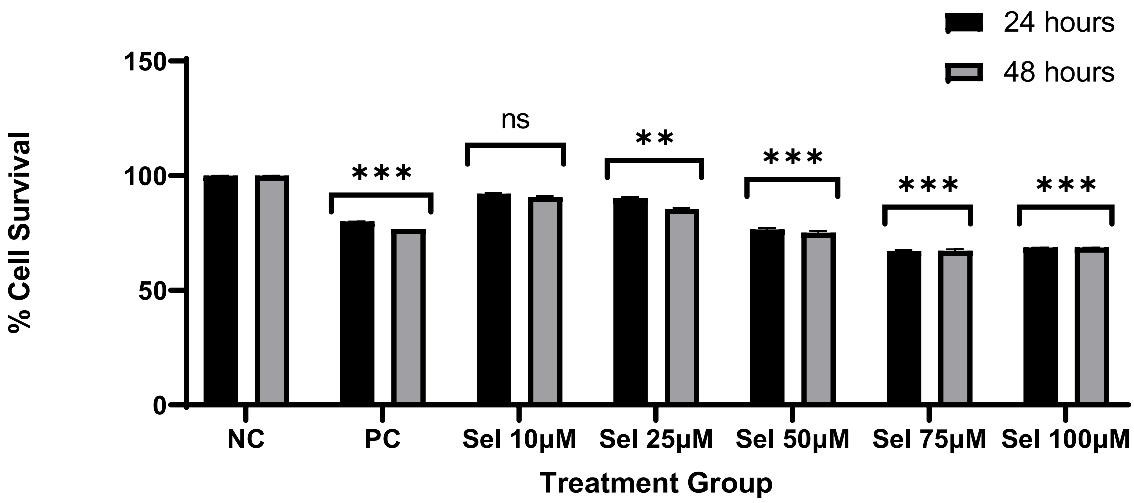

Figure 10. Survival (%) of 10 × 10^4 lymphocytes, from healthy individuals, exposed to 75 µM H_2O_2 (PC) and treated with the Se concentrations indicated. Viability was determined using the CCK-8 assay at 24 h and 48 h. Error bars show mean ± SEM, n = 3 (* $p < 0.05$; ** $p < 0.01$; *** $p < 0.001$; ns = not significant). Pairwise comparisons are against untreated cells (NC).

3.3.1.3 Cytotoxicity of Se in Stressed CHL-1 MM Cells

Similarly, to the above experiment, CHL-1 melanoma cells were stressed with 75 µM H_2O_2 (PC) and treated with different concentrations of Se (10, 25, 50, 75 and 100 µM), then incubated for 24 h or 48 h. The treatment significantly induced growth inhibition of melanoma cells at low doses (*** $p < 0.001$), as revealed by cell viability measurements using the CCK-8 assay. The IC_{50} of Se on melanoma cells was estimated as 10 µM at both time points (

Figure 11). Therefore, 10 µM Se was selected to study melanoma cells using the comet assay, in comparison with untreated cells.

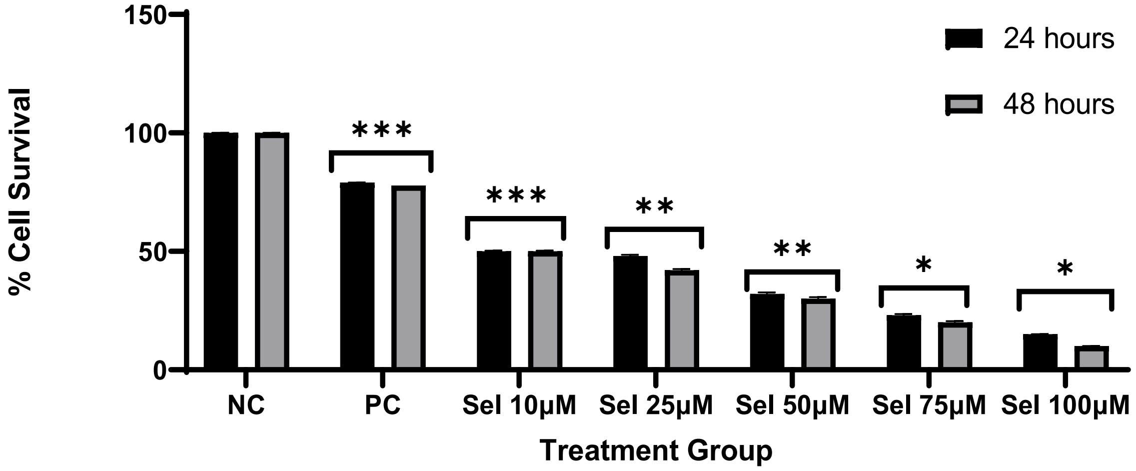

Figure 11. Selenium reduces the viability of CHL-1 melanoma cells. Cytotoxicity was assessed by CCK-8 assay at 24 h and 48 h, after treatment with the concentrations shown. There is a clear dose–response relationship, with the IC_{50} estimated as 10 µM. All values are presented as mean ± SEM, n ≥ 3 (* p <0.05; ** p <0.01; *** p <0.001; ns = not significant).

3.3.1.4 Effect of Se on Genotoxicity in Healthy Lymphocytes

To determine the genotoxicity of Se towards lymphocytes from healthy individuals, the comet assay was performed with dosing at three different concentrations (10, 25 and 75 µM), as well as using 10 µM Se in combination with 75 µM H_2O_2, for 20 healthy volunteers. As seen in **Figure 12**, there was no significant change in OTM with 10 µM or 25 µM Se, but significant DNA damage was seen at 75 µM. Similar results were observed in terms of % tail DNA, except there was no significant effect of 75 µM Se (**Figure 13**). The genotoxic effect of 75 µM H_2O_2 (PC) was fully rescued by 10 µM Se (i.e., for PC + 10 µM Se; *** p <0.001). Consequently, for subsequent comet assays, 10 µM and 25 µM Se were considered suitable since they do not induce any significant genotoxicity, and 10 µM seemed ideal since it can fully protect against oxidative stress. Numerical data for these experiments are presented in Table 5.

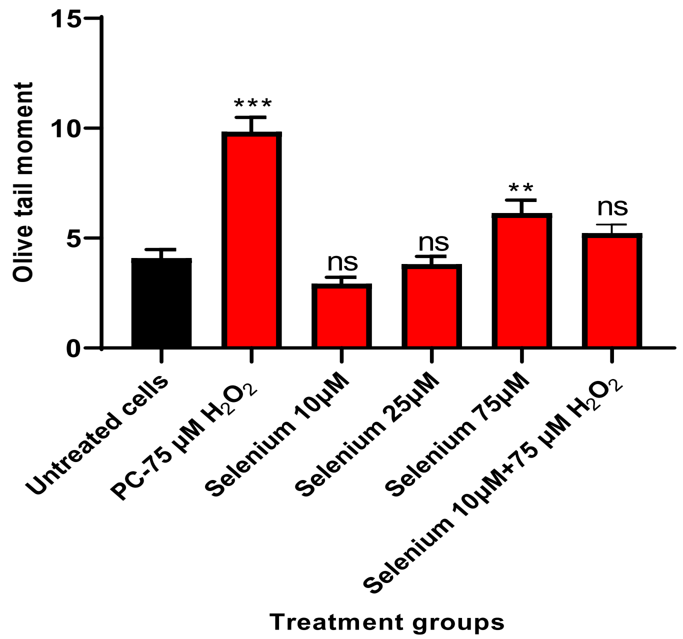

Figure 12. Effect of Se at the concentrations shown, with/without the presence of 75 µM H_2O_2 (as indicated), on the DNA of lymphocytes from healthy individuals, as judged by OTM. All outcomes for the treatment groups were compared to the relevant negative control group. Error bars show mean ± SEM, n = 20 (* p<0.05; ** p <0.01; *** p <0.001; ns = not significant).

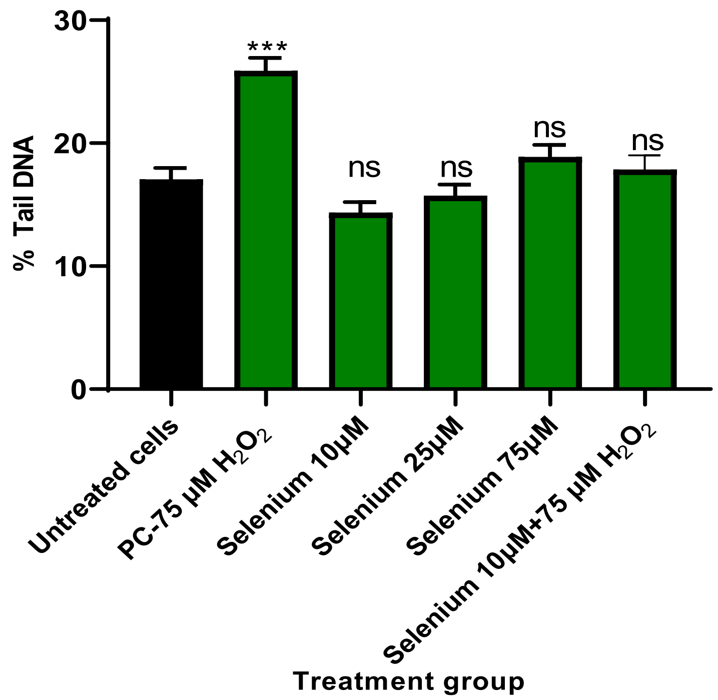

Figure 13. Companion results to Figure 12. Effect of Se at the concentrations shown, with/without the presence of 75 µM H_2O_2 (as indicated), on the DNA of lymphocytes from healthy individuals, as judged by % tail DNA. All outcomes for the treatment groups were compared to the relevant negative control group. Error bars show mean ± SEM, n = 20 (* p<0.05; ** p <0.01; *** p <0.001; ns = not significant).

Table 5. Mean results of comet assays on blood samples (lymphocytes) from 20 healthy individuals, expressed as OTM and % tail DNA, including SEM and statistical significance.

Treatment	OTM (mean ± SEM)	% Tail DNA (mean ± SEM)
Untreated	4.09 ± 0.07	17.07 ± 0.36
75 µM H_2O_2 (PC)	9.84 ± 0.18 (***)	25.89 ± 0.68 (***)
10 µM Se	2.93 ± 0.08 (ns)	14.36 ± 0.38 (ns)
25 µM Se	3.82 ± 0.08 (ns)	15.73 ± 0.33 (ns)
75 µM Se	6.13 ± 0.15 (***)	18.90 ± 0.32 (ns)
75 µM H_2O_2 + 10 µM Se	5.22 ± 0.09 (***)	17.85 ± 0.38 (ns)

3.3.1.5 Effect of Se on Genotoxicity in MM Patient Lymphocytes

Lymphocytes from 20 individuals with MM were subjected to the comet assay under the same treatment conditions as used for the lymphocytes from healthy volunteers (i.e., NC; PC; 10, 25 and 75 µM Se; PC + 10 µM Se). In terms of both OTM and % tail DNA, 10 µM Se reduced the DNA damage in comparison to NC (*** $p < 0.001$;
Figure 14, **Figure 15**). When stressed melanoma lymphocytes were treated with 10 µM of Se (i.e., 10 µM Se + 75 µM H_2O_2), the DNA damage was significantly reduced in comparison to the PC, according to both parameters. The rescue effect was statistically significant (*** $p < 0.001$) for lymphocytes from both healthy individuals and MM patients (see below; Section 3.3.1.6 Comparing Se Treatment of Healthy versus MM Lymphocytes). The results are also presented numerically in Table 6. Mean results of comet assays on blood samples (lymphocytes) from 20 melanoma patients, expressed as OTM and % tail DNA, including SEM and statistical significance..

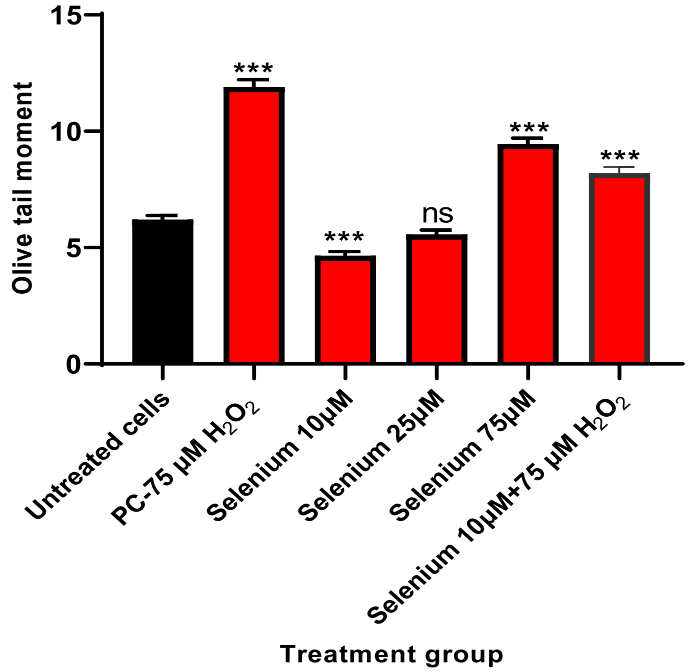

Figure 14. Effect of Se at the concentrations shown, with/without the presence of 75 µM H_2O_2 (as indicated), on the DNA of lymphocytes from MM patients, as judged by OTM. All outcomes for the treatment groups were compared to the relevant negative control group. Error bars show mean ± SEM, n = 20 (* p<0.05; ** p <0.01; *** p <0.001; ns = not significant).

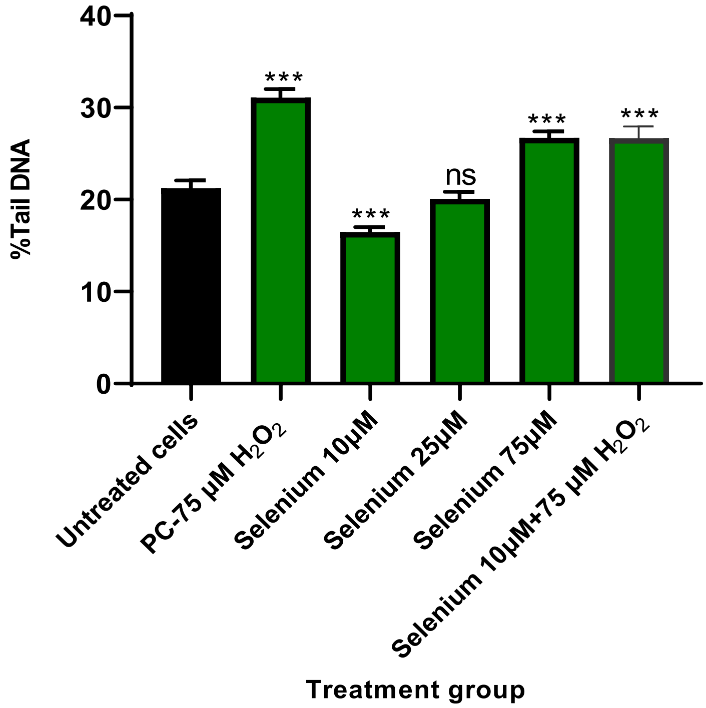

Figure 15. Effect of Se at the concentrations shown, with/without the presence of 75 µM H_2O_2 (as indicated), on the DNA of lymphocytes from MM patients, as judged by % tail DNA. All outcomes for the treatment groups were compared to the relevant negative control group. Error bars show mean ± SEM, n = 20 (* p<0.05; ** p <0.01; *** p <0.001; ns = not significant).

Table 6. Mean results of comet assays on blood samples (lymphocytes) from 20 melanoma patients, expressed as OTM and % tail DNA, including SEM and statistical significance.

Treatment	OTM (mean ± SEM)	% Tail DNA (mean ± SEM)
Untreated	6.20 ± 0.12	21.25 ± 0.47
75 µM H_2O_2 (PC)	11.91 ± 0.19 (***)	31.09 ± 0.58 (***)
10 µM Se	4.65 ± 0.08 (***)	16.49 ± 0.41 (***)
25 µM Se	5.56 ± 0.10 (ns)	20.07 ± 0.42 (ns)
75 µM Se	9.45 ± 0.08 (***)	26.71 ± 0.39 (***)
75 µM H_2O_2 + 10 µM Se	8.2 ± 0.12 (***)	26.69 ± 0.47 (***)

3.3.1.6 Comparing Se Treatment of Healthy versus MM Lymphocytes

The comet assay was done for healthy lymphocytes and melanoma lymphocytes (20 patients per group) at three different Se concentrations (10 µM, 25 µM and 75 µM), also comparing PC (75 µM H_2O_2), either alone or in combination with 10 µM Se, as before. For both parameters (OTM and % tail DNA), 10 µM Se was well tolerated, and significantly attenuated the genotoxic effect of H_2O_2 (i.e., relative to PC; *** $p < 0.001$), with a full rescue effect in the lymphocytes from healthy individuals (**Figure 16** and **Figure 17**). In other words, cells co-treated with 75 µM H_2O_2 and 10 µM Se showed a significant decrease in OTM and % tail DNA compared with the PC (75 µM H_2O_2 only; *** $p < 0.001$). In MM lymphocytes, there was a significant decrease in % tail DNA and OTM upon 10 µM Se treatment, from 21.3% and 6.2, respectively, in the NC, to 16.4% and 4.65, respectively, in the treatment group. This suggests that 10 µM Se protects against DNA damage and genotoxicity in MM lymphocytes (more than in healthy lymphocytes, where the effect was not statistically significant), presumably due to its antioxidant properties. However, higher doses were genotoxic. With 75 µM Se, the % tail DNA (26.7%) and OTM (9.45) were both significantly higher than control values (Table 6).

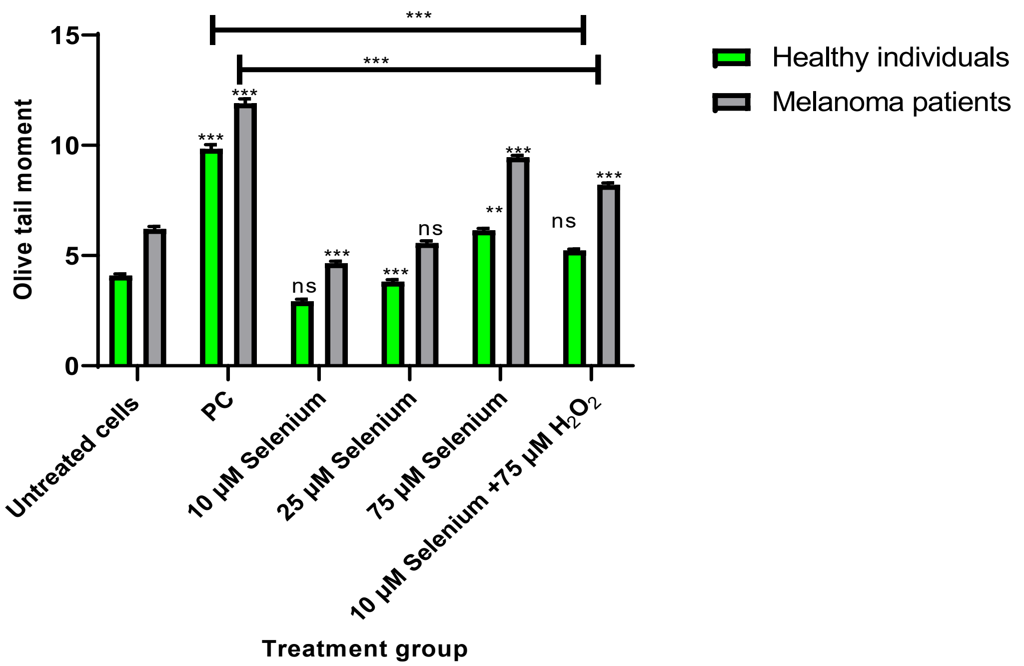

Figure 16. Comparison of DNA damage between healthy individuals and MM patients, after lymphocytes were treated with Se at various concentrations, with/without 75 µM H_2O_2 (as indicated), according to comet assay OTM measurements. Error bars show mean ± SEM, n = 20 (* p <0.05; ** p <0.01; *** p <0.001; ns = not significant).

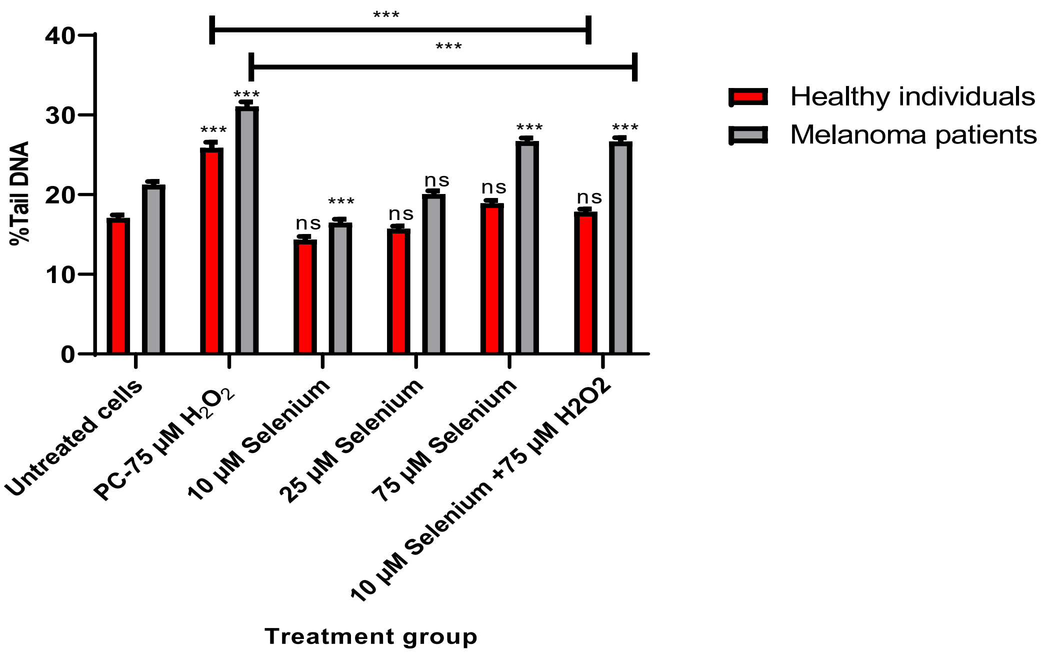

Figure 17. Comparison of DNA damage between healthy individuals and MM patients, after lymphocytes were treated with Se at various concentrations, with/without 75 µM H_2O_2 (as indicated), according to comet assay % tail DNA measurements. Error bars show mean ± SEM, n = 20 (* p <0.05; ** p <0.01; *** p <0.001; ns = not significant).

3.3.1.7 Effect of Se on Genotoxicity in CHL-1 MM Cells

The comet assay was performed on the CHL-1 cell line (n = 3) comparing PC, 10 µM Se and combined treatment (75 µM H_2O_2 + 10 µM Se) versus NC (untreated cells). As shown in Figure 18 (OTM) and Figure 19 (% tail DNA), treatment with 10 µM Se induced significant DNA damage in this cell line (** $p < 0.01$), albeit to a lesser extent than PC. Rather than exerting a rescue effect, as seen in lymphocytes, 10 µM Se exacerbated the genotoxicity of 75 µM H_2O_2 (PC) in CHL-1 cells (*** $p < 0.001$).

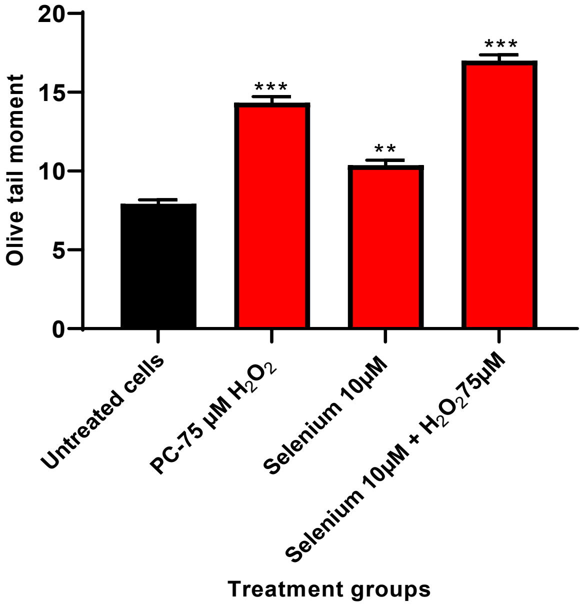

Figure 18. Effect of 10 µM Se on DNA damage in stressed/unstressed CHL-1 cells (with/without 75 µM H_2O_2, respectively), based on OTM measured in comet assays, relative to untreated cells. Error bars show mean ± SEM, n = 3 (* $p < 0.05$; ** $p < 0.01$; *** $p < 0.001$; ns = not significant).

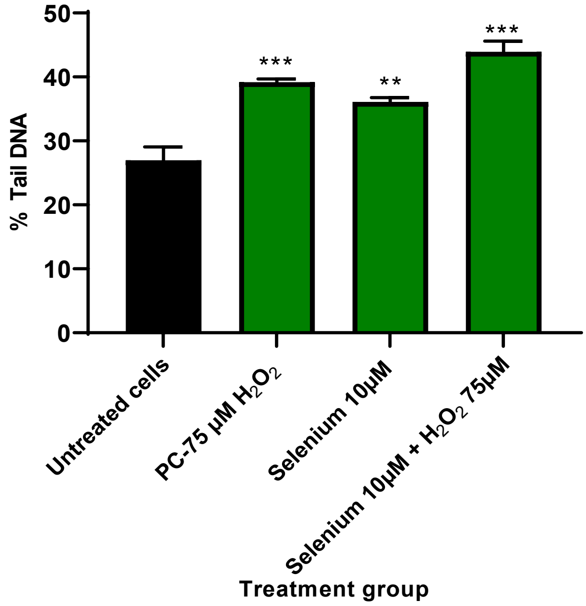

Figure 19. Effect of 10 µM Se on DNA damage in stressed/unstressed CHL-1 cells (with/without 75 µM H_2O_2, respectively), based on % tail DNA measured in comet assays, relative to untreated cells. Error bars show mean ± SEM, n = 3 (* p <0.05; ** p <0.01; *** p <0.001; ns = not significant).

3.3.2 CBSC-Derived Exosomes for MM Treatment

3.3.2.1 Cytotoxicity of Exosomes in Stressed Healthy Lymphocytes

Lymphocytes from healthy individuals were stressed (PC; 75 µM H_2O_2) and treated with CBSC-derived exosomes at five different concentrations (10, 30, 60, 90 and 120 µL). Cell viability was measured using the CCK-8 assay at six different time points (30 min, 3 h, 12 h, 16 h, 24 h and 48 h). Most concentrations (except 60 µL) were able to protect the cells against H_2O_2-induced cytotoxicity (

Figure **20**). The three most effective exosome concentrations at 48 h were regarded as 10 µL, 90 µL and 120 µL, since their protective effect was stable and did not change significantly over the full course of the experiment. These concentrations were therefore selected for further study in comet assays.

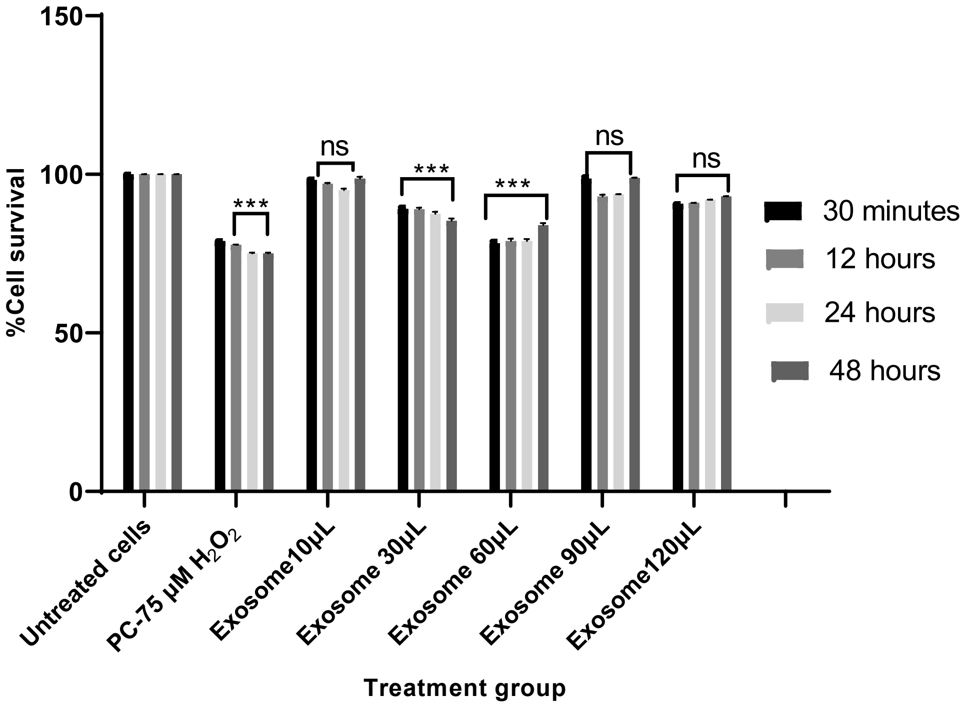

Figure 20. Cell survival (%) for lymphocytes from healthy individuals (10×10^4 cells) stressed (PC) and treated with the indicated exosome concentrations. Cell viability was measured using the CCK-8 assay at 30 min, then 3, 12, 16, 24 and 48 h (with data for the four indicated time points shown). Error bars show mean ± SEM, n = 20 (* $p < 0.05$; ** $p < 0.01$; *** $p < 0.001$; ns = not significant). Pairwise comparisons were made between the different exosome concentrations and the NC.

3.3.2.2 Cytotoxicity of Exosomes in Stressed MM Patient Lymphocytes

Analogous experiments to those above (Section 3.3.2.1 Cytotoxicity of Exosomes in Stressed Healthy Lymphocytes) were carried out using lymphocytes from MM patients, assessing the same five concentrations of CBSC-derived exosomes in oxidatively stressed cells (PC; 75 µM H_2O_2), at the same time points. Similar results were obtained (Figure 21), and at 48 h, the best three concentrations to take forward to comet assays were again identified as 10 µL, 90 µL and 120 µL.

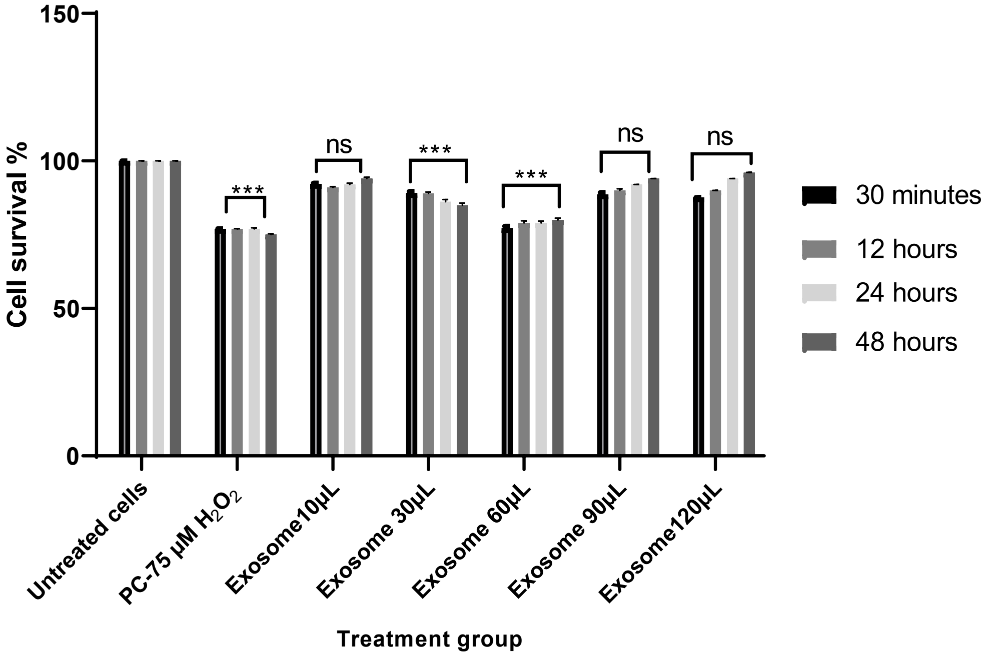

Figure 21. Cell survival (%) for lymphocytes from MM patients (10×10^4 cells) stressed (PC) and treated with the indicated exosome concentrations. Cell viability was measured using the CCK-8 assay at 30 min, then 3, 12, 16, 24 and 48 h (with data for the four indicated time points shown). Error bars show mean ± SEM, n = 3 (* $p < 0.05$; ** $p < 0.01$; *** $p < 0.001$; ns = not significant). Pairwise comparisons were made between the different exosome concentrations and the NC.

3.3.2.3 Cytotoxicity of Exosomes in CHL-1 MM Cells

The initial screen of various exosome concentrations (10, 30, 60, 90 and 120 µL) was also carried out using the CHL-1 MM cell line, with cytotoxicity again assessed using the CCK-8 assay. In this case, measurements were made at four time points (30 min, 12 h, 24 h and 48 h). The exosomes reduced the viability of the melanoma cells with an apparent IC_{50} of 120 µL after 24 h and 48 h (Figure 22). A concentration of 120 µL exosomes was chosen to study their effect in the comet assay.

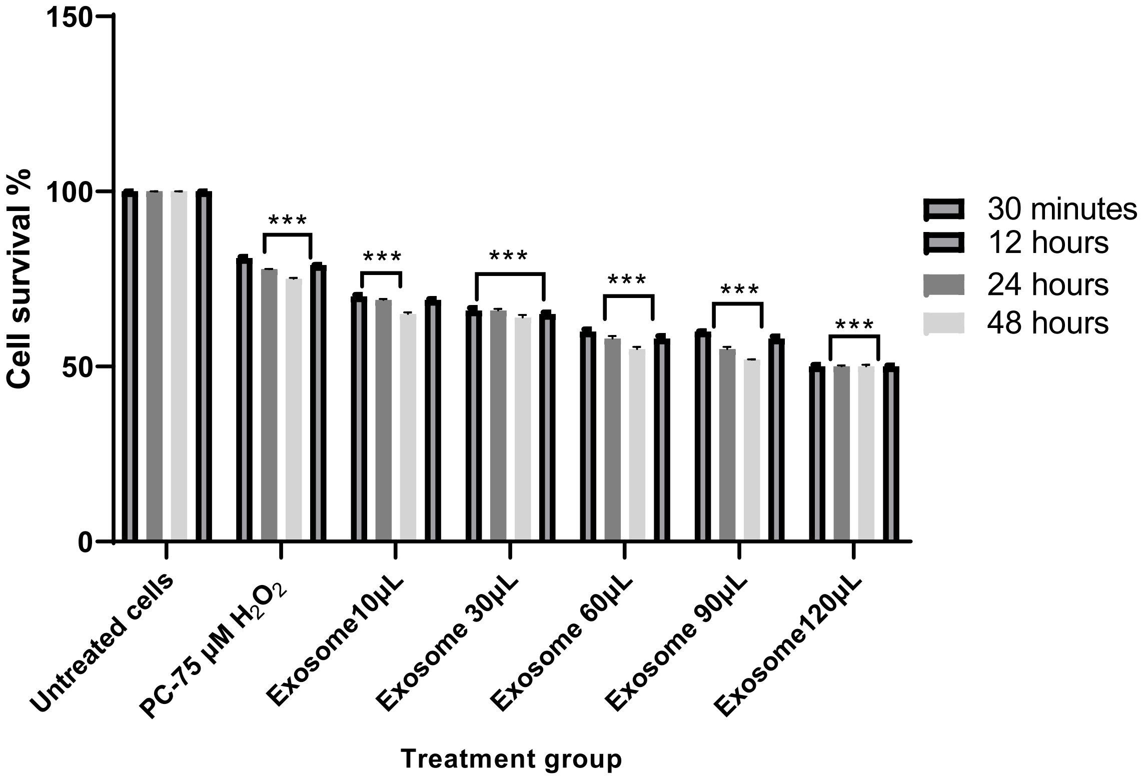

Figure 22. Exosomes reduce the viability of melanoma cells. Cytotoxicity of CBSC-derived exosomes towards stressed (75 µM H_2O_2; PC) CHL-1 cells was assessed by CCK-8 assay at the time points shown. A clear dose–response relationship is seen with an estimated IC_{50} of 120 µL. All results are expressed as mean ± SEM, n ≥ 3. (* $p < 0.05$; ** $p < 0.01$; *** $p < 0.001$; ns = not significant). All treated groups were compared (according to exosome concentration) against the NC (untreated) group, as in previous examples.

3.3.2.4 Effect of Exosomes on Genotoxicity in Healthy Lymphocytes

The comet assay was done on lymphocytes from 20 healthy individuals, treated with the three exosome concentrations determined above (10, 90 and 120 µL), under either stressed or unstressed conditions (i.e, with/without 75 µM H_2O_2). In terms of OTM (Figure 23), all three concentrations appeared to induce a positive response in unstressed cells, although the effect did not reach statistical significance. However, 120 µL exosomes generated the best response and also reduced the DNA damage caused by H_2O_2 (* $p < 0.05$). Similar results were observed for % tail DNA (Figure 24). Thus, for lymphocytes from healthy individuals, the optimum exosome concentration is 120 µL, according to the comet assay.

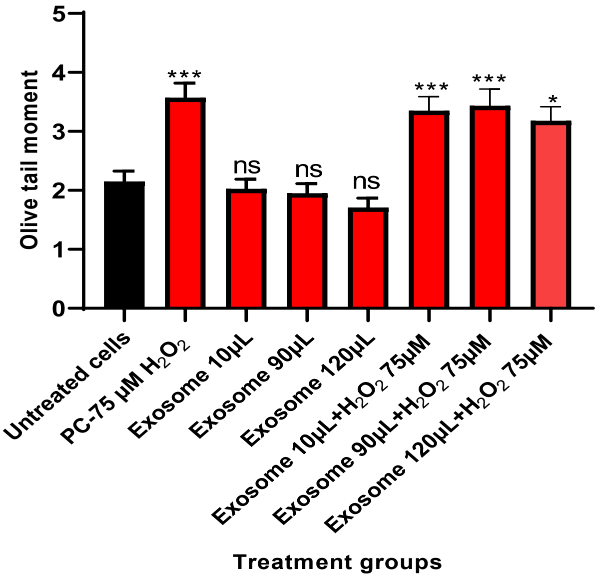

Figure 23. Effect of 10, 90 and 120 µL exosomes, with/without the presence of 75 µM H_2O_2 (as indicated), on DNA damage in lymphocytes from heathy individuals, based on OTM. Error bars show mean ± SEM, n = 20 (* p <0.05; ** p <0.01; *** p <0.001; ns = not significant). All results for treatment groups were compared against the respective NC group.

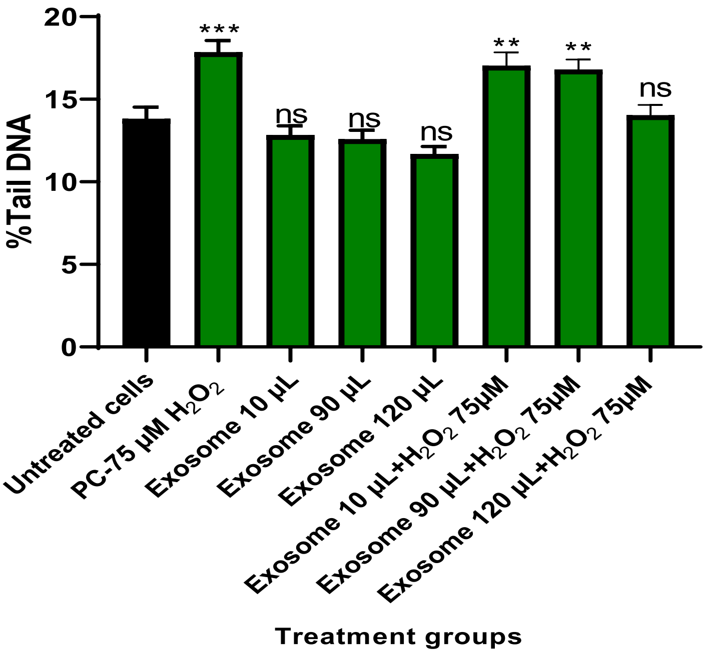

Figure 24. Effect of 10, 90 and 120 µL exosomes, with/without the presence of 75 µM H_2O_2 (as indicated), on DNA damage in lymphocytes from heathy individuals, based on % tail DNA. Error bars show mean ± SEM, n = 20 (* p <0.05; ** p <0.01; *** p <0.001; ns = not significant). All results for treatment groups were compared against the respective NC group.

3.3.2.5 Effect of Exosomes on Genotoxicity in MM Lymphocytes

Comet assays were similarly performed on lymphocytes from 20 MM patients, using the same three optimal exosome concentrations (10, 90 and 120 µL), with or without 75 µM H_2O_2. The results for OTM (Figure 25) showed that all three concentrations of exosomes reduced the DNA damage, but the observed effect was only statistically significant at 120 µL (** $p < 0.01$). The addition of 120 µL exosomes also attenuated the DNA damage caused by H_2O_2 (* $p < 0.05$ relative to PC). As before, similar results were seen for % tail DNA (Figure 26). Therefore, according to the comet assay observations, the optimal concentration of exosomes for MM patient lymphocytes is also 120 µL.

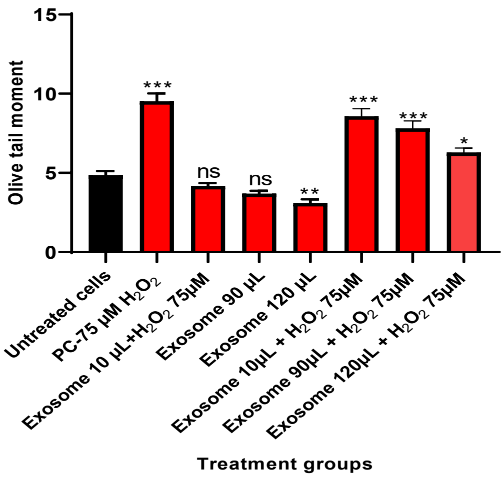

Figure 25. Effect of 10, 90 and 120 µL exosomes, with/without the presence of 75 µM H_2O_2 (as indicated), on DNA damage in lymphocytes from MM patients, based on OTM. Error bars show mean ± SEM, n = 20 (* $p < 0.05$; ** $p < 0.01$; *** $p < 0.001$; ns = not significant). All results for treatment groups were compared against the respective NC group.

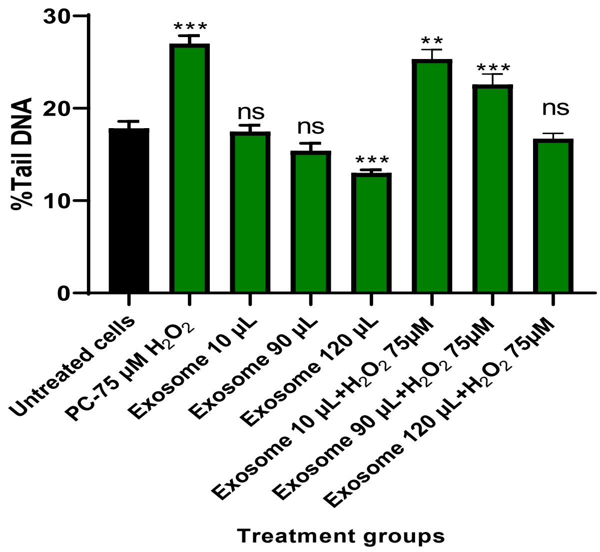

Figure 26. Effect of 10, 90 and 120 µL exosomes, with/without the presence of 75 µM H_2O_2 (as indicated), on DNA damage in lymphocytes from MM patients, based on % tail DNA. Error bars show mean ± SEM, n = 20 (* $p <0.05$; ** $p <0.01$; *** $p <0.001$; ns = not significant). All results for treatment groups were compared against the respective NC group.

3.3.2.6 Comparing Exosome Treatment of Healthy versus MM Lymphocytes

The comet assay was used to assess exosome treatment at three different concentrations (30, 90 and 120 µL) on H_2O_2-induced genotoxicity in lymphocytes from 20 healthy individuals and 20 MM patients. For both OTM (Figure 27) and % tail DNA (Figure 28), the DNA damage was decreased in lymphocytes from all study subjects after treatment with 120 µL of exosomes. However, this effect was not statistically significant in the healthy samples, but only for the MM patient samples (*** $p <0.001$, for tail DNA), compared with untreated cells. Although treatment with 120 µL exosomes was able to significantly reduce DNA damage in all cases, the results also showed that MM lymphocytes exhibited more DNA damage than those from healthy individuals. The horizontal lines in Figure 27 and Figure 28 (on top of the histograms) show the statistical comparisons between the PC and the three concentrations of exosomes (10, 90 and 120 µL), highlighting a significant protective effect only at the highest concentration.

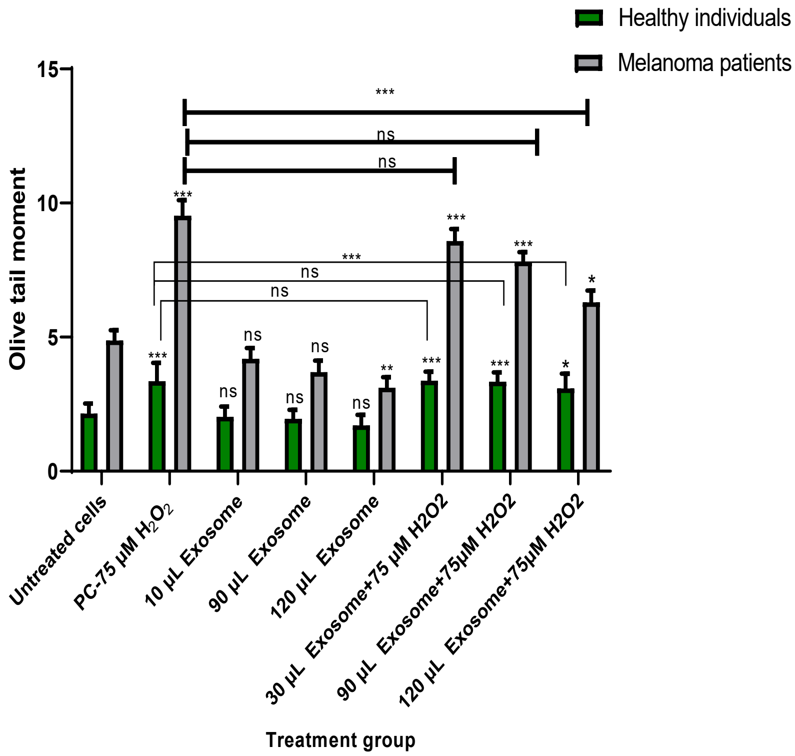

Figure 27. Comparison of lymphocyte DNA damage between healthy individuals and MM patients, after treatment with exosomes (at the concentrations shown), in the presence/absence of 75 µM H_2O_2 (as indicated), based on OTM measurements. Error bars show mean ± SEM, n = 20 (* p <0.05; ** p <0.01; *** p <0.001; ns = not significant). Pairwise comparisons are indicated by horizontal lines, or were otherwise made against the NC group.

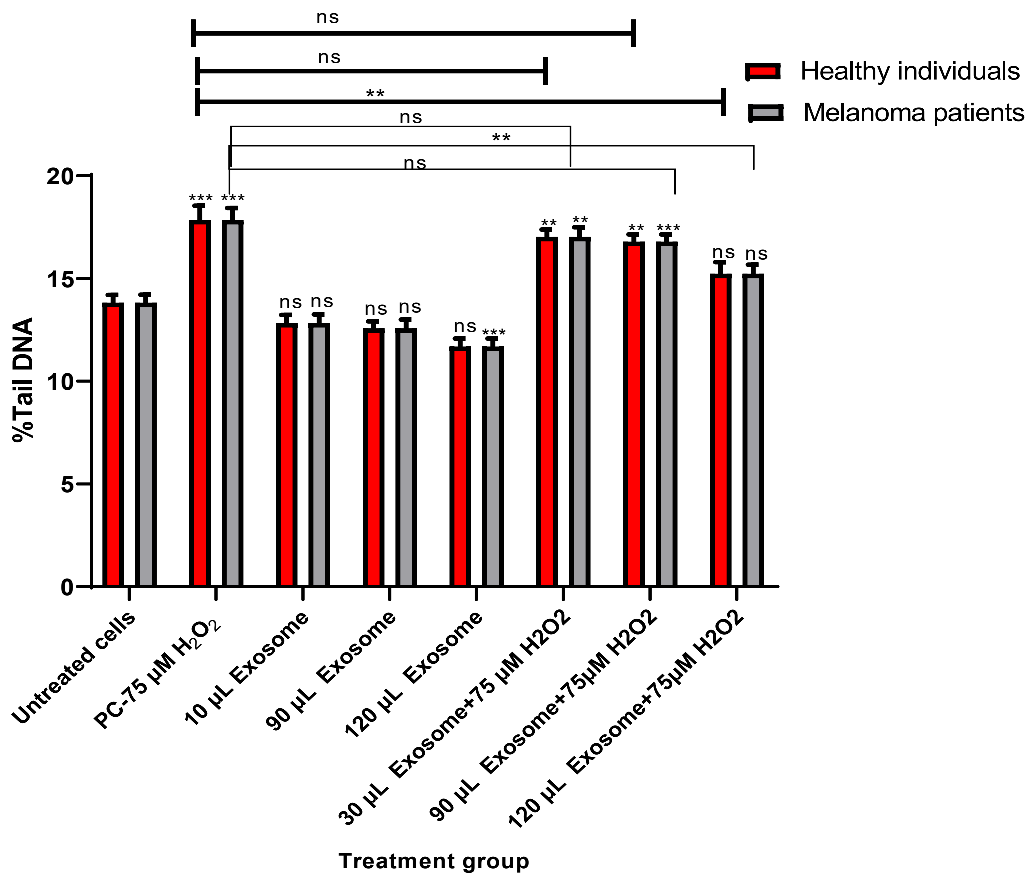

Figure 28. Comparison of lymphocyte DNA damage between healthy individuals and MM patients, after treatment with exosomes (at the concentrations shown), in the presence/absence of 75 μM H_2O_2 (as indicated), based on % tail DNA measurements. Error bars show mean ± SEM, n = 20 (* $p <0.05$; ** $p <0.01$; *** $p <0.001$; ns = not significant). Pairwise comparisons are indicated by horizontal lines, or were otherwise made against the NC group.

3.3.2.7 Effect of Exosomes on Genotoxicity in CHL-1 MM Cells

For the CHL-1 melanoma cell line, the effect of exosome treatment at the best concentration (120 μL) on genotoxicity induced by 75 μM H_2O_2 (PC) was investigated by comet assay. The experiment was repeated three times. Figure 29 (OTM) and Figure 30 (% tail DNA) demonstrate that exosome treatment significantly increased DNA damage relative to both NC and PC conditions, in terms of both parameters (*** $p <0.001$ in both cases, for OTM). In other words, the DNA damage induced by H_2O_2 was exacerbated by the addition of 120 μL exosomes, in contrast to the beneficial effects seen in human lymphocytes.

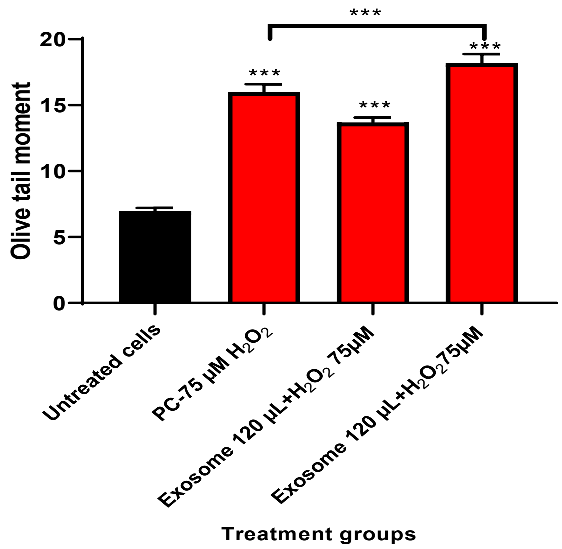

Figure 29. The effect of 120 μL exosomes, with/without 75 μM H_2O_2 treatment (as indicated), on DNA damage in CHL-1 MM cells, based on OTM measurements. Error bars show mean ± SEM, n = 3 (* p <0.05; ** p <0.01; *** p <0.001; ns = not significant). Pairwise comparisons were made against the NC group, unless indicated otherwise (horizontal line).

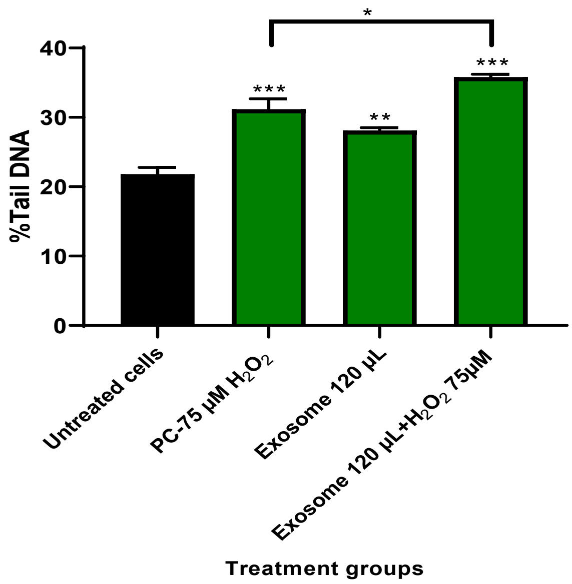

Figure 30. The effect of 120 μL exosomes, with/without 75 μM H_2O_2 treatment (as indicated), on DNA damage in CHL-1 MM cells, based on % tail DNA measurements. Error bars show mean ± SEM, n = 3 (* p <0.05; ** p <0.01; *** p <0.001; ns = not significant). Pairwise comparisons were made against the NC group, unless indicated otherwise (horizontal line).

3.3.3 Combined Treatment with Se and CBSC-Derived Exosomes

3.3.3.1 Cytotoxicity of Combined Treatment in CHL-1 MM Cells

Four different combination treatments (90 μL exosomes + 5 μM Se, 120 μL exosomes + 10 μM

Se, 90 µL exosomes + 15 µM Se, and 120 µL exosomes + 20 µM Se) were tested against the CHL-1 cell line, using the CCK-8 assay to evaluate their effect on viability in cells exposed to oxidative stress (PC, 75 µM H_2O_2). Measurements were done at four different time points (30 min, 12 h, 24 h and 48 h). All treatments reduced the viability of cells, with the strongest effect seen for 120 µL CBSC-derived exosomes combined with 10 µM Se (**Figure 31**). These treatment conditions were therefore chosen for further study using the comet assay, compared with untreated CHL-1 melanoma cells.

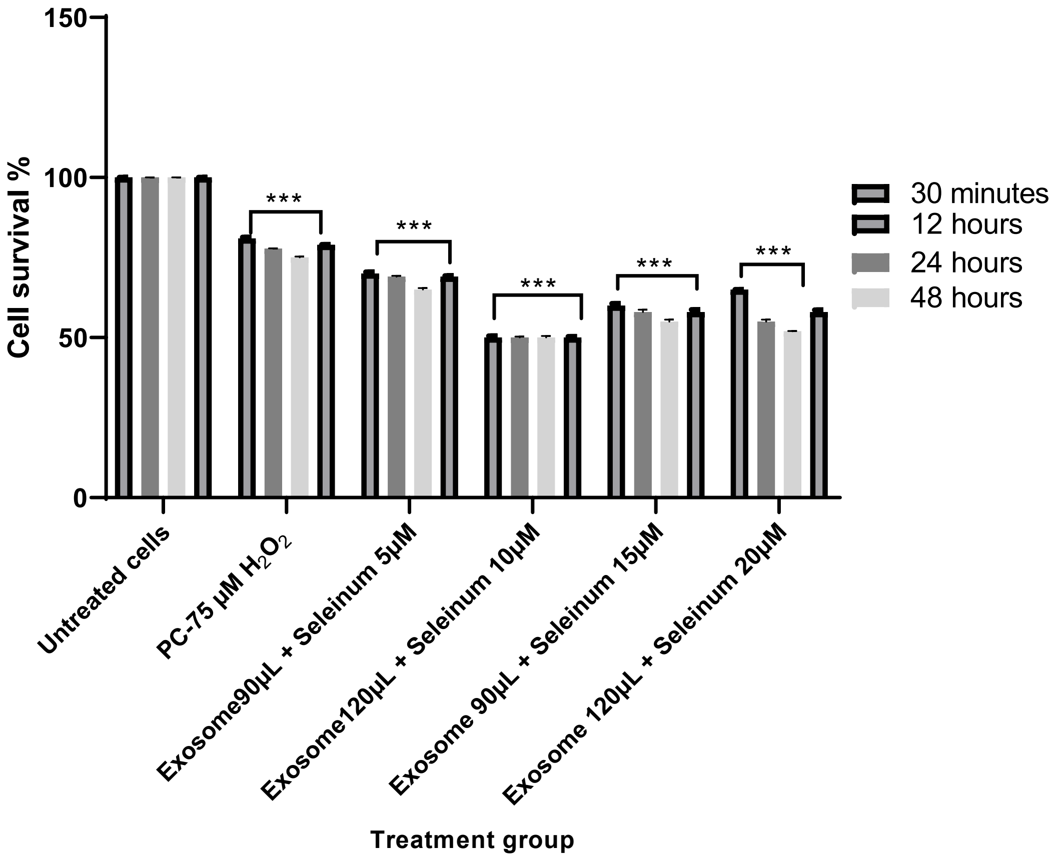

Figure 31. Combined exosome and Se treatments reduce the viability of melanoma cells. Cytotoxicity of the specified treatments in CHL-1 cells was assessed by CCK-8 assay at four time points (up to 48 h, as indicated). Values are expressed as mean ± SEM, n ≥ 3 (* p <0.05; ** p <0.01; *** p <0.001; ns = not significant). The different treatment combinations were compared against the NC, as shown.

3.3.3.2 Effect of Combined Treatment on Genotoxicity in CHL-1 MM Cells

The genotoxic effects of exosomes, Se, and both together, on the CHL-1 MM cell line were analysed using the comet assay (for three biological replicates). The treatment effects on DNA damage were investigated both in isolation, and in conjunction with oxidative stress conditions (i.e., 75 µM H_2O_2). Compared with untreated controls, exposure to 120 µL exosomes produced a significant increase in both OTM (12.5 versus 6.9) and % tail DNA (28.2% versus 21.8%) in these cells (*** p ≤0.001; Figure 32 and Figure 33). Moreover, cells treated with 120 µL exosomes and 10 µM Se showed a greater increase in DNA damage relative to controls, with an OTM of 15 and 40.1% tail DNA (*** p ≤0.001). Highly significant genotoxicity (*** p <0.001) was also observed with co-treatment (120 µL exosomes and 10 µM Se) in cells stressed with 75 µM H_2O_2, relative to the PC conditions alone.

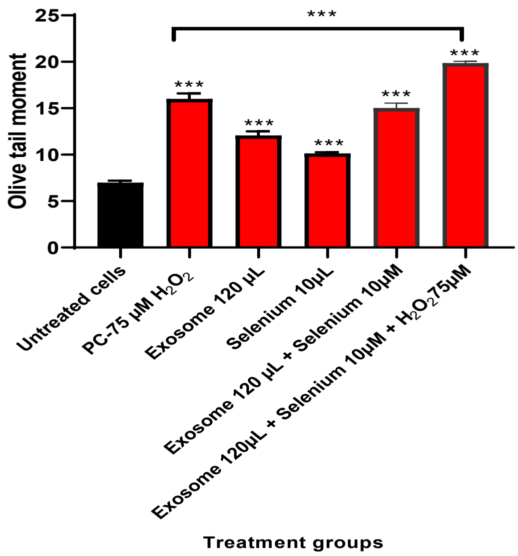

Figure 32. Effect of 120 µL exosomes and 10 µM Se, either individually or in combination, on DNA damage in CHL-1 MM cells stressed (or not) with 75 µM H_2O_2, as indicated, based on measurements of OTM. Error bars show mean ± SEM, n = 3 (* p <0.05; ** p <0.01; *** p <0.001; ns = not significant). Pairwise comparisons were made against the NC group, unless indicated otherwise (horizontal line).

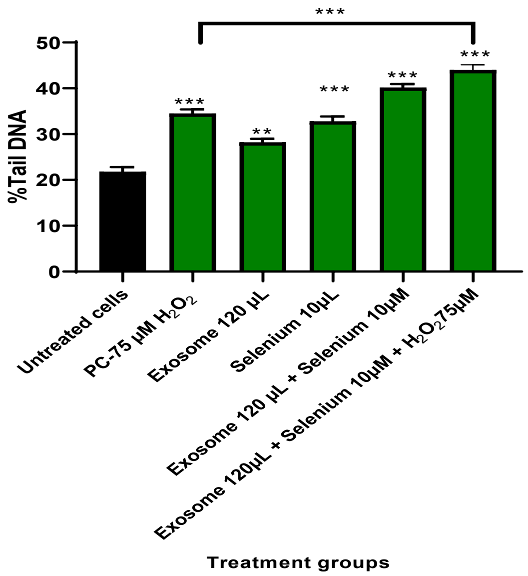

Figure 33. Effect of 120 µL exosomes and 10 µM Se, either individually or in combination, on DNA damage in CHL-1 MM cells stressed (or not) with 75 µM H_2O_2, as indicated, based on measurements of % tail DNA. Error bars show mean ± SEM, n = 3 (* $p < 0.05$; ** $p < 0.01$; *** $p < 0.001$; ns = not significant). Pairwise comparisons were made against the NC group, unless indicated otherwise (horizontal line).

3.4 Discussion

In this chapter, cytotoxicity and genotoxicity assays were employed to investigate the potential of Se or CBSC-derived exosomes, either separately or in combination, as potential treatments for MM. In human lymphocytes, 10 µM Se was able to protect against H_2O_2-induced DNA damage. The effect was more significant in lymphocytes from healthy controls (full rescue), with only partial rescue observed in MM patient lymphocytes (Figure 16 and Figure 17). However, for both sets of lymphocyte samples, treatment with 120 µL exosomes was also able to attenuate the genotoxicity induced by oxidative stress, with a similar effect in both groups of subjects (Figure 25 and Figure 26).

In the aforementioned experiments, a higher basal level of DNA damage (i.e., in untreated lymphocytes) was also observed in the MM patients compared with healthy individuals. This is important, given the suggestion that increased basal damage levels make cells more susceptible to the effects of oxidative stress (Vinoth et al., 2015), and especially given that genomic instability is a recognised feature of MM (Osrodek & Wozniak, 2021). Although it is tempting to speculate that elevated basal DNA damage in MM lymphocytes is associated with cancer development, this would have to be confirmed in age-matched cohorts (which does not apply in the current study), since oxidative stress and accumulation of DNA damage could also be consequences of ageing.

In the CHL-1 melanoma cell line, Se treatment caused greater cell death and also exacerbated genomic damage, under either basal or oxidative stress conditions (

Figure **11**, Figure 18 and Figure 19). Similarly, CBSC-derived exosomes (120 µL) reduced the viability of H_2O_2-exposed melanoma cells (Figure 22), but had no such effect on lymphocytes from either healthy individuals or MM patients (

Figure **20** and Figure 21). In combination, these treatments were also cytotoxic to melanoma cells—especially for 120 µL exosomes with 10 µM Se (Figure 31)—and co-administration seemed to have an additive effect on DNA damage, even in unstressed cells (Figure 32 and Figure 33). Thus, the proposed treatments exhibited both cytotoxicity and genotoxicity towards CHL-1 melanoma cells, while generally demonstrating genoprotective effects in human lymphocytes, as long as optimal concentrations were used.

Given the growing understanding of MM as an oxidative stress-associated disease (Section 1.2.2.2 Aetiology of MM), it may be that CHL-1 cells have higher basal ROS levels than either group of lymphocytes, and this could be tested in future experiments. Alternatively, mutated *TP53* (found in this cell line, as noted above) has previously been associated with increased genome instability (Hanel & Moll, 2012; Eischen, 2016), perhaps suggesting why these cells were adversely impacted by the treatments, whereas lymphocytes were not. It might also be the case that p53-dependent apoptosis is activated in the melanoma cells, and this possibility will be explored in the following chapters.

4) Gene Expression Analysis (RT–qPCR)

4.1 Introduction

Treatment of lymphocytes with Se and/or CBSC-derived exosomes consistently showed protection against DNA damage and generally did not induce significant cytotoxicity. In contrast, however, both treatments caused a substantial reduction in viability in CHL-1 melanoma cells. It was therefore decided to investigate the underlying mechanisms in more detail, with a focus on the key cell cycle and apoptosis-related proteins introduced earlier (Section 1.3 The Cell Cycle and its Checkpoints).

The tumour suppressor *TP53* (p53) is a master co-ordinator of multiple cellular processes, but generally acts as an antiproliferative factor by serving as a negative regulator of the cell cycle (Lee et al., 2014) to prevent uncontrolled cellular growth. In mediating responses to genotoxic stress, p53 can activate apoptosis if the cell has experienced extensive genome damage (Aubrey et al., 2018). This process is also likely to involve induction of the p53 downstream target gene *CDKN1A* (p21), which induces cell cycle arrest as described above (Brown et al., 2007).

Canonical apoptotic signalling results in activation of caspases, including *CASP3* (caspase-3), which commit the cell to apoptosis. This pathway is negatively regulated by anti-apoptotic genes including *BCL2* (Bcl-2) and related family members, as also outlined above, although *BCL2* is of particular relevance given the currently mixed evidence regarding its role in MM (Section 1.3.4 Role of the Apoptosis Proteins Caspase-3 and Bcl-2 in MM). Expression of all four of the aforementioned genes was investigated in CHL-1 cells, noting also that p53-mediated apoptosis has been previously characterised under H_2O_2-induced oxidative stress in glioma cells (Datta et al., 2002). The expression of *S100B* was also measured, given that it is one of the most strongly expressed S100 proteins in MM (as explained in Section 1.3.2 S100 Family Proteins in MM). Importantly, S100B is known to interact with p53 (van Dieck et al., 2010), which represents another regulatory mechanism that might affect apoptosis in MM cells.

Expression of the five aforementioned genes (*TP53*, *CDKN1A*, *BCL2*, *CASP3* and *S100B*) was measured at the transcriptional (i.e., mRNA) level using RT–qPCR (Section 1.6.3 Reverse Transcription–Quantitative PCR (RT-qPCR)) in conjunction with gene-specific primers. As outlined above, this method first involves reverse transcription of extracted cellular RNA to cDNA, to provide a template for PCR. By adding a fluorescent DNA-binding dye (SYBR Green) to PCR reactions, amplification of the target sequences can be followed in real time (using successive rounds of thermal cycling), and relative transcript levels can be determined by reference to a housekeeping gene (Figure 7); in this case, *ACTB* (β-actin).

4.2 Materials and Methods

The materials and equipment used in the RT–qPCR experiments are listed in Section 2.1 Materials(in Table 1 and Table 2, respectively). All stages of the experimental procedure, including final data analysis, are described in detail above, in Section 2.3.11 Gene Expression Analysis by RT–qPCR.

4.3 Results

4.3.1 Treatment Effects on Cell Cycle and Apoptosis Protein Expression

The transcriptional response to 120 µL CBSC-derived exosomes, 10 µM Se, or a combination of both, was investigated in stressed (PC; 75 µM H_2O_2) CHL-1 melanoma cells, for the stated target genes (*TP53*, *CDKN1A*, *BCL2*, *CASP3* and *S100B*). This experiment was intended to give insight into the molecular mechanisms underlying the observed cytotoxicity for all of these treatments. According to the findings of RT–qPCR, depicted in Figure 34, the PC conditions robustly induced the cell cycle genes *TP53* (p53) and *CDNK1A* (p21), along with the pro-apoptotic gene *CASP3* (caspase-3) (in all cases, *** $p \leq 0.001$), while *BCL2* and *S100B* were slightly downregulated, although the change was not statistically significant. In the treatment groups, similar effects were seen: 10 µM Se or 120 µL exosomes both significantly increased the same three upregulated genes relative to untreated cells (*** $p \leq 0.001$). However, for 10 µM Se, induction of all three upregulated genes was not as strong as for the PC, and in fact, *CDKN1A* was not significantly changed relative to the untreated cells. For 120 µL exosomes, the transcriptional response was only slightly attenuated relative to PC conditions, and the combination treatment (10 µM Se + 120 µL exosomes) showed slightly higher expression of all three genes. In all groups with H_2O_2, there was a substantial elevation in pro-apoptotic *CASP3* compared with untreated control cells (*** $p \leq 0.001$).

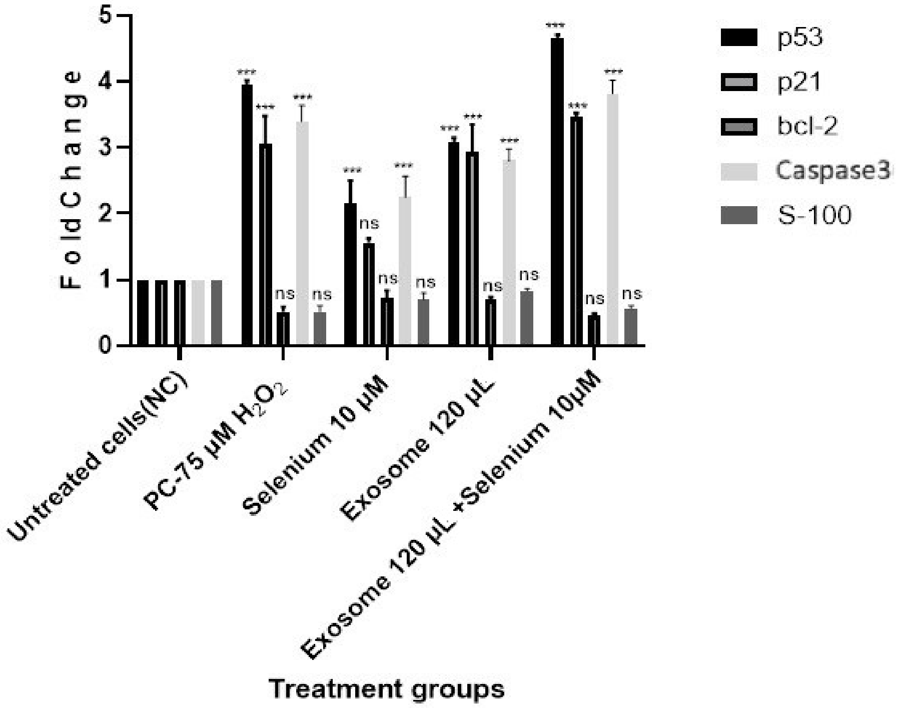

Figure 34. Effect of 10 µL Se, 120 µL exosomes, or both, in stressed (75 µM H_2O_2; PC) CHL-1 MM cells, on gene expression levels of *TP53* (p53), *CDKN1A* (p21), *BCL2* (Bcl-2), *CASP3* (caspase-3) and *S100B*. Relative expression levels were determined using the $2^{-\Delta\Delta CT}$ method with *ACTB* (β-actin) as internal housekeeping gene. All values denote the mean ± SEM of three independent experiments (*** p <0.001; ns = not significant).

4.4 Discussion

Under oxidative stress (75 µM H_2O_2), expression of *TP53*, *CDKN1A* and *CASP3* was strongly upregulated in CHL-1 MM cells (Figure 34). This suggests induction of canonical responses to DNA damage; namely, cell cycle arrest (*CDKN1A*) and apoptosis (*CASP3*), both mediated by *TP53*. In turn, these findings indicate that normal p53-mediated pathways are functional, at least to some extent, in CHL-1 cells, even though they carry a *TP53* mutation (Wu et al., 2017). Treatment with 10 µM Se appeared to dampen these responses—especially for *CDKN1A*, where the increase in mRNA levels was no longer statistically significant—and 120 µL exosomes had a similar, but more marginal, impact. Combined treatment, using the same concentrations of Se and exosomes together, appeared to amplify the transcriptional response slightly, and all three genes remained strongly significantly upregulated. Although there was some evidence for variation in *S100B* and the anti-apoptotic gene *BCL2* in all treatment groups, these expression changes were not statistically significant at the transcript level.

The above observations are potentially important, given that both treatments (Se and CBSC-derived exosomes) induced heightened cytotoxicity and genotoxicity in stressed CHL-1 cells (as reported earlier, in Section 3.3 Results). If the enhanced cell death with these treatments was mediated through p53-dependent apoptosis, it might be expected that *TP53*, *CDKN1A* and *CASP3* would be transcriptionally induced more strongly than under the PC conditions (75 µM H_2O_2), and perhaps much more so, but this was not the case. It therefore appears likely that the Se or exosome treatments, either individually or in combination, are able to induce cell death via p53-independent mechanisms (even when the p53-dependent pathway is still functional), or at least, by caspase-3-independent pathways. This is important because of the known mutation and/or inactivation of p53 commonly found in MM, as noted above (Box et al., 2014), and marks out the current therapeutic approach as a promising avenue for treatment of melanoma. To confirm these findings, expression changes at the protein level were also measured for the same genes, using Western blotting as the experimental approach. This is described in the next chapter.

5) Protein Expression Analysis (Western Blotting)

5.1 Introduction

The results of gene expression analysis using RT–qPCR showed substantial transcriptional upregulation for three of the five genes analysed (i.e., at the mRNA level), indicating that p53-mediated cell cycle arrest and apoptosis are activated in CHL-1 MM cells exposed to H_2O_2. The same genes generally remained significantly upregulated in the treatment groups with 10 µM Se, 120 µL exosomes, or both. To further understand the functional impact of the observed changes, and to validate the RT–qPCR results, it is important to also consider how expression is affected at the protein level.

This was approached using Western blotting, which is an ideal technique for this kind of analysis (as explained in Section 1.6.4 Western Blotting). Here, it was used to measure changes in the protein levels derived from the same five genes of interest (p53, p21, Bcl-2, caspase-3 and S100B), in the same MM cell line as above (CHL-1 cells), after exposure to 75 µM H_2O_2 and treatment with 10 µM Se, 120 µL exosomes, or both.

5.2 Materials and Methods

The materials and equipment used for Western blotting are listed in Section 2.1 Materials(in Table 1 and Table 2, respectively). All stages of the experimental procedure, including data analysis, are described in detail above, in Section 2.3.12 Western Blot Assay.

5.3 Results

5.3.1 Treatment Effects on Cell Cycle and Apoptosis Protein Expression

A series of Western blotting experiments was conducted, as described above, to evaluate the protein expression of p53, p21, Bcl-2, caspase-3 and S100B in melanoma cells exposed to 75 µM H_2O_2 and treated with 10 µM Se, 120 µL CBSC-derived exosomes, or both in combination. Analysis of the data revealed a significant upregulation in the expression of p53, p21 and caspase-3 proteins (Figure 35), in good general agreement with the RT–qPCR data. As before, the extent of upregulation was lowest for 10 µM Se alone, highest for the combination treatment, and intermediate for 120 µL exosomes only. The extent of upregulation (2–3-fold change) was slightly less than seen in the RT–qPCR results (3–4-fold change), but nevertheless, the Western blotting results support the conclusions drawn from the transcriptional analysis. More specifically, expression of p53 increased by 1.9-fold in 10 µM Se-treated cells (relative to NC). Under the same conditions, expression of p21 protein increased 1.6-fold and expression of caspase-3 by 1.8-fold. Exosome treatment showed stronger upregulation of p53, p21 and caspase-3, with increases of 2.2-, 2.0- and 1.9-fold, respectively, compared with the control group.

Interestingly, protein expression of Bcl-2 was significantly reduced, especially in the presence of exosomes (*** p <0.001). This is also consistent with apoptosis induction, since Bcl-2 is an anti-apoptotic factor. A reduction in S100B levels was also evident, although this change did not reach statistical significance in any case. As also depicted in Figure 35, the combination of Se and exosome treatment produced the strongest response, with significant (*** p <0.001) upregulation of the p53 (2.7-fold), p21 (2.4-fold) and caspase-3 (2.4-fold) proteins in oxidatively stressed (75 µM H_2O_2) CHL-1 melanoma cells. As already noted, these conditions resulted in downregulation of Bcl-2 and S100B at the protein level, although this was only significant for the former.

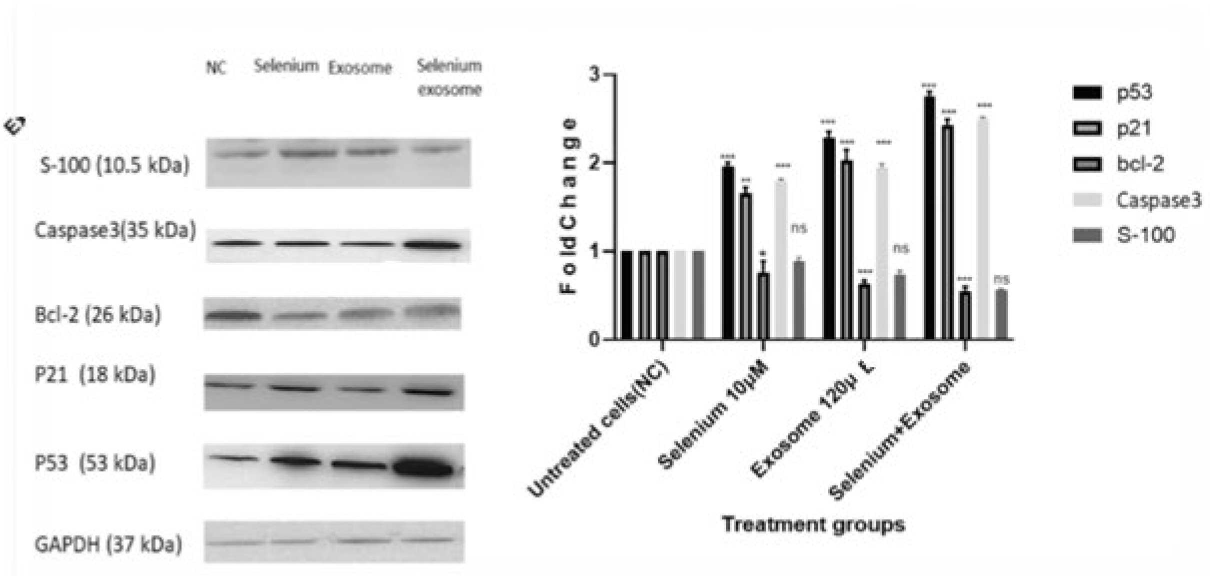

Figure 35. Effect of 10 µM Se, 120 µL exosomes, or both, on the protein expression levels of p53, p21, Bcl-2, caspase-3 and S100B in CHL-1 melanoma cells stressed with 75 µM H_2O_2. Relative quantification used GAPDH as an internal loading control. For all treatments, there was significant upregulation of the p53, p21 and caspase-3 proteins (with combination treatment producing the strongest effect), and there was also significant downregulation of Bcl-2 in all treatment groups. Data shows mean ± SEM values, n = 3 (* p <0.05, ** p <0.01, *** p <0.001, ns = not significant).

5.4 Discussion

In general, the Western blotting results support the conclusions from the RT–qPCR experiments, although the extent of upregulation of p53, p21 and caspase-3 was slightly less than at the mRNA level. Nevertheless, significant activation of apoptosis is clear in all treatment groups, especially for the combined Se and exosome treatment. Thus, induction of p53-mediated apoptosis is significant in CHL-1 MM cells. An important additional finding from the Western blotting experiments is downregulation of Bcl-2 in all treatment groups, but especially where the CBSC-derived exosomes were used (*** $p < 0.001$, Figure 35). This was apparent at the transcript level, but importantly, it reached statistical significance at the protein (i.e., functional) level. This is noteworthy for two reasons. First, it indicates repression of anti-apoptotic signalling, which may contribute to the cytotoxicity of these treatments towards melanoma cells, and is seemingly a desirable characteristic of a potential new cancer therapy. Second, it is important in the specific context of MM, since recent evidence suggests that high levels of Bcl-2 are found in at least a subset of melanoma patients, and may correlate with decreased survival (Trisciuoglio & Del Bufalo, 2021). Taken together, the RT–qPCR and Western blotting analysis, which has focused on key genes of interest, has identified relevant molecular mechanisms for the action of Se and CBSC-derived exosomes (especially when used in combination), on a melanoma cell line. This approach therefore appears to offer promise as a therapeutic strategy for MM.

6) General Discussion

6.1 Overview

The current study has investigated the impact of external Se and CBSC-derived exosomes on a melanoma cell line, in addition to lymphocytes from healthy individuals and MM patient donors. The aim has been to study the potential of using these agents as a safe and effective antioxidant and antitumour therapy in MM. As well as functional evidence, mechanistic understanding of potential new cancer therapies is also crucial, to help establish which patients will most benefit from them, but also to ensure a good therapeutic window (i.e., no harm to healthy cells). Here, we present both of these aspects of the present results in relation to current knowledge. As far as we are aware, no previous studies have focused on the combined effects of Se and CBSC-derived exosomes on DNA damage in human lymphocytes from MM patients, or in melanoma cells.

Here, peripheral lymphocytes were used to identify genotoxicity, since they are the most suitable option due to the ease of collection. Lymphocytes circulate throughout the body's organs and are present in the bloodstream, meaning that a significant proportion of them are exposed to both exogenous and endogenous substances that might cause genotoxic damage (Li, et al., 2010). Additionally, because subpopulations of lymphocytes survive for a long period and may have been exposed to mutagenic stresses and accumulating genomic damage for more than 40 years, they are an ideal model for studying genome sensitivity (Neel et al., 1989).

In this work, genotoxicity was assessed using the comet assay due to its sensitivity, simplicity, time-efficiency and cost-effectiveness for assessing the integrity of cellular DNA (Azqueta et al., 2022). It is a very economical, reliable and sensitive assay, and can also quickly and accurately identify the apoptotic effects of various therapies or medications in cells, thereby explaining its choice in this study. The alkaline comet assay is frequently applied to quantify DNA damage in peripheral human lymphocytes, which can be brought on by a variety of agents including mutagenic chemicals, oxidative stress and radiation. The information it provides is used to help protect people against potentially genotoxic exposures, for example, to harmful chemicals and pollutants (Dusinska & Collins, 2008). By measuring the ratio between two components—namely, the comet head (undamaged, non-migrating DNA) and comet tail (damaged, migrating DNA)—the assay allows for quantification of DNA damage. In this research, the OTM and % tail DNA parameters were used to express the extent of DNA damage, since they were previously found to be the most accurate indicators of this (Dusinska & Collins, 2008). Here, the comet assay was initially employed to identify the ideal H_2O_2 concentration that caused the most DNA damage. In cells from MM patients and lymphocytes from healthy individuals, 75 µM H_2O_2 was found to be optimal in this regard, and was therefore used for the remainder of the study.

In vitro investigations have often employed H_2O_2 to induce cellular oxidative stress, with earlier investigations identifying it as a contributing factor to DNA damage. Here, it was used as a model of MM-associated oxidative stress, which is increasingly emerging as a characteristic feature of the disease, as noted above (e.g., Emanuelli et al., 2022). The Fenton reaction [$Fe^{2+} + H_2O_2 \rightarrow Fe^{3+} + HO\cdot + HO^-$] produces hydroxyl free radicals from H_2O_2 in the presence of ferrous iron (Fe^{2+}). The hydroxyl radical ($HO\cdot$) is one of the main ROS that can damage DNA by accessing the nucleus through aquaporins, also called water channels, which can be expressed on the nuclear membrane. These radicals can damage DNA via multiple mechanisms; for example, by attacking the sugar component to cause single-stranded DNA breaks (Das et al., 2015).

We determined cell survival/viability, and the cytotoxicity of treatments, using the trypan blue dye exclusion method and CCK-8 assay, with lymphocytes from both healthy individuals and MM patients. Groups were included with Se treatment at different concentrations and for various time periods. Analysis of the trypan blue exclusion results demonstrated that cell viability remained within the range of 75–85% after 48 h of treatment with 10 µM Se. The CCK-8 assay gave similar results: cell survival did not drop below 80% in lymphocytes from healthy individuals and MM patients in any considered treatment group (
Figure **10**). However, the IC_{50} for Se in the CHL-1 melanoma cell line was estimated as 10 µM
(
Figure **11**).

Selenium has been under intense investigation for the last few years because of its potential use in MM treatment. Selenoproteins are now known as key mediators of redox homeostasis, including in MM, suggesting that melanoma sensitivity to free radical-inducing therapies, including ascorbate, may depend on Se (Jankowski & Rabinowitz, 2022). The effectiveness of Se is dependent on both the dosage and the chemical form. For example, methylselenol (MeSeH), a small-molecule metabolite that can be generated *in vivo* from various forms of Se (Zeng et al., 2009), triggers cell cycle arrest, induction of apoptosis, and induction of the unfolded protein response, in cell cultures. Prodrugs of MeSeH have also been found to be effective in melanoma prevention, and as treatment agents in both transgenic and xenograft models of human MM (Cassidy et al., 2013).

To explore the relationship between Se and cancer, The Nutritional Prevention of Cancer Trial (Karp et al., 2013), conducted three RCTs using Se as a cancer treatment in 2002. High levels of Se were used in each of these trials. The study authors concluded that high amounts were safe and well-tolerated, but offered no benefits over placebo (Algotar et al., 2013; Karp et al., 2013; Vinceti et al., 2018). However, recent observational and cohort studies have demonstrated efficacy for low-dose Se in cancer treatment; and as is evident from the results presented above, the current investigation does support this finding. Major cellular responses have been reported in pancreatic ductal adenocarcinoma (PDAC) cell lines, at sodium selenite (Na_2SeO_3) concentrations between 15–30 μM (Moro et al., 2022), and we were able to determine the ideal Se dosage for treating melanoma in the present study. According to our data, 10 μM Se is non-toxic for healthy cells but toxic to CHL-1 melanoma cells.

Having established low off-target cytotoxicity for Se, we then investigated its genotoxic effects on lymphocytes and melanoma cells. Lymphocytes from 20 healthy volunteers were exposed to three different dosages of Se (10 μM, 25 μM and 75 μM), with 10 μM Se also being evaluated for its protective effect against 75 μM H_2O_2 (PC). The comet assay revealed the least DNA damage at 10 μM (Figure 12 and Figure 13), with Se treatment showing a beneficial (albeit not statistically significant) effect on OTM and % tail DNA at both 10 μM and 25 μM. Importantly, 10 μM Se fully rescued the genotoxic effect of 75 μM H_2O_2. Therefore, the optimal concentration of Se was 10 μM. Our findings are in agreement with the study of Zuo et al. (2022), which also demonstrated excellent responses for 10 μM and 25 μM dosages of Se, in terms of both OTM and % tail DNA. In contrast, in the MM patient lymphocytes, 10 μM Se significantly reduced the DNA damage in comparison with untreated cells, in terms of both OTM and % tail DNA (*** $p < 0.001$; Figure 14 and Figure 15). Furthermore, when stressed (75 μM H_2O_2) MM lymphocytes were treated with 10 μM Se, the genotoxic impact was again significantly reduced.

The comet assay was also performed on the CHL-1 melanoma cell line, with Se treatment at the estimated IC_{50} concentration of 10 μM, either alone or in combination with oxidative stress (PC; 75 μM H_2O_2). In either case, Se exposure increased DNA damage in these cells (as judged by both OTM and % tail DNA), and caused significant DNA damage when combined with the PC conditions (Figure 18 and Figure 19). Thus, 10 μM Se is more genotoxic and more cytotoxic towards melanoma cells than it is towards healthy cells. These results in CHL-1 MM cells suggested that the observed cytotoxicity might stem from DNA damage-induced apoptosis.

To explore this possibility, expression of cell cycle (*TP53*, *CDKN1A*) and apoptosis (*TP53*, *BCL2*, *CASP3*) associated genes was assessed at the mRNA and protein levels using RT–qPCR and Western blotting, respectively. The results from the two techniques were generally in good agreement, and showed induction of cell cycle arrest and apoptosis in CHL-1 cells stressed with H_2O_2. Upon treatment with 10 µM Se, induction of *TP53* (p53) and caspase-3 (*CASP3*) was maintained, although the slight dampening in response (relative to PC conditions) also hinted that other mechanisms may be involved—e.g., suppression of Bcl-2 anti-apoptotic signalling—as discussed earlier (in Sections 4.4 Discussion and 5.4 Discussion). Additionally, no significant change was identified for the putative MM biomarker *S100B*, which has previously been shown to inhibit p53-dependent apoptosis in MM (including lower caspase-3 enzyme activity) (Lin et al., 2010). The fact that our treatment conditions did not induce this potential anti-apoptotic factor would therefore seem to be an advantage.

As illustrated by the above, it is generally known that Se compounds mainly exert their anticancer activity through apoptosis (Garbo et al., 2023), which includes activation of caspase-3 (i.e., the intrinsic apoptosis pathway). For example, sodium selenite (Na2SeO3) was able to induce caspase-3 activity in LNCaP prostate cancer cells, as measured by functional enzyme assay (Xiang et al., 2009). In another prostate cancer cell line (PC-3), sodium selenite (Na2SeO3) was found to downregulate Bcl-2 by using Western blotting (Chen et al., 2013). Various studies have investigated the anticancer effects of another important Se metabolite, methylseleninic acid (MSA), which has the chemical formula $MeSeO_2H$. This is an oxidised form of methylselenol that is derived from Se-containing amino acids (Tan et al., 2018). Qiu et al. (2019) used the CCK-8 assay to show that MSA reduces the viability of breast cancer cells, and also used combined Western blotting and RT–qPCR approaches to demonstrate downregulation of Bcl-2 and upregulation of caspase-3 in response to treatment, similarly to the results reported here.

However, with Se metabolites, other cell death pathways can be involved (Varlamova & Turovsky, 2021). In one important study, Lobb et al. (2018) investigated the anticancer properties of MSA. In healthy cells (peripheral blood mononuclear cells), this treatment downregulated caspase-8 (associated with the extrinsic apoptosis pathway) and increased glutathione levels, whereas the opposite effects were observed in malignant cells (THP-1 leukaemia cells); i.e., caspase-8 was upregulated and glutathione levels were depleted (Lobb et al., 2018). Thus, MSA may exert antitumour effects by two mechanisms: by activation of apoptosis, but also through increased ROS, which is consistent with other reports implicating elevated production of ROS in the anticancer properties of various Se metabolites (Kim et al., 2021).

In this study, Se may therefore have acted against CHL-1 melanoma cells in two important ways. First, the additional DNA damage induced by Se might be explained by the increased ROS production that it seems to promote selectively in cancer cells (Kim et al., 2021), which was not apparent in lymphocytes, consistent with the findings of Lobb et al. (2018). Second, it may activate the extrinsic apoptosis pathway (which is associated with caspase-8), as observed by the same authors in leukaemia cells, and also by Chen et al. (2013). This would be consistent with the interpretation of the RT–qPCR and Western blotting results suggested above (as mentioned in Section 4.4 Discussion), and it is quite plausible for both apoptosis pathways to be relevant, given that p53 can induce both caspase-3 and caspase-8 (Chen, 2016). Overall, these considerations offer a possible explanation for the observed effects with Se, and it would be interesting to investigate this further in future work.

In this study, we have also explored the effects of CBSC-derived exosomes on the same cell types as above. Exosomes carry information from the parent cells to other cells, meaning that they can exert a paracrine effect on both healthy and malignant cells. Here, we used CBSC-derived exosomes because numerous reports have documented their immunomodulatory properties and their value in managing cancer (Zhu et al., 2022). There has previously been some controversy over whether MSC-derived exosomes can inhibit or promote cancer cell proliferation, but Karaoz et al. (2019) recently demonstrated that exosomes derived from Wharton's jelly (WJ)—part of the umbilical cord—do not promote cancer growth, using multiple cell lines. Thus, some concerns over CBSC-derived exosomes for cancer treatment seem to have now been alleviated. However, defining the optimal dosage of these exosomes has not been the subject of many studies. Through the current experiments, we have determined the best dose for melanoma. The CBSC-derived exosomes were essentially non-toxic to lymphocytes from either healthy individuals or MM patients, over a range of doses, but they were cytotoxic towards CHL-1 MM cells with an estimated IC_{50} of 120 μM, according to the CCK-8 assay results (Figure 22). Using the comet assay, we found that treatment of lymphocytes from healthy individuals with 120 μM exosomes did not significantly alter DNA damage levels (Figure 23 and Figure 24), but the same treatment reduced DNA damage compared with untreated cells in

MM patient lymphocytes (Figure 25 and Figure 26). Furthermore, in the same set of experiments, treatment with 120 μL CBSC-derived exosomes exhibited a protective effect against H_2O_2-induced DNA damage in lymphocytes from both groups of donors.

In contrast, in the CHL-1 melanoma cell line, comet assay results showed that CBSC-derived exosome treatment (120 μM) significantly increased DNA damage in both stressed (PC) and unstressed (NC) cells (Figure 29 and Figure 30). Thus, these exosomes both inhibited the growth of cancer cells and induced significant genotoxicity, without causing such harmful effects in healthy lymphocytes. Analysis by RT–qPCR and Western blotting, focusing on the same five genes as above, indicated that p53- and p21-mediated cell cycle arrest, and caspase-3-dependent apoptosis, remained active in CHL-1 cells treated with 120 μL exosomes. At the protein level, there was also evidence for significant downregulation of Bcl-2 (*** $p < 0.001$) (Figure 35), supporting a pro-apoptotic effect of the CBSC-derived exosome treatment. As in the case of Se, no significant change in *S100B* was observed.

The present results for CBSC-derived exosome treatment are similarly in agreement with earlier research where exosomes derived from WJ stem cells were found to inhibit proliferation of T24 bladder cancer cells (Wu et al., 2013). Using Western blotting, the same authors showed that this effect was due to cell cycle arrest and apoptosis via upregulation of p53, p21 and caspase-3, as seen here. The exosomes also strongly inhibited tumour growth in mouse xenografts of the same cell line, presumably by the same mechanism. Similarly, Bruno et al. (2013) used bone marrow MSC-derived exosomes to inhibit the growth of three different cancer cell lines *in vitro* and *in vivo*. For example, in Kaposi's sarcoma cells, exosome treatment was associated with an approximately fivefold increase in p21 expression (by RT–qPCR) and caspase-3/7 activity (by functional assay). In another example, camel milk exosomes were shown to be more cytotoxic towards HepaRG hepatoma cells than normal liver cells (El-Kattawy et al., 2021). Comet assays revealed that the exosomes caused DNA damage in the cancer cells, and RT–qPCR experiments showed activation of apoptosis through upregulation of caspase-3 and downregulation of Bcl-2, in common with the results presented here.

Together, the aforementioned studies illustrate that exosome from diverse sources (generally originating from stem cells) can arrest tumour cell growth through genotoxicity and apoptosis. The current findings build on this previous work to establish the utility of CBSC-derived exosomes in MM, showing how they can similarly induce genotoxicity and apoptosis in melanoma cells. It is interesting to note, however, that exosomes derived from tumour cells appear to have the opposite effect, inducing anti-apoptotic signalling in both normal and transformed cells through upregulation of Bcl-2 and downregulation of caspase-3, at the protein level (Huang et al., 2019). This suggests that stem cell-derived exosomes, such as the CBSC-derived exosomes used here, can inhibit cancer growth by modifying the malignant phenotype through cellular reprogramming, in line with the evidence discussed earlier (Section 3.1 Introduction), to ‘tip the balance’ back towards apoptosis. The findings of this study, and those mentioned above, also suggest that this reprogramming may involve reactivation of cell cycle checkpoints (e.g., p21 induction), which are often inhibited in cancer, as mentioned earlier (Molinari, 2000).

In other studies, CBSC-derived exosomes have demonstrated immunomodulatory properties, as noted above, inducing peripheral tolerance and modulation of the immune response (Xin et al., 2012; Ludwig et al., 2012; Mokarizadeh et al., 2012). Such exosomes promote more proliferation and differentiation of endothelial cells than any other type of exosomes. Also, human umbilical cord MSC-derived exosomes have been found to kill liver cancer cells (Zhu et al., 2022) by preventing cellular growth and causing programmed cell death. Moreover, they prevented metastasis of the cancer cells. Exosomes therefore have an excellent treatment profile, and Xu et al. (2020) recently reviewed the preceding 10 years of work on utilisation of human umbilical cord MSC-derived exosomes in cancer treatment. According to their report, this class of exosomes will become the preferred method for treating cancers in the future (Xu et al., 2020). For example, exosomes have been suggested as a possible therapeutic strategy for PDAC, from various perspectives—namely, cellular reprogramming (to overcome drug resistance), immunomodulation and drug delivery (Papadakos et al., 2022)—but interestingly, a combination with antioxidant therapy (such as Se) does not yet seem to have been considered.

The most promising results from this study concern the additive effect of combined Se and CBSC-derived exosome treatment in CHL-1 MM cells. Both functionally (Figure 31, Figure 32 and Figure 33) and mechanistically (Figure 34 and Figure 35), the present findings suggest complementary and/or synergistic actions of these treatments in cancer cells. The combination treatment (10 μM Se + 120 μL CBSC-derived exosomes) caused more DNA damage in melanoma cells than either agent alone (Figure 32 and Figure 33), and was also associated with higher levels of cell cycle arrest (*TP53*, *CDKN1A*) and pro-apoptotic (*TP53*, *CASP3*) gene expression than the individual treatments (Figure 34 and Figure 35). The previous studies outlined above may offer some rationale for these findings. For example, Se (and its metabolites) can activate multiple mechanisms of cell death in cancer cells, including both the intrinsic and extrinsic apoptosis pathways, as well as through elevated DNA damage. On the other hand, CBSC-derived exosomes can induce cellular reprogramming to suppress anti-apoptotic signalling, attenuate the malignant phenotype, and activate the intrinsic apoptosis pathway. While there is some overlap in these functions, there are also differences, and these distinct functional profiles may explain the beneficial effects of the combination therapy seen here.

Building on this, some evidence points to a potential synergistic immunomodulatory effect of Se and CBSC-exosomes. Although the immune-modulating potential of the latter has already been mentioned, Se may also have immunomodulatory effects in cancer cells, especially given its known role in the immune system (as introduced in Section 1.5 Selenium and its Roles in Biology and Cancer). A study by Lennicke et al. (2017) identified expression changes in cell surface antigens in melanoma cells exposed to MSA, suggesting that Se might be able to restore normal T cell responses during immune surveillance; and in the context of this study, to complement the effects of exosome therapy. Thus, Se and CBSC-derived exosomes might represent a form of complementary cancer immunotherapy, as well as acting by distinct (but overlapping) mechanisms to induce greater genotoxicity and cytotoxicity in cancer cells than either treatment alone. Given these multiple modes of action, together with the current experimental results, this marks out the combination therapy described herein as a promising therapeutic strategy for MM.

In cancer therapy, exosomes have also been tried together with melatonin, as an alternative antioxidant to Se, with promising results so far (Alonso Novais et al., 2021); although the combination with Se appears to be new in this study, and certainly for MM (as noted above). Meanwhile, other research has suggested that including an additional antioxidant, such as ascorbic acid, may be able to further augment the anticancer effects of Se, since this combination was recently shown to increase apoptosis and reduce viability in both breast cancer (MCF-7) and colon cancer (HCT-116) cell lines (Ganash, 2021).

Finally, it is important to note that the present study is not an exhaustive investigation of all possible concentrations and combinations of Se and CBSC-derived exosomes for the treatment of MM; nevertheless, we have presented strong evidence that they can be beneficial for patients, with seemingly no substantial adverse effects on the immunogenic response of healthy individuals. However, further studies are required to establish a tighter timeline for translational research and clinical application.

6.2 Conclusion

For the treatment of MM, low-dose Se is a practical therapeutic approach. The use of high, optimal doses of CBSC-derived exosomes also appears promising in the treatment of this disease, and the present research may serve as a ‘standard shift’ towards more in-depth investigations; especially considering the *in vitro* results that were obtained for combination treatment, which we have consequently identified as the most promising approach. We now require preclinical studies—followed by clinical research with high sample numbers—to validate, optimise and administer effective MM therapy with ideal doses of Se and CBSC-derived exosomes. The next logical step would be to investigate the *in vivo* efficacy of our new combination treatment (Se plus CBSC-derived exosomes) in mouse models of MM, especially metastatic melanoma, where there is an urgent need for new treatments. The combination of Se and CBSC-derived exosomes could also be employed in targeted treatment for other illnesses, including various disorders where exosome treatments are also under investigation. The future prospects for CBSC-derived exosomes appear promising, as does the outlook for newer exosome mimetics in cancer treatment (Vázquez-Ríos et al., 2019). These mimetics have already been prepared from bone marrow-derived and umbilical cord-derived MSCs (Kalimuthu et al., 2018; Zhang et al., 2022), and the same technology could also be applied to CBSC-derived exosomes once their clinical use in MM treatment has been established.

6.3 Further Perspectives

The results presented in this *in vitro* study have shown that CBSC-derived exosomes and Se (an antioxidant) can decrease DNA damage in human lymphocytes from MM patients. The present work has also established that Se and CBSC-derived exosomes can protect lymphocytes against oxidative stress-associated DNA damage induced by H_2O_2. Moreover, the CBSC-derived exosomes exerted cytotoxic and pro-apoptotic effects against the CHL-1 MM cell line, perhaps through their induction of elevated DNA damage. The observed effects against cancer cells were stronger in combination with Se. Further research is required to fully identify the mechanism of action of these exosomes, and of the combination therapy with Se, to evaluate the impact of genotoxicity on apoptosis using Western blotting, RT–qPCR and other appropriate techniques to study relevant genes such as *TP53* and *CDKN1A*. The tumour suppressor *TP53* (p53) can induce apoptosis, perpetual (but short-lived) cell cycle arrest, metabolic homeostasis and DNA repair

(Aubrey et al., 2018). For example, the first p53 downstream target gene to be identified, *CDKN1A* (p21), encodes a CDK inhibitor that plays a prominent role in cell cycle regulation, and also has a critical role in tumour suppression by regulating DNA replication and repair (Georgakilas et al., 2017). When stimulated by p53, p21 binds to CDK2, causing downregulation of the latter and inducing G1 cell cycle arrest (Bostwick & Cheng, 2020) (i.e., preventing S phase entry). These processes, and related pathways, should be explored in more detail. Given the potential for treatment-associated p53-independent mechanisms of apoptosis, other options could be considered. These include the extrinsic pathway (as discussed above), and also the ERK1/2 pathway, whose activity can also be modulated by exosomes from a variety of sources, including CBSC-derived exosomes (Fröhlich et al., 2014; Wang et al., 2018).

References

Abbasi, N. R., Shaw, H. M., & Rigel, D. S. (2004). Early diagnosis of cutaneous melanoma: Revisiting the ABCD criteria. *Journal of the American Medical Association*, *292*(22), 2771–2776. https://doi.org/10.1001/jama.292.22.2771

Algotar, A. M., Hsu, C. H., Singh, P., & Stratton, S. P. (2013). Selenium supplementation has no effect on serum glucose levels in men at high risk of prostate cancer. *Journal of Diabetes*, *5*(4), 465–470. https://doi.org/10.1111/1753-0407.12041

Alonso Novais, A., de Almeida Chuffa, L. G., de Campos Zuccari, D. A. P., & Reiter, R. J. (2021). Exosomes and melatonin: Where their destinies intersect. *Frontiers in Immunology*, *12*, Article 692022. https://doi.org/10.3389/fimmu.2021.692022

Aubrey, B. J., Kelly, G. L., Janic, A., Herold, M. J. & Strasser, A. (2018). How does p53 induce apoptosis and how does this relate to p53-mediated tumour suppression? *Cell Death & Differentiation*, *25*, 104–113. https://doi.org/10.1038/cdd.2017.169

Avery, J. C., & Hoffmann, P. R. (2018). Selenium, selenoproteins, and immunity. *Nutrients*, *10*(9), Article 1203. https://doi.org/10.3390/nu10091203

Azqueta, A., Stopper, H., Zegura, B., Dusinska, M., & Møller, P. (2022). Do cytotoxicity and cell death cause false positive results in the *in vitro* comet assay? *Mutation Research/Genetic Toxicology and Environmental Mutagenesis*, *881*, Article 503520. https://doi.org/10.1016/j.mrgentox.2022.503520

Bajpayee M, Kumar A, Dhawan A. The comet assay: assessment of in vitro and in vivo DNA damage. Methods Mol Biol. 2013;1044:325-45. doi: 10.1007/978-1-62703-529-3_17. PMID: 23896885.

Barnum, K. J., & O'Connell, M. J. (2014). Cell cycle regulation by checkpoints. In E. Noguchi & M. Gadaleta (Eds.), *Cell cycle control. Methods in molecular biology, vol. 1170* (pp. 29–40). Humana Press. https://doi.org/10.1007/978-1-4939-0888-2_2

Beckett, G. J., & Arthur, J. R. (2005). Selenium and endocrine systems. *The Journal of Endocrinology*, *184*(3), 455–465. https://doi.org/10.1677/joe.1.05971

Bisevac, J. P., Djukic, M., Stanojevic, I., Stevanovic, I., Mijuskovic, Z., Djuric, A., Gobeljic, B., Banovic, T., & Vojvodic, D. (2018). Association between oxidative stress and melanoma progression. *Journal of Medical Biochemistry*, *37*(1), 12–20. https://doi.org/10.1515/jomb-2017-0040

Bostwick, D. G., & Cheng, L. (2020). Neoplasms of the prostate. In L. Cheng, G. T. Maclennan, & D. G. Bostwick (Eds.), *Urologic surgical pathology* (4th ed., pp. 415–525). Elsevier.

Boutry, J., Tissot, S., Ujvari, B., Capp, J.-P., Giraudeau, M., Nedelcu, A. M., & Thomas, F. (2022). The evolution and ecology of benign tumors. *Biochimica et Biophysica Acta (BBA) – Reviews on Cancer*, *1877*, Article 188643. https://doi.org/10.1016/j.bbcan.2021.188643

Box, N. F., Vukmer, T. Q., & Terzian, T. (2013). Targeting p53 in melanoma. *Pigment Cell & Melanoma Research*, *27*(1), 8–10. https://doi.org/10.1111/pcmr.12180

Brown, L., Boswell, S., Raj, L., & Lee, S. W. (2007). Transcriptional targets of p53 that regulate cellular proliferation. *Critical Reviews in Eukaryotic Gene Expression*, *17*(1), 73–86. https://doi.org/10.1615/CritRevEukarGeneExpr.v17.i1.50

Bruno, S., Collino, F., Deregibus, M. C., Grange, C., Tetta, C., & Camussi, G. (2013). Microvesicles derived from human bone marrow mesenchymal stem cells inhibit tumor growth. *Stem Cells and Development*, *22*(5), 758–771. https://doi.org/10.1089/scd.2012.0304

Bai, X., Shoushtari, A. N., Warner, A. B., Si, L., Tang, B., Cui, C., Yang, X., Wei, X., Quach, H. T., Cann, C. G., Zhang, M. Z., Pallan, L., Harvey, C., Kim, M. S., Kasumova, G., Sharova, T., Cohen, J. V., Lawrence, D. P., Freedman, C., Fadden, R. M., … Guo, J. (2022). Benefit and toxicity of programmed death-1 blockade vary by ethnicity in patients with advanced melanoma: An international multicentre observational study. *British Journal of Dermatology*, *187*(3), 401–410. https://doi.org/10.1111/bjd.21241

Cannavò, S. P., Tonacci, A., Bertino, L., Casciaro, M., Borgia, F., & Gangemi, S. (2019). The role of oxidative stress in the biology of melanoma: A systematic review. *Pathology – Research and Practice*, *215*(1), 21–28. https://doi.org/10.1016/j.prp.2018.11.020

Cassidy, P. B., Fain, H. D., Cassidy Jr, J. P., Tran, S. M., Moos, P. J., Boucher, K. M., Gerads, R., Florell, S. R., Grossman, D., & Leachman, S. A. (2013). Selenium for the prevention of cutaneous melanoma. *Nutrients, 5*, 725–749. https://doi.org/10.3390/nu5030725

Cavalcante, G. C., Schaan, A. P., Cabral, G. F., Santana-da-Silva, M. N., Pinto, P., Vidal, A. F., & Ribeiro-dos-Santos, Â. (2019). A cell's fate: An overview of the molecular biology and genetics of apoptosis. *International Journal of Molecular Sciences*, *20*(17), Article 4133. https://doi.org/10.3390/ijms20174133

Chatterjee, N., & Walker, G. C. (2017). Mechanisms of DNA damage, repair, and mutagenesis. *Environmental and Molecular Mutagenesis*, *58*(5), 235–263. https://doi.org/10.1002/em.22087

Chen, J. (2016). The cell-cycle arrest and apoptotic functions of p53 in tumor initiation and progression. *Cold Spring Harbor Perspectives in Biology*, *6*, Article a026104. https://doi.org/10.1101/cshperspect.a026104

Chen, P., Wang, L., Li, N., Liu, Q., & Ni, J. (2013). Comparative proteomics analysis of sodium selenite-induced apoptosis in human prostate cancer cells. *Metallomics*, *5*(5), 541–550. https://doi.org/10.1039/c3mt00002h

Chung, J. H., & Bunz, F. (2010). CDK2 is required for p53-independent G_2/M checkpoint control. *PLoS Genetics*, *6*(2), Article e1000863. https://doi.org/10.1371/journal.pgen.1000863

Colicchia, M., Jones, D. A., Beirne, A. M., Hussain, M., Weeraman, D., Rathod, K., Veerapen, J., Lowdell, M., & Mathur, A. (2019). Umbilical cord-derived mesenchymal stromal cells in cardiovascular disease: Review of preclinical and clinical data. *Cytotherapy*, *21*(10), 1007–1018. https://doi.org/10.1016/j.jcyt.2019.04.056

Cordelli, E., Bignami, M., & Pacchierotti, F. (2021). Comet assay: A versatile but complex tool in genotoxicity testing. *Toxicology Research*, *10*(1), 68–78. https://doi.org/10.1093/toxres/tfaa093

Cortéz-Gutiérrez, E. I., Dávila-Rodríguez, M. I., Fernández, J. L., López-Fernández, C., Gosálbez, A., & Gosálvez, J. (2011). New application of the comet assay: Chromosome–comet assay. *Journal of Histochemistry & Cytochemistry*, *59*(7), 655–660. https://doi.org/10.1369/0022155411410884

Coyle, C. H., Martinez, L. J., Coleman, M. C., Spitz, D. R., Weintraub, N. L., & Kader, K. N. (2006). Mechanisms of H_2O_2-induced oxidative stress in endothelial cells. *Free Radical Biology and Medicine*, *40*(12), 2206–2213. https://doi.org/10.1016/j.freeradbiomed.2006.02.017

Cui, X., Chen, H., Zhang, Q., Xu, M., Yuan, G., & Zhou, J. (2019). Exploration of the structure and recognition of a G-quadruplex in the *HER2* proto-oncogene promoter and its transcriptional regulation. *Scientific Reports*, *9*, Article 3966. https://doi.org/10.1038/s41598-019-39941-5

Da Silva, M. T., Silva-Jardim, I., & Thiemann, O. H. (2014). Biological implications of selenium and its role in *Trypanosomiasis* treatment. *Current Medicinal Chemistry*, *21*(15), 1772–1780. https://doi.org/10.2174/0929867320666131119121108

D'Arrigo, D., Roffi, A., Cucchiarini, M., Moretti, M., Candrian, C., & Filardo, G. (2019). Secretome and extracellular vesicles as new biological therapies for knee osteoarthritis: A systematic review. *Journal of Clinical Medicine*, *8*(11), Article 1867. https://doi.org/10.3390/jcm8111867

Das, T. K., Wati, M. R., & Fatima-Shad, K. (2015). Oxidative stress gated by Fenton and Haber Weiss reactions and its association with Alzheimer's disease. *Archives of Neuroscience*, *2*(2), Article e60038. https://doi.org/10.5812/archneurosci.20078

Datta, K., Babbar, P., Srivastava, T., Sinha, S., & Chattopadhyay, P. (2002). p53-dependent apoptosis in glioma cell lines in response to hydrogen peroxide induced oxidative stress. *The International Journal of Biochemistry & Cell Biology*, *34*(2), 148–157. https://doi.org/10.1016/S1357-2725(01)00106-6

Davis, L. E., Shalin, S. C., & Tackett, A. J. (2019). Current state of melanoma diagnosis and treatment. *Cancer Biology & Therapy*, *20*(11), 1366–1379. https://doi.org/10.1080/15384047.2019.1640032

Dixit, P., & Katare, R. (2015). Challenges in identifying the best source of stem cells for cardiac regeneration therapy. *Stem Cell Research & Therapy*, *6*(1), Article 26. https://doi.org/10.1186/s13287-015-0010-8

Döhner, H., Weisdorf, D. J., & Bloomfield, C. D. (2015). Acute myeloid leukemia. *The New England Journal Of Medicine*, *373*(12), 1136–1152. https://doi.org/10.1056/nejmra1406184

Donato, R., Cannon, B. R., Sorci, G., Ruizzi, F., Hsu, K., Weber, D. J., & Geczy, C. L. (2013). Functions of S100 proteins. *Current Molecular Medicine*, *13*(1), 24–57. https://doi.org/10.2174/156652413804486214

Đorđević Brlek, Z., Radoš, J., Bradamante, M., & Jurakić Tončić, R. (2019). Melanoma with comedo-like openings: A rare dermoscopic finding. *Dermatology Practical & Conceptual*, *9*(2), 148–149. https://doi.org/10.5826/dpc.0902a12

Dunkenberger, L., Reiss, K., & Del Valle, L. (2022). Comet assay for the detection of single and double-strand DNA breaks. In L. Del Valle (Ed.), *Immunohistochemistry and immunocytochemistry: Methods and protocols. Methods in molecular biology, vol. 2422* (pp. 263–269). Humana Press. https://doi.org/10.1007/978-1-0716-1948-3_18

Dusinska, M., & Collins, A. R. (2008). The comet assay in human biomonitoring: Gene–environment interactions. *Mutagenesis*, *23*(3), 191–205. https://doi.org/10.1093/mutage/gen007

Duthie, S. J., Collins, A. R., Duthie, G. G., & Dobson, V. L. (1999). Quercetin and myricetin protect against hydrogen peroxide-induced DNA damage (strand breaks and oxidised pyrimidines) in human lymphocytes. *Mutation Research/Genetic Toxicology and Environmental Mutagenesis*, *393*(3), 223–231. https://doi.org/10.1016/S1383-5718(97)00107-1

Eischen, C. M. (2016). Genome stability requires p53. *Cold Spring Harbor Perspectives in Biology*, *6*, Article a026096. https://doi.org/10.1101/cshperspect.a026096

El-Kattawy, A. M., Algezawy, O., Alfaifi, M. Y., Noseer, E. A., Hawsawi, Y. M., Alzahrani, O. R., Algarni, A., Kahilo, K. A., & El-Magd, M. A. (2021). Therapeutic potential of camel milk exosomes against HepaRG cells with potent apoptotic, anti-inflammatory, and anti-angiogenesis effects for colostrum exosomes. *Biomedicine & Pharmacotherapy*, *143*, Article 112220. https://doi.org/10.1016/j.biopha.2021.112220

Emanuelli, M., Sartini, D., Molinelli, E., Campagna, R., Pozzi, V., Salvolini, E., Simonetti, E., Campanati, A., & Offidani, A. (2022). The double-edged sword of oxidative stress in skin damage and melanoma: From pathophysiology to therapeutical approaches. *Antioxidants*, *11*(4), Article 612. https://doi.org/10.3390/antiox11040612

Falk, M. H., & Issels, R. D. (2001). Hyperthermia in oncology. *International Journal of Hyperthermia*, *17*(1), 1–18. https://doi.org/10.1080/02656730118511

Felicetti, F., De Feo, A., Coscia, C., Puglisi, R., Pedini, F., Pasquini, L., Bellenghi, M., Errico, M. C., Pagani, E., & Carè, A. (2016). Exosome-mediated transfer of miR-222 is sufficient to increase tumor malignancy in melanoma. *Journal of Translational Medicine*, *14*, Article 56. https://doi.org/10.1186/s12967-016-0811-2

Fernandes, A. R., dos Santos, T., Granja, P. L., Sanchez-Lopez, E., Santini, A., Garcia, M. L., Silva, A. M., & Souto, E. B. (2021). DABCO-customized nanoemulsions: Characterization, cell viability and genotoxicity in retinal pigmented epithelium and microglia cells. *Pharmaceutics*, *13*(10), Article 1652. https://doi.org/10.3390/pharmaceutics13101652

Filosa, A., & Filosa, G. (2018). Melanoma diagnosis: The importance of histopathological report. *Dermatopathology*, *5*(1), 41–43. https://doi.org/10.1159/000486670

Friedman, R. J., Rigel, D. S., & Kopf, A. W. (1985). Early detection of malignant melanoma: The role of physician examination and self-examination of the skin. *CA: A Cancer Journal for Clinicians*, *35*(3), 130–151. https://doi.org/10.3322/canjclin.35.3.130

Fröhlich, D., Kuo, W. P., Frühbeis, C., Sun, J.-J., Zehendner, C. M., Luhmann, H. J., Pinto, S., Toedling, J., Trotter, J., & Krämer-Albers, E.-M. (2014). Multifaceted effects of oligodendroglial exosomes on neurons: Impact on neuronal firing rate, signal transduction and gene regulation. *Philosophical Transactions of the Royal Society B*, *369*(1652), Article 20130510. https://doi.org/10.1098/rstb.2013.0510

Fulda, S., & Debatin, K.-M. (2006). Extrinsic versus intrinsic apoptosis pathways in anticancer chemotherapy. *Oncogene*, *25*, 4798–4811. https://doi.org/10.1038/sj.onc.1209608

Gandini, S., Autier, P., & Boniol, M. (2011). Reviews on sun exposure and artificial light and melanoma. *Progress in Biophysics and Molecular Biology*, *107*(3), 362–366. https://doi.org/10.1016/j.pbiomolbio.2011.09.011

Gao, Y., Gao, W., Chen, X., Cha, N., Wang, X., Jia, X., Wang, B., Ren, M., & Ren, J. (2016). Enhancing the treatment effect on melanoma by heat shock protein 70-peptide complexes purified from human melanoma cell lines. *Oncology Reports*, *36*(3), 1243–1250. https://doi.org/10.3892/or.2016.4947

Ganash, M. A. (2021). Anticancer potential of ascorbic acid and inorganic selenium on human breast cancer cell line MCF-7 and colon carcinoma HCT-116. *Journal of Cancer Research and Therapeutics*, *17*(1), 122–129. https://doi.org/10.4103/jcrt.jcrt_989_17

Garbo, S., Di Giacomo, S., Łażewska, D., Honkisz-Orzechowska, E., Di Sotto, A., Fioravanti, R., Zwergel, C., & Battistelli, C. (2023). Selenium-containing agents acting on cancer—a new hope? *Pharmaceutics*, *15*(1), Article 104. https://doi.org/10.3390/pharmaceutics15010104

García-Silva, S., & Peinado, H. (2016). Melanosomes foster a tumour niche by activating CAFs. *Nature Cell Biology*, *18*, 911–913. https://doi.org/10.1038/ncb3404

Georgakilas, A. G., Martin, O. A., & Bonner, W. M. (2017). p21: A two-faced genome guardian. *Trends in Molecular Medicine*, *23*(4), 310–319. https://doi.org/10.1016/j.molmed.2017.02.001

Gilani, S. J., Imam, S. S., Jafar, M., Alshehri, S., Taleuzzaman, M., & Jahangir, M. A. (2021). Curcumin nanomedicine and their application in the management of disease. In M. Rahman, S. Beg, M. A. Zamzami, H. Choudhry, A. Ahmad, & K. S. Alharbi (Eds.), *Biomarkers as targeted herbal drug discovery* (pp. 43–63). Apple Academic Press.

Girard, P. M., Francesconi, S., Pozzebon, M., Graindorge, D., Rochette, P., Drouin, R., & Sage, E. (2011). UVA-induced damage to DNA and proteins: Direct versus indirect photochemical processes. *Journal of Physics: Conference Series*, *261*, Article 012002. https://doi.org/10.1088/1742-6596/261/1/012002

Gottesman, M. M., Lavi, O., Hall, M. D., & Gillet, J.-P. (2016). Toward a better understanding of the complexity of cancer drug resistance. *Annual Review of Pharmacology and Toxicology*, *56*, 85–102. https://doi.org/10.1146/annurev-pharmtox-010715-103111

Goydos, J. S., & Shoen, S. L. (2016). Acral lentiginous melanoma. In H. L. Kaufman & J. M. Mehnert (Eds.), *Melanoma* (pp. 321–329). Springer. https://doi.org/10.1007/978-3-319-22539-5_14

Grau-Pérez, M., Borrego, L., Carretero, G., Almeida, P., & Cano, J. (2022). Assessing the effect Of environmental and socio-economic factors on skin melanoma incidence: An island-wide spatial study in Gran Canaria (Spain), 2007–2018. *Cancer Causes & Control*, *33*(10), 1261–1272. https://doi.org/10.1007/S10552-022-01614-6

Gupta, A., Kashte, S., Gupta, M., Rodriguez, H. C., Gautam, S. S., & Kadam, S. (2020). Mesenchymal stem cells and exosome therapy for Covid-19: Current status and future perspective. *Human Cell*, *33*(4), 907–918. https://doi.org/10.1007/s13577-020-00407-w

Haider, A., Kanwal, A., Nadeem, H., Azeem, F., Zameer, R., Rafique, M. U., & Rasul, I. (2022). Applications of nanoparticles-based enzymes in the diagnosis of diseases. In T. A. Inamuddin, J. N. Cruz, & M. Luqman (Eds,), *Nanomaterial-supported enzymes* (pp. 162–191). Materials Research Forum LLC.

Hall, M. D., Handley, M. D., & Gottesman, M. M. (2009). Is resistance useless? Multidrug resistance and collateral sensitivity. *Trends in Pharmacological Sciences*, *30*(10), 546–556. https://doi.org/10.1016/j.tips.2009.07.003

Hanel, W., & Moll, U. M. (2012). Links between mutant p53 and genomic instability. *Journal of Cellular Biochemistry*, *113*(2), 433–439. https://doi.org/10.1002/jcb.23400

Hazen, B. P., Bhatia Ac Fau - Zaim, T., Zaim T Fau - Brodell, R. T., & Brodell, R. T. (1999). The clinical diagnosis of early malignant melanoma: Expansion of the ABCD criteria to improve diagnostic sensitivity. *Dermatology Online Journal*, 5*(2)*, Article 3.

Heistein, J. B., Acharya, U., & Mukkamalla, S. K. R. (2022). Malignant melanoma. In *Statpearls*. Statpearls Publishing. https://www.ncbi.nlm.nih.gov/books/NBK470409/

Henderson, L., Wolfreys, A., Fedyk, J., Bourner, C., & Windebank, S. (1998). The ability of the comet assay to discriminate between genotoxins and cytotoxins. *Mutagenesis*, *13*(1), 89–94. https://doi.org/10.1093/mutage/13.1.89

Heo, J., & Kang, H. (2022). Exosome-based treatment for atherosclerosis. *International Journal of Molecular Sciences*, *23*(2), Article 1002. https://doi.org/10.3390/ijms23021002

Hida, T., Kamiya, T., Kawakami, A., Ogino, J., Sohma, H., Uhara, H., & Jimbow, K. (2020). Elucidation of melanogenesis cascade for identifying pathophysiology and therapeutic approach of pigmentary disorders and melanoma. *International Journal Of Molecular Sciences*, *21*(17), Article 6129. https://doi.org/10.3390/ijms21176129

Hu, W., Song, X., Yu, H., Sun, J., & Zhao, Y. (2020). Released exosomes contribute to the immune modulation of cord blood-derived stem cells. *Frontiers in Immunology*, *11*, Article 165. https://doi.org/10.3389/fimmu.2020.00165

Huang, A. C., & Zappasodi, R. (2022). A decade of checkpoint blockade immunotherapy in melanoma: Understanding the molecular basis for immune sensitivity and resistance. *Nature Immunology*, *23*(5), 660–670. https://doi.org/10.1038/s41590-022-01141-1

Huang, J., Ding, Z., Luo, Q., & Xu, W. (2019). Cancer cell-derived exosomes promote cell proliferation and inhibit cell apoptosis of both normal lung fibroblasts and non-small cell lung cancer cell through delivering alpha-smooth muscle actin. *American Journal of Translational Research*, *11*(3), 1711–1723.

Huang, M. B., Gao, Z., Xia, M., Zhao, X., Fan, X., Lin, S., Zhang, L., Huang, L., Wei, A., Zhou, H., Wu, J. Y., Roth, W. W., Bond, V. C., & Leng, J. (2022). Improved Aitongxiao prescription (I-ATXP) induces apoptosis, cell cycle arrest and blocks exosomes release in hepatocellular carcinoma (HCC) cells. *International Journal of Physiology, Pathophysiology and Pharmacology*, *14*(2), 90–113.

Huang, Z., Rose, A. H., & Hoffmann, P. R. (2012). The role of selenium in inflammation and immunity: From molecular mechanisms to therapeutic opportunities. *Antioxidants & Redox Signaling*, *16*(7), 705–743. https://doi.org/10.1089/ars.2011.4145

Hussein, M. R., Haemel, A. K., & Wood, G. S. (2003). Apoptosis and melanoma: Molecular mechanisms. *The Journal of Pathology*, *199*(3), 275–288. https://doi.org/10.1002/path.1300

Intranuovo, G., Schiavulli, N., Cavone, D., Birtolo, F., Cocco, P., Vimercati, L., Macinagrossa, L., Giordano, A., Perrone, T., Ingravallo, G., Mazza, P., Strusi, M., Spinosa, C., Specchia, G., & Ferri, G. M. (2018). Assessment of DNA damages in lymphocytes of agricultural workers exposed to pesticides by comet assay in a cross-sectional study. *Biomarkers*, *23*(5), 462–473. https://doi.org/10.1080/1354750X.2018.1443513

Istlifi, E. S., Hüsunet, M. T., & İla, H. B. (2019). Cell division, cytotoxicity, and the assays used in the detection of cytotoxicity. In E. S. Istlifi & H. B. İla (Eds.), *Cytotoxicity – definition, identification, and cytotoxic compounds*. IntechOpen. https://doi.org/10.5772/intechopen.88368

Jankowski, C. S. R., & Rabinowitz, J. D. (2022). Selenium modulates cancer cell response to pharmacologic ascorbate. *Cancer Research*, *82*(19), 3486–3498. https://doi.org/10.1158/0008-5472.can-22-0408

Jenkins, R. W., & Fisher, D. E. (2021). Treatment of advanced melanoma in 2020 and beyond. *Journal of Investigative Dermatology*, *141*(1), 23–31. https://doi.org/10.1016/j.jid.2020.03.943

Jerome-Morais, A., Bera, S., Rachidi, W., Gann, P. H., & Diamond, A. M. (2013). The effects of selenium and the GPx-1 selenoprotein on the phosphorylation of H2AX. *Biochemica et Biophysica Acta (BBA) – General Subjects*, *1830*(6), 3399–3406. https://doi.org/10.1016/j.bbagen.2013.03.010

Kalimuthu, S., Gangadaran, P., Rajendran, R. L., Zhu, L., Oh, J. M., Lee, H. W., Gopal, A., Baek, S. H., Jeong, S. Y., Lee, S.-W., Lee, J., & Ahn, B.-C. (2018). A new approach for loading anticancer drugs into mesenchymal stem cell-derived exosome mimetics for cancer therapy. *Frontiers in Pharmacology*, *9*, Article 1116. https://doi.org/10.3389/fphar.2018.01116

Kallini, J. R., Hamed, N., & Khachemoune, A. (2015). Squamous cell carcinoma of the skin: Epidemiology, classification, management, and novel trends. *International Journal of Dermatology*, *54*(2), 130–140. https://doi.org/10.1111/ijd.12553

Kallini, J. R., Jain, S. K., & Khachemoune, A. (2013). Lentigo maligna: Review of salient characteristics and management. *American Journal of Clinical Dermatology*, *14*, 473–480. https://doi.org/10.1007/s40257-013-0044-6

Karami Fath, M., Azargoonjahromi, A., Jafari, N., Mehdi, M., Alavi, F., Daraei, M., Mohammadkhani, N., Mueller, A. L., Brockmueller, A., Shakibaei, M., & Payandeh, Z. (2022). Exosome application in tumorigenesis: Diagnosis and treatment of melanoma. *Medical Oncology*, *39*(2), Article 19. https://doi.org/10.1007/s12032-021-01621-8

Karaoz, E., Sun, E., & Demir, C. S. (2019). Mesenchymal stem cell-derived exosomes do not promote the proliferation of cancer cells *in vitro*. *International Journal of Physiology, Pathophysiology and Pharmacology*, *11*(4), 177–189.

Karp, D. D., Lee, S. J., Keller, S. M., Wright, G. S., Aisner, S., Belinsky, S. A., Johnson, D. H., Johnston, M. R., Goodman, G., & Clamon, G. (2013). Randomized, double-blind, placebo-controlled, phase III chemoprevention trial of selenium supplementation in patients with resected stage I non-small-cell lung cancer: ECOG 5597. *Journal of Clinical Oncology*, *31*(33), 4179–4187. https://doi.org/10.1200/JCO.2013.49.2173

Khan, A. Q., Travers, J. B., & Kemp, M. G. (2018). Roles of UVA radiation and DNA damage responses in melanoma pathogenesis. *Environmental and Molecular Mutagenesis*, *59*(5), 438–460. https://doi.org/10.1002/em.22176

Khan, M. A., Singh, D., Ahmad, A., & Siddique, H. R. (2021). Revisiting inorganic nanoparticles as promising therapeutic agents: A paradigm shift in oncological theranostics. *European Journal of Pharmaceutical Sciences*, *164*, Article 105892. https://doi.org/10.1016/j.ejps.2021.105892

Kim, D. P., Kus, K. J. B., & Ruiz, E. (2019). Basal cell carcinoma review. *Hematology/Oncology Clinics*, *33*(1), 13–24. https://doi.org/10.1016/j.hoc.2018.09.004

Kim, J., & Zaret, K. S. (2015). Reprogramming of human cancer cells to pluripotency for models of cancer progression. *EMBO Journal*, *34*, 739–747. https://doi.org/10.15252/embj.201490736

Kim, S. J., Choi, M. C., Park, J. M., & Chung, A. S. (2021). Antitumor effects of selenium. *International Journal of Molecular Sciences*, *22*(21), Article 11844. https://doi.org/10.3390/ijms222111844

Kim, Y.-S., Park, G. S., Bang, C. H., & Chung, Y.-J. (2022). Genomic landscape of multiple Bowen's disease using whole-exome sequencing. *The Journal of Dermatology*. Advance online publication. https://doi.org/10.1111/1346-8138.16584

Kocarnik, J. M., Compton, K., Dean, F. E., Fu, W., Gaw, B. L., Harvey, J. D., Henrikson, H. J., Lu, D., Pennini, A., Xu, R., Ababneh, E., Abbasi-Kangevari, M., Abbastabar, H., Abd-Elsalam, S. M., Abdoli, A., Abedi, A., Abidi, H., Abolhassani, H., Adedeji, I. A., … Force, L. M. (2022). Cancer incidence, mortality, years of life lost, years lived with disability, and disability-adjusted life years for 29 cancer groups from 2010 to 2019: A systematic analysis for the Global Burden Of Disease Study 2019. *JAMA Oncology*, *8*(3), 420–444. https://doi.org/10.1001/jamaoncol.2021.6987

Kurien, B. T., & Scofield, R. H. (2006). Western blotting. *Methods*, *38*(4), 283–293. https://doi.org/10.1016/j.ymeth.2005.11.007

Lacy, K. E., Karagiannis, S. N., & Nestle, F. O. (2012). Advances in the treatment of melanoma. *Clinical Medicine Journal*, *12*(2), 168–171. https://doi.org/10.7861/clinmedicine.12-2-168

Lee, D.-H., Ha, J.-H., Kim, Y., Jang, M., Park, S. J., Yoon, H. S., Kim, E.-H., Bae, K.-H., Park, B. C., Park, S. G., Yi, G.-S., & Chi, S.-W. (2014). A conserved mechanism for binding of p53 DNA-binding domain and anti-apoptotic Bcl-2 family proteins. *Molecules and Cells*, *37*(3), 264–269. https://doi.org/10.14348/molcells.2014.0001

Lee, E. Y. H. P., & Muller, W. J. (2010). Oncogenes and tumor suppressor genes. *Cold Spring Harbor Perspectives in Biology*, *2*, Article a003236. https://doi.org/10.1101/cshperspect.a003236

Lennicke, C., Rahn, J., Bukur, J., Hochgräfe, F., Wessjohann, L. A., Lichtenfels, R., & Seliger, B. (2017). Modulation of MHC class I surface expression in B16F10 melanoma cells by methylseleninic acid. *OncoImmunology*, *6*(6), Article e1259049. https://doi.org/10.1080/2162402X.2016.1259049

Lens, M. B., & Eisen, T. G. (2003). Systemic chemotherapy in the treatment of malignant melanoma. *Expert Opinion on Pharmacotherapy*, *4*(12), 2205–2211. https://doi.org/10.1517/14656566.4.12.2205

Lewis, S. E., & Aitken, R. J. (2005). DNA damage to spermatozoa has impacts on fertilization and pregnancy. *Cell And Tissue Research*, *322*(1), 33–41. https://doi.org/10.1007/s00441-005-1097-5

Li, C., Zhou, T., Chen, J., Li, R., Chen, H., Luo, S., Chen, D., Cai, C., & Li, W. (2022). The role of exosomal miRNAs in cancer. *Journal Of Translational Medicine*, *20*(1), Article 6. https://doi.org/10.1186/s12967-021-03215-4

Li, X., Pei, D., & Zheng, H. (2014). Transitions between epithelial and mesenchymal states during cell fate conversions. *Protein & Cell*, *5*, 580–591. https://doi.org/10.1007/s13238-014-0064-x

Li, X., Liu, L., Yang, J., Yu, Y., Chai, J., Wang, L., Ma, L. & Yin, H. (2016). Exosome derived from human umbilical cord mesenchymal stem cell mediates miR-181c attenuating burn-induced excessive inflammation. *eBioMedicine*, *8*, 72–82. https://doi.org/10.1016/j.ebiom.2016.04.030

Li, Y., Shen, M., Jin, C., Gao, L., Liang, B., Wang, Z., Tan, S., Chen, A., Zhang, F., & Zhang, Z. (2020). Regulation of ferroptosis by ncRNA: A new direction. *IUBMB Life*, *72*(11), 2290–2302. https://doi.org/10.1002/iub.2381

Li, Z., Branham, W. S., Dial, S. L., Wang, Y., Guo, L., Shi, L., & Chen, T. (2010). Genomic analysis of microRNA time-course expression in liver of mice treated with genotoxic carcinogen *N*-ethyl-*N*-nitrosourea. *BMC Genomics*, *11*, Article 609. https://doi.org/10.1186/1471-2164-11-609

Lin, J., Yang, Q., Wilder, P. T., Carrier, F., & Weber, D. J. (2010). The calcium-binding protein S100B down-regulates p53 and apoptosis in malignant melanoma. *Journal of Biological Chemistry*, *285*(35), 27487–27498. https://doi.org/10.1074/jbc.M110.155382

Lin, P., Tian, X.-H., Yi, Y.-S., Jiang, W.-S., Zhou, Y.-J., & Cheng, W.-J. (2015). Luteolin-induced protection of H_2O_2-induced apoptosis in PC12 cells and the associated pathway. *Molecular Medicine Reports*, *12*(5), 7699–7704. https://doi.org/10.3892/mmr.2015.4400

Linares, M. A., Zakaria, A., & Nizran, P. (2015). Skin cancer. *Primary Care: Clinics in Office Practice*, *42*(4), 645–59. https://doi.org/10.1016/j.pop.2015.07.006

Liu, M., Du, H., Khan, A. R., Ji, J., Yu, A., & Zhai, G. (2018a). Redox/enzyme sensitive chondroitin sulfate-based self-assembled nanoparticles loading docetaxel for the inhibition of metastasis and growth of melanoma. *Carbohydrate Polymers*, *184*, 82–93. https://doi.org/10.1016/j.carbpol.2017.12.047

Liu, M., Khan, A. R., Ji, J., Lin, G., Zhao, X., & Zhai, G. (2018b). Crosslinked self-assembled nanoparticles for chemo-sonodynamic combination therapy favoring antitumor, antimetastasis management and immune responses. *Journal of Controlled Release*, *290*, 150–164. https://doi.org/10.1016/j.jconrel.2018.10.007

Liu, Y.-R., Sun, B., Zhao, X.-L., Gu, Q., Liu, Z.-Y., Dong, X.-Y., Che, N., & Mo, J. (2013). Basal caspase-3 activity promotes migration, invasion, and vasculogenic mimicry formation of melanoma cells. *Melanoma Research*, *23*(4), 243–253. https://doi.org/10.1097/cmr.0b013e3283625498

Lobb, R. J., Jacobson, G. M., Cursons, R. T., & Jameson, M. B. (2018). The interaction of selenium with chemotherapy and radiation on normal and malignant human mononuclear blood cells. *International Journal of Molecular Sciences*, *19*(10), Article 3167. https://doi.org/10.3390/ijms19103167

Ludwig, A., Kordelas, L., Rebmann, V., Radtke, S., Felderhoff-Müser, U., Horn, P., Beelen, D., & Giebel, B. (2012). Exosomes – from bench to bedside. *Klinische Pädiatrie*, *224*, Article A6. https://doi.org/10.1055/s-0032-1330775

Mackie, R. M., Hauschild, A., & Eggermont, A. M. (2009). Epidemiology of invasive cutaneous melanoma. *Annals if Oncology*, *20*(Suppl. 6), vi1–vi7. https://doi.org/10.1093/annonc/mdp252

Mahmood, T., & Yang, P.-C. (2012). Western blot: Technique, theory, and trouble shooting. *North American Journal of Medical Sciences*, *4*(9), 429–434. https://doi.org/10.4103/1947-2714.100998

Maroni P., & Bendinelli, P. (2020). Bone, a secondary growth site of breast and prostate carcinomas: Role of osteocytes. *Cancers*, *12*(7), Article 1812. https://doi.org/10.3390/cancers12071812

Matthews, H. K., Bertoli, C., & de Bruin, R. A. M. (2022). Cell cycle control in cancer. *Nature Reviews Molecular Cell Biology*, *23*, 74–88. https://doi.org/10.1038/s41580-021-00404-3

Mi, X., Bekerman, W., Sims, P. A., Canoll, P. D., & Hu, J. (2021). *RZiMM-scRNA: A regularized zero-inflated mixture model framework for single-cell RNA-Seq data*. ArXiv. https://doi.org/10.48550/arXiv.2110.12964

Miura, K., & Green, A. C. (2015). Dietary antioxidants and melanoma: Evidence from cohort and intervention studies. *Nutrition and Cancer*, *67*(6), 867–876. https://doi.org/10.1080/01635581.2015.1053499

Mokarizadeh, A., Delirezh, N., Morshedi, A., Mosayebi, G., Farshid, A.-A., & Mardani, K. (2012). Microvesicles derived from mesenchymal stem cells: Potent organelles for induction of tolerogenic signaling. *Immunology Letters*, *147*, 47–54. https://doi.org/10.1016/j.imlet.2012.06.001

Molinari, M. (2000). Cell cycle checkpoints and their inactivation in human cancer. *Cell Proliferation*, *33*(5), 261–274. https://doi.org/10.1046/j.1365-2184.2000.00191.x

Møller, P., Azqueta, A., Boutet-Robinet, E., Koppen, G., Bonassi, S., Milić, M., Gajski, G., Costa, S., Teixeira, J. P., Costa Pereira, C., Dusinska, M., Godschalk, R., Brunborg, G., Gutzkow, K. B., Giovannelli, L., Cooke, M. S., Richling, E., Laffon, B., Valdiglesias, V., Basaran, N., Del Bo', C., Zegura, B., Novak, M., Stopper, H., Vodicka, P., Vodenkova, S., De Andrade, V. M., Sramkova, M., Gabelova, A., Collins, A., & Langie, S. A. S. (2020). Minimum information for reporting on the comet assay (MIRCA): Recommendations for describing comet assay procedures and results. *Nature Protocols*, *15*, 3817–3826. https://doi.org/10.1038/s41596-020-0398-1

Moloudizargari, M., Abdollahi, M., Asghari, M. H., Zimta, A. A., Neagoe, I. B., & Nabavi, S. M. (2019). The emerging role of exosomes in multiple myeloma. *Blood Reviews*, *38*, Article 100595. https://doi.org/10.1016/j.blre.2019.100595

Moncayo, V. M., Grady, E. E., Alazraki, N. P., & Aarsvold, J. N. (2020). Sentinel-lymph-node multicenter trials. *Seminars in Nuclear Medicine*, *50*(1), 56–74. https://doi.org/10.1053/j.semnuclmed.2019.10.001

Moro, C. F., Selvam, A. K., Ghaderi, M., Pimenoff, V. N., Gerling, M., Bozóky, B., Elduayen, S. P., Dillner, J., & Björnstedt, M. (2022). Drug-induced tumor-specific cytotoxicity in a whole tissue ex vivo model of human pancreatic ductal adenocarcinoma. *Frontiers in Oncology*, *12*, Article 965182. https://doi.org/10.3389/fonc.2022.965182

Mullis, K. B. (1990). The unusual origin of the polymerase chain reaction. *Scientific American*, *262*(4), 56–61. https://doi.org/10.1038/scientificamerican0490-56

Mundekkad, D., & Cho, W. C. (2022). Nanoparticles in clinical translation for cancer therapy. *International Journal of Molecular Sciences*, *23*(3), Article 1685. https://doi.org/10.3390/ijms23031685

Muthu, S., Bapat, A., Jain, R., Jeyaraman, N., & Jeyaraman, M. (2021). Exosomal therapy—a new frontier in regenerative medicine. *Stem Cell Investigation*, *8*, Article 7. https://doi.org/10.21037/sci-2020-037

Najafzadeh, M., Normington, C., Jacob, B. K., Isreb, M., Gopalan, R. C., & Anderson, D. (2016). DNA damage in healthy individuals and respiratory patients after treating whole blood *in vitro* with the bulk and nano forms of NSAIDs. *Frontiers in Molecular Biosciences*, *3*, Article 50. https://doi.org/10.3389/fmolb.2016.00050

Neagu, T. P., Ţigliş, M., Botezatu, D., Enache, V., Cobilinschi, C. O., Vâlcea-Precup, M. S., & Grinţescu, I. M. (2017). Clinical, histological and therapeutic features of Bowen's disease. *Romanian Journal of Morphology and Embryology*, *58*, 33–40.

Neel, J. V., Schull, W. J., Awa, A. A., Satoh, C., Otake, M., Kato, H., & Yoshimoto, Y. (1989). Implications of the Hiroshima-Nagasaki genetic studies for the estimation of the human "doubling dose" Of radiation. *Genome*, *31*(2), 853–859. https://doi.org/10.1139/g89-150

NIH. (2022). *What is cancer?* National Cancer Institute. https://www.cancer.gov/about-cancer/understanding/what-is-cancer

Nowak, W. N., Deng, J., Ruan, X. Z., & Xu, Q. (2017). Reactive oxygen species generation and atherosclerosis. *Arteriosclerosis, Thrombosis, and Vascular Biology*, *37*, e41–e52. https://doi.org/10.1161/ATVBAHA.117.309228

Obrador, E., Liu-Smith, F., Dellinger, R. W., Salvador, R., Meyskens, F. L., & Estrela, J. M. (2019). Oxidative stress and antioxidants in the pathophysiology of malignant melanoma. *Biological Chemistry*, 400, 589–612. https://doi.org/10.1515/hsz-2018-0327

Olive, P. L. (2002). The comet assay. In V. V. Didenko (Ed.), *In situ detection of DNA damage. Methods in molecular biology, vol. 203* (pp. 179–194). Humana Press. https://doi.org/10.1385/1-59259-179-5:179

Osrodek, M., & Wozniak. M. (2021). Targeting genome stability in melanoma—a new approach to an old field. *International Journal of Molecular Sciences*, *22*(7), Article 3485. https://doi.org/10.3390/ijms22073485

Palaniappan, V., & Karthikeyan, K. (2022). Bowen's disease. *Indian Dermatology Online Journal*, *13*(2), 177–189. https://doi.org/10.4103/idoj.idoj_257_21

Papadakos, S. P., Dedes, N., Pergaris, A., Gazouli, M., & Theocharis, S. (2022). Exosomes in the treatment of pancreatic cancer: A moonshot to PDAC treatment? *International Journal of Molecular Sciences*, *23*(7), Article 3620. https://doi.org/10.3390/ijms23073620

Phillips, H. J. (1973). Dye exclusion tests for cell viability. In P. F. Kruse & M. K. Patterson, Jr. (Eds.), *Tissue Culture* (pp. 406–408). Academic Press.

Pillai-Kastoori, L., Schutz-Geschwender, A., & Harford, J. A. (2020). A systematic approach to quantitative Western blot analysis. *Analytical Biochemistry*, *593*, Article 113608. https://doi.org/10.1016/j.ab.2020.113608

Qazi, I. H., Angel, C., Yang, H., Zoidis, E., Pan, B., Wu, Z., Ming, Z., Zeng, C. J., Meng, Q., Han, H., & Zhou, G. (2019). Role of selenium and selenoproteins in male reproductive function: A review of past and present evidences. *Antioxidants*, *8*(8), Article 268. https://doi.org/10.3390/antiox8080268

Qiu, C., Zhang, T., Zhu, X., Qiu, J., Jiang, K., Zhao, G., Wu, H., & Deng, G. (2019). Methylseleninic acid suppresses breast cancer growth via the JAK2/STAT3 pathway. *Reproductive Sciences*, *26*, 829–838. https://doi.org/10.1177/1933719118815582

Quartuccio, N., Siracusa, M., Pappalardo, M., Arnone, A., & Arnone, G. (2020). Sentinel node identification in melanoma: Current clinical impact, new emerging SPECT radiotracers and technological advancements. An update of the last decade. *Current Radiopharmaceuticals*, *13*(2), 32–41. https://doi.org/10.2174/1874471012666191015100837

Radu, O., & Pantanowitz, L. (2013). Kaposi sarcoma. *Archives of Pathology & Laboratory Medicine*, *137*(2), 289–294. https://doi.org/10.5858/arpa.2012-0101-rs

Rastrelli, M., Tropea, S., Rossi, C. R., & Alaibac, M. (2014). Melanoma: Epidemiology, risk factors, pathogenesis, diagnosis and classification. *In Vivo*, *28*(6), 1005–1011.

Ravindranathan, D., Master, V. A., & Bilen, M. A. (2021). Inflammatory markers in cancer immunotherapy. *Biology*, *10*(4), Article 325. https://doi.org/10.3390/biology10040325

Rebecca, V. W., Somasundaram, R., & Herlyn, M. (2020). Pre-clinical modelling of cutaneous melanoma. *Nature Communications*, *11*, Article 2858. https://doi.org/10.1038/s41467-020-15546-9

Revythis, A., Shah, S., Kutka, M., Moschetta, M., Ozturk, M. A., Pappas-Gogos, G., Ioannidou, E., Sheriff, M., Rassy, E., & Boussios, S. (2021). Unraveling the wide spectrum of melanoma biomarkers. *Diagnostics*, *11*(8), Article 1341. https://doi.org/10.3390/diagnostics11081341

Rigel D. S. (2010). Epidemiology of melanoma. *Seminars in Cutaneous Medicine and Surgery*, *29*(4), 204–209. https://doi.org/10.1016/j.sder.2010.10.005

Rogoża-Janiszewska, E., Malińska, K., Baszuk, P., Marciniak, W., Derkacz, R., Lener, M., Jakubowska, A., Cybulski, C., Huzarski, T., Masojć, B., Gronwald, J., Rudnicka, H., Kram, A., Kiedrowicz, M., Boer, M., Dębniak, T., & Lubiński, J. (2021). Serum selenium level and 10-year survival after melanoma. *Biomedicines*, *9*(8), Article 991. https://doi.org/10.3390/biomedicines9080991

Rutgers E. J. (2008). Sentinel node biopsy: Interpretation and management of patients with immunohistochemistry-positive sentinel nodes and those with micrometastases. *Journal of Clinical Oncology*, *26*(5), 698–702. https://doi.org/10.1200/jco.2007.14.4667

Saginala, K., Barsouk, A., Aluru, J. S., Rawla, P., & Barsouk, A. (2021). Epidemiology of melanoma. *Medical Sciences*, *9*(4), Article 63. https://doi.org/10.3390/medsci9040063

Schins, R. P. F., & Knaapen, A. M. (2006). Genotoxicity of poorly soluble particles. *Inhalation Toxicology*, *19*(Suppl. 1), 189–198. https://doi.org/10.1080/08958370701496202

Šestáková, B., Ondrušová, L., & Vachtenheim, J. (2010). Cell cycle inhibitor p21/WAF1/CIP1 as a cofactor of MITF expression in melanoma cells. *Pigment Cell & Melanoma Research*, *23*(2), 238–251. https://doi.org/10.1111/j.1755-148X.2010.00670.x

Shah, S. U. (2012). Importance of genotoxicity & S2A guidelines for genotoxicity testing for pharmaceuticals. *IOSR Journal of Pharmacy and Biological Sciences*, *1*(2), 43–54.

Sorenson, E., Mcandrew, R., Patel, V., Logan, A. C., Koo, J., & Levin, E. (2015). Narrowband UV-B phototherapy for steroid-refractory sclerotic chronic cutaneous graft-vs-host disease. *JAMA Dermatology*, *151*(6), 635–637. https://doi.org/10.1001/jamadermatol.2015.0175

Speit, G., Kojima, H., Burlinson, B., Collins, A. R., Kasper, P., Plappert-Helbig, U., Uno, Y., Vasquez, M., Beevers, C., & De Boeck, M. (2015). Critical issues with the *in vivo* comet assay: A report of the comet assay working group in the 6th International Workshop on Genotoxicity Testing (IWGT). *Mutation Research/Genetic Toxicology and Environmental Mutagenesis*, 783, 6–12. https://doi.org/10.1016/j.mrgentox.2014.09.006

Stern, R. S., Laird, N., Melski, J., Parrish, J. A., Fitzpatrick, T. B., & Bleich, H. L. (1984). Cutaneous squamous-cell carcinoma in patients treated with PUVA. *New England Journal of Medicine*, *310*, 1156–1161. https://doi.org/10.1056/NEJM198405033101805

Tan, H. W., Mo, H.-Y., Lau, A. T. Y., & Xu, Y.-M. (2018). Selenium species: Current status and potentials in cancer prevention and therapy. *International Journal of Molecular Sciences*, *20*(1), Article 75. https://doi.org/10.3390/ijms20010075

Tanese, K. (2019). Diagnosis and management of basal cell carcinoma. *Current Treatment Options in Oncology*, *20*, Article 13. https://doi.org/10.1007/s11864-019-0610-0

Trindade, F. M., De Freitas, M. L. P., & Bittencourt, F. V. (2021). Dermoscopic evaluation of superficial spreading melanoma. *Anais Brasileiros de Dermatologia*, *96*, 139–147. https://doi.org/10.1016/j.abd.2020.06.012

Trisciuoglio, D., & Del Bufalo, D. (2021). New insights into the roles of antiapoptotic members of the Bcl-2 family in melanoma progression and therapy. *Drug Discovery Today*, *26*(5), 1126–1135. https://doi.org/10.1016/j.drudis.2021.01.027

Tucci, M., Mannavola, F., Passarelli, A., Stucci, L. S., Cives, M., & Silvestris, F. (2018). Exosomes in melanoma: A role in tumor progression, metastasis and impaired immune system activity. *Oncotarget*, *9*(29), 20826–20837. https://doi.org/10.18632/oncotarget.24846

Tyrrell, R. M., & Webb, R. B. (1973). Reduced dimer excision in bacteria following near ultraviolet (365 nm) radiation. *Mutation Research/Fundamental and Molecular Mechanisms of Mutagenesis*, *19*(3), 361–364. https://doi.org/10.1016/0027-5107(73)90238-8

van Dieck, J., Brandt, T., Teufel, D. P., Veprintsev, D. B., Joerger, A. C., & Fersht, A. R. (2010). Molecular basis of S100 proteins interacting with the p53 homologs p63 and p73. *Oncogene*, *29*, 2024–2035. https://doi.org/10.1038/onc.2009.490

VanGuilder, H. D., Vrana, K. E., & Freeman, W. M. (2008). Twenty-five years of quantitative PCR for gene expression analysis. *BioTechniques*, *44*(5), 619–626. https://doi.org/10.2144/000112776

Varamo, C., Occelli, M., Vivenza, D., Merlano, M., & Lo Nigro, C. (2017). MicroRNAs role as potential biomarkers and key regulators in melanoma. *Genes, Chromosomes & Cancer*, *56*(1), 3–10. https://doi.org/10.1002/gcc.22402

Varlamova, E. G., & Turovsky, E. A. (2021). The main cytotoxic effects of methylseleninic acid on various cancer cells. *International Journal of Molecular Sciences*, *22*(12), Article 6614. https://doi.org/10.3390/ijms22126614

Vázquez-Ríos, A. J., Molina-Crespo, A., Bouzo, B. L., López-López, R., Moreno-Bueno, G., & de la Fuente, M. (2019). Exosome-mimetic nanoplatforms for targeted cancer drug delivery. *Journal of Nanobiotechnology*, *17*, Article 85. https://doi.org/10.1186/s12951-019-0517-8

Villani, A., Potestio, L., Fabbrocini, G., Troncone, G., Malapelle, U., & Scalvenzi, M. (2022). The treatment of advanced melanoma: Therapeutic update. *International Journal of Molecular Sciences*, *23*(12), Article 6388. https://doi.org/10.3390/ijms23126388

Vinceti, M., Filippini, T., Del Giovane, C., Dennert, G., Zwahlen, M., Brinkman, M., Zeegers, M. P., Horneber, M., D'Amico, R., & Crespi, C. M. (2018). Selenium for preventing cancer. *Cochrane Database of Systematic Reviews*, *2018*(1), Article CD005195. https://doi.org/10.1002/14651858.CD005195.pub4

Vinoth, K. J., Manikandan, J., Sethu, S., Balakrishnan, L., Heng, A., Lu, K., Poonepalli, A., Hande, M. P., & Cao, T. (2015). Differential resistance of human embryonic stem cells and somatic cell types to hydrogen peroxide-induced genotoxicity may be dependent on innate basal intracellular ROS levels. *Folia Histochemica et Cytobiologica*, *53*(2), 169–174. https://doi.org/10.5603/FHC.a2015.0016

Wang, J. H., Li, J., Wu, Q., Yang, P., Pawar, R. D., Xie, S., Timares, L., Raman, C., Chaplin, D. D., Lu, L., Mountz, J. D., & Hsu, H. C. (2010). Marginal zone precursor B cells as cellular agents for type I IFN-promoted antigen transport in autoimmunity. *Journal of Immunology*, *184*(1), 442–451. https://doi.org/10.4049/jimmunol.0900870

Wang, L.-H., Wu, C.-F., Rajasekaran, N., & Shin, Y. K. (2018). Loss of tumor suppressor gene function in human cancer: An overview. *Cellular Physiology and Biochemistry*, *51*, 2647–2693. https://doi.org/10.1159/000495956

Wang, W., Li, Z., & Feng, J. (2018). The potential role of exosomes in the diagnosis and therapy of ischemic diseases. *Cytotherapy*, *20*(10), 1204–1219. https://doi.org/10.1016/j.jcyt.2018.06.012

Wang, X.-Y., Lin, C., Chang, W.-J., Huang, Y.-H., & Mi, F.-L. (2022). Thiolated hyaluronic acid and catalase-enhanced CD44-targeting and oxygen self-supplying nanoplatforms with photothermal/photodynamic effects against hypoxic breast cancer cells. *International Journal of Biological Macromolecules*, *221*, 121–134. https://doi.org/10.1016/j.ijbiomac.2022.08.164

Watson, M., Holman, D. M., & Maguire-Eisen, M. (2016). Ultraviolet radiation exposure and its impact on skin cancer risk. *Seminars in Oncology Nursing*, *32*(3), 241–254. https://doi.org/10.1016/j.soncn.2016.05.005

Wei, Y., Zhu, Z., Hu, H., Guan, J., Yang, B., & Zhao, H. (2022). Eupaformosanin induces apoptosis and ferroptosis through ubiquitination of mutant p53 in triple-negative breast cancer. *European Journal of Pharmacology*, *924*, Article 174970. https://doi.org/10.1016/j.ejphar.2022.174970

Williams, A. B., & Schumacher, B. (2016). p53 in the DNA-damage-repair process. *Cold Spring Harbor Perspectives in Medicine*, *6*, Article a026070. https://doi.org/10.1101/cshperspect.a026070

Wong, S. L., Faries, M. B., Kennedy, E. B., Agarwala, S. S., Akhurst, T. J., Ariyan, C., Balch, C. M., Berman, B. S., Cochran, A., Delman, K. A., Gorman, M., Kirkwood, J. M., Moncrieff, M. D., Zager, J. S., & Lyman, G. H. (2018). Sentinel lymph node biopsy and management of regional lymph nodes in melanoma: American Society of Clinical Oncology and Society of Surgical Oncology Clinical Practice guideline update. *Annals of Surgical Oncology*, *25*, 356–377. https://doi.org/10.1245/s10434-017-6267-7

Wu, C.-E., Esfandiari, A., Ho, Y.-H., Wang, N., Mahdi, A. K., Aptullahoglu, E., Lovat, P., & Lunec, J. (2018). Targeting negative regulation of p53 by MDM2 and WIP1 as a therapeutic strategy in cutaneous melanoma. *British Journal of Cancer*, *118*, 495–508. https://doi.org/10.1038/bjc.2017.433

Wu, P., Zhang, B., Han, X., Sun, Y., Sun, Z., Li, L., Zhou, X., Jin, Q., Fu, P., Xu, W., & Qian, H. (2021). HucMSC exosome-delivered 14-3-3ζ alleviates ultraviolet radiation-induced photodamage via SIRT1 pathway modulation. *Aging*, *13*(8), 11542–11563. https://doi.org/10.18632/aging.202851

Wu, S., Ju, G.-Q., Du, T., Zhu, Y.-J., & Liu, G.-H. (2013). Microvesicles derived from human umbilical cord Wharton's jelly mesenchymal stem cells attenuate bladder tumor cell growth *in vitro* and *in vivo*. *PLoS One*, *8*(4), Article e61366. https://doi.org/10.1371/journal.pone.0061366

Xin, H., Li, Y., Buller, B., Katakowski, M., Zhang, Y., Wang, X., Shang, X., Zhang, Z. G., & Chopp, M. (2012). Exosome-mediated transfer of miR-133b from multipotent mesenchymal stromal cells to neural cells contributes to neurite outgrowth. *Stem Cells*, *30*, 1556–1564. https://doi.org/10.1002/stem.1129

Xiang, N., Zhao, R., & Zhong, W. (2009). Sodium selenite induces apoptosis by generation of superoxide via the mitochondrial-dependent pathway in human prostate cancer cells. *Cancer Chemotherapy and Pharmacology*, *63*, 351–362. https://doi.org/10.1007/s00280-008-0745-3

Xiong, T.-F., Pan, F.-Q., & Li, D. (2019). Expression and clinical significance of S100 family genes in patients with melanoma. *Melanoma Research*, *29*(1), 23–29. https://doi.org/10.1097/cmr.0000000000000512

Xu, L., Shoaie, N., Jahanpeyma, F., Zhao, J., Azimzadeh, M., & Al Jamal, K. T. (2020). Optical, electrochemical and electrical (nano)biosensors for detection of exosomes: A comprehensive overview. *Biosensors & Bioelectronics*, *161*, Article 112222. https://doi.org/10.1016/j.bios.2020.112222

Yan, Y., Jiang, W., Tan, Y., Zou, S., Zhang, H., Mao, F., Gong, A., Qian, H., & Xu, W. (2017). hucMSC exosome-derived GPX1 is required for the recovery of hepatic oxidant injury. *Molecular Therapy*, *25*(2), 465–479. https://doi.org/10.1016/j.ymthe.2016.11.019

Yao, Y., Gu, X., Xu, X., Ge, S., & Jia, R. (2022). Novel insights into *RB1* mutation. *Cancer Letters*, *547*, Article 215870. https://doi.org/10.1016/j.canlet.2022.215870

Yousefzadeh, M., Henpita, C., Vyas, R., Soto-Palma, C., Robbins, P., & Niederhofer, L. (2021). DNA damage—how and why we age? *eLife*, *10*, Article e62852. https://doi.org/10.7554/eLife.62852

Zeng, H., Wu, M., Botnen, J. H. (2009). Methylselenol, a selenium metabolite, induces cell cycle arrest in G1 phase and apoptosis via the extracellular-regulated kinase 1/2 pathway and other cancer signaling genes. *The Journal of Nutrition*, *139*(9), 1613–1618. https://doi.org/10.3945/jn.109.110320

Zhang, B., Wu, X., Zhang, X., Sun, Y., Yan, Y., Shi, H., Zhu, Y., Wu, L., Pan, Z., Zhu, W., Qian, H., & Xu, W. (2015). Human umbilical cord mesenchymal stem cell exosomes enhance angiogenesis through the Wnt4/ß-catenin pathway. *Stem Cells Translational Medicine*, *4*(5), 513–522. https://doi.org/10.5966/sctm.2014-0267

Zhang, X., Zhang, L., Xia, K., Dai, J., Huang, J., Wang, Y., Zhu, G., Hu, Z., Zeng, Z., & Jia, Y. (2022). Effects of dietary selenium on immune function of spleen in mice. *Journal of Functional Foods*, *89*, Article 104914. https://doi.org/10.1016/j.jff.2021.104914

Zhang, Z., Mi, T., Jin, L., Li, M., Zhanghuang, C., Wang, J., Tan, X., Lu, H., Shen, L., Long, C., Wei, G., & He, D. (2022). Comprehensive proteomic analysis of exosome mimetic vesicles and exosomes derived from human umbilical cord mesenchymal stem cells. *Stem Cell Research & Therapy*, *13*, Article 312. https://doi.org/10.1186/s13287-022-03008-6

Zhao, Y., Huang, Z., & Peng, H. (2021). Molecular mechanisms of ferroptosis and its roles in hematologic malignancies. *Frontiers in Oncology*, *11*, Article 743006. https://doi.org/10.3389/fonc.2021.743006

Zhou, J., Tan, X., Tan, Y., Li, Q., Ma, J., & Wang, G. (2018). Mesenchymal stem cell derived exosomes in cancer progression, metastasis and drug delivery: A comprehensive review. *Journal of Cancer*, *9*(17), 3129–3137. https://doi.org/10.7150/jca.25376

Zhou, S., Abdouh, M., Arena, V., Arena, M., & Arena, G. O. (2017). Reprogramming malignant cancer cells toward a benign phenotype following exposure to human embryonic stem cell microenvironment. *PLoS One*, *12*(1), Article e0169899. https://doi.org/10.1371/journal.pone.0169899

Zhu, D., Li, W., Fang, C., Yin, R., Jiang, M., Lv, X., & Chen, Y. (2022). Proteomic analysis of human umbilical cord serum exosomes using mass spectrometry and preliminary study of their biological activities in liver cancer cell lines. *Experimental and Therapeutic Medicine*, *23*(1), Article 44. https://doi.org/10.3892/etm.2021.10966

Zuo, Y.-B., Zhang, Y.-F., Zhang, R., Tian, J.-W., Lv, X.-B., Li, R., Li, S.-P., Cheng, M.-D., Shan, J., & Zhao, Z. (2022). Ferroptosis in cancer progression: Role of noncoding RNAs. *International Journal of Biological Sciences*, *18*(5), 1829–1843. https://doi.org/10.7150/ijbs.66917

Appendix

UNIVERSITY OF BRADFORD
MAKING KNOWLEDGE WORK

School of Life Sciences

DATA COLLECTION FORM
(To be completed by the Doctor)

STUDY TITLE: Genetic and environmental effects in lymphocytes from different cancerous, precancerous and inflammatory conditions using various genetic endpoints
REVIEWED BY LEEDS East RESEARCH ETHICS COMMITTEE (REC)
(REC REFERENCE NUMBER: 12/YH/0464)

PATIENT NUMBER		DATE OF SAMPLE	
AGE			
SEX (PLEASE TICK)	M / F	CONSENT	Y / N
ETHNIC GROUP		INFORMATION SHEET	Y / N
OCCUPATION			

CURRENT SMOKER	Y/N	PAST SMOKER	Y/N	HOW MANY/MUCH PER DAY?	
CIGARETTES		CIGARS		PIPE	
ALCOHOL	Y/N	UNITS PER WEEK			

DIET	WESTERN	ASIAN	OMNIVORE	VEGETARIAN	VEGAN

VITAMINS / ANTI-OXIDANTS (PLEASE LIST)

PRESCRIBED DRUG USE (PLEASE LIST)

RECREATIONAL DRUG USE Y/N

IF YES PLEASE LIST

MEDICAL **Asthma** **COPD** **others**

CANCER |
Inflammatory disease

EXTENT		SITE		HISTOLOGY		SURGERY	

CANCER	
Inflammatory disease	
Pre cancerous state	
OTHER MEDICAL CONDITIONS (PLEASE LIST)	
Family history of cancer and Inflammatory disease	
Chemotherapy or radiotherapy	

MOST RECENT MEASURE

	RESULT	DATE		RESULT	DATE
WEIGHT			OTHERS		
HEIGHT					
BMI					

Participant Information Sheet for patients (Version 4, 28/01/2019).

Study title: Genetic and environmental effects in lymphocytes from different cancerous, precancerous and inflammatory conditions using various genetic endpoints.

Reviewed by Leeds East Research Ethics Committee (REC)
(REC reference number: 12/YH/0464)

Invitation to the research study

We should like to invite you to take part in a research study. Before you decide you need to understand why the research is being done and what it would involve for you. Please take time to read the following information carefully. Talk to others about the study if you wish and you will be allowed around 24 hours to consider this.

(Part 1 tells you the purpose of this study and what will happen to you if you take part.

Part 2 gives you more detailed information about the conduct of the study).

Ask us if there is anything that is not clear or if you would like more information. Take time to decide whether you want to take part.

Part 1

What is the purpose of the study?

In this study blood cells will be treated in a test tube with very small chemical particles or UVA (Ultraviolet A light) to determine if patients with different diseases are more at risk after exposure compared to healthy individuals. For example, chemicals and UV (Ultraviolet) can break and damage the DNA of white blood cells. Further examination of this resulting damage may improve our knowledge of the cancers and other inflammatory diseases. The tests are not predictive for any kind of diseases and the test results will not impact on you or the healthy volunteers with whom you are compared.
Blood samples for the study will be taken during the clinic visit in which you are recruited, if possible, at the same time as the samples taken for your routine care.
A blood sample of around 2-4 teaspoons (20 ml) will be taken. Samples will be stored only until the end of the study (after 8 years) and used for studies of similar nature or to check original responses. The research is also used for some PhD programmes.

Why have I been invited?

Because you are a patient at the Clinic, and we should like to determine if these small chemical particles or UVA could be more harmful to you than to people without the disease.

Do I have to take part?

No, it is up to you to decide. We shall outline the study and go through this information sheet, which we shall then give to you. We shall ask you to sign a consent form to show you have agreed to take part. You are free to withdraw at any time, without giving a reason. This would not affect the standard of care you receive.

Part 2

What will happen to me if I take part?

Only a single blood sample will be taken for this research study. A brief questionnaire will need to be completed by the researchers. Everyone will be given a coded study number so that your clinical data will be linked in an anonymous way with the research results.

<u>The study tests are not predictive for you.</u>

The data obtained will only be available to the research team and will not be returned to you. Responses will be compared only on group basis i.e., collective responses from patients with that individual disease compared to collective responses from people without that disease. Results could be published in the form of scientific papers. The work may benefit the medical and scientific community at large but will not be of direct benefit to you as an individual. If, however, you would like more information, the appropriate consultant will be prepared to talk to you individually about study results.

The data will be stored until the study is completed at the end of 8 years.

People who cannot take part in the study.

People who are not well enough to take part will be excluded e.g., those with anaemia.

If you have any further questions, you could contact the research team:

Prof Badie Jacob, NHS Trust, St Luke's Hospital
Bradford Teaching Hospitals NHS Foundation Trust, BD5 0NA .
Telephone: 01274 542200

Professor Diana Anderson, Established Chair in Biomedical Sciences, BSc, MSc, PhD, DipEd, FIBiol, FATS, FRCPath, FIFST, FBTS, FHEA, University of Bradford, Richmond Road, Bradford, BD7 1DP and Honorary Research Consultant to Bradford NHS Trust.
e-mail: d.anderson1@bradford.ac.uk

Dr Mojgan Najafzadeh MD, PhD, Postdoctoral Research Fellow, Division of Medical Sciences, University of Bradford, Richmond Road, Bradford, BD7 1DP Honorary Research Consultant to Bradford NHS Trust.